CORBYS
Cognitive Control Framework for Robotic Systems

SEVENTH FRAMEWORK PROGRAMME

CORBYS

Cognitive Control Framework for Robotic Systems

(FP7 – 270219)

Deliverable D3.2
Physical/Physiological sensing devices

Contractual delivery date: Month 20
Actual submission date: 30st September 2012

Start date of project: 01.02.2011 Duration: 48 months

Lead beneficiary: BBT Responsible person: Marco Creatura

Revision: 1.0

Project co-funded by the European Commission within the seventh Framework Program		
Dissemination Level		
PU	Public	**X**
PP	Restricted to other program participants (including the Commission Services)	
RE	Restricted to a group specified by the consortium (including the Commission Services)	
CO	Confidential, only for members of the consortium (including the Commission Services)	

Document History

Author(s)	Revision	Date	Contributions
Anders Liverud	0.1	02-07-2012	Draft document structure
Marco Creatura	0.2	23-07-2012	Revision of the BBT contribution
Anders Liverud	0.3	10-09-2012	Added IMU Sensor module documentation
Anders Liverud, Steffen Dalgard	0.4	14-09-2012	Reset of "track changes" after much editing
Anders Liverud	0.6	21-09-2012	Draft document
Marco Creatura	0.8	24-09-2012	BCI section
Anders Liverud	0.9	26-09-2012	Input from review on HSS
Marco Creatura	0.10	26-09-2012	BCI section – internal review changes
Anders Liverud	0.11	27-09-2012	HSS sections updated
Marco Creatura	0.12	28-09-2012	Executive Summary, Introduction and BCI section (including Safety , Requirements, and Conclusion) updated
Marco Creatura	1.0	30-09-2012	Release version

CORBYS Definition of Terms

Term		Definition
CORBYS Demonstrators		
The 1st CORBYS Demonstrator (Demonstrator I)		Mobile Robot-assisted Gait Rehabilitation System
The 2nd CORBYS Demonstrator (Demonstrator II)		Reconnaissance Robot for Investigation of Hazardous Environments – (RecoRob)
CORBYS Roles		
User		Any user interacting with the CORBYS systems, for example, in case of gait rehabilitation system, users with the following roles: a patient, therapist or an engineer; In the case of reconnaissance robot, users with the following role: (tele) operator or a hazardous area examination officer.
CORBYS End-user		The companies/entities that use/exploit (aspects of) CORBYS technology in their commercial products or services.
Mobile Robotic Gait Rehabilitation System Roles	Patient	The person receiving gait rehabilitation therapy aided by the CORBYS system
	Therapist	The medical professional configuring and assessing rehabilitation therapy aided by the CORBYS system.
	Engineer	A professional dealing with the CORBYS system based on a need to do technical maintenance, repairs or system configurations.
Reconnaissance robot for Investigation of Hazardous Environments Roles	Operator	The person steering the robot by remote control
	Hazardous Area Examination Officer	The person that robot follows in a team work on investigation of hazardous areas
	Engineer	A professional dealing with the CORBYS system based on a need to do technical maintenance, repairs or system configurations.
CORBYS Domain Knowledge		
Sensor Fusion		Method used to combine multiple independent sensors to extract and refine information not available through single sensors alone.
Situation Assessment		Estimation and prediction of relation among objects in the context of their environment.
Cognitive Control		Capability to process variety of stimuli in parallel, to "filter" those that are the most important for a given task to be executed, to create an adequate response in time and to learn new motor actions with minimum assistance (Kawamura et al., 2008).
Human-Robot Interaction		Ability of a robotic system to mutually communicate with humans.
Neural Plasticity		Ability of neural circuits, both in the brain and the spinal cord, to reorganise or change function.
Cognitive Processes		Processes responsible for knowledge and awareness, they include the processing of experience, perception and memory.
CORBYS Technology Components		
SAWBB		Situation Awareness Blackboard
SOIAA		Self-Organising Informational Anticipatory Architecture
User Interface		User interface designed to meet the needs of the various users in exchanging information between the robot and human user
Brain Computer Interface (BCI)		The sensor system measuring the brain waves using EEG and detecting patterns identifying movement actions
Human Sensory System (HSS)	HSS	The sensors measuring aspects of the human physiology and movement patterns.
	Chest Unit (CU)	Sensor unit located at chest of patient.
	IMU Sensor Unit	Sensor Unit located at back of patient.

	Chest Belt	Belt around patient chest with Chest Unit at front and IMU Sensor Unit at back.
	HSS Controller	Computer and software system that receives data from HSS sensors and forward these to the General Purpose Network.
Low Level Control		Localised control of actuators, usually torque, current or position control. Sensory data is passed to the real-time control, actuation commands are calculated and sent to the actuators.
Smart Actuators		Highly integrated mechatronic units incorporating a motor and the complete motion control electronics in one single unit.
Generic CORBYS Robot Control Components		
Cognitive System		Incorporates situation awareness and intention detection to enable optimal man-machine interaction towards achievement of set goals in the specific usage context.
Executive Layer		The executive layer is responsible for translating the high-level plans (cognitive inputs) into low-level actions, invoking actions at the appropriate times, monitoring the action execution, and handling exceptions. The executive layer can also allocate and monitor resource usage.
Communication Server		Manage subscriptions of sensor data between different control modules. The sensor data to the cognitive modules are not flowing through the Communication Server, but are forwarded directly.
Task manager		The task manager manages operation modes to be executed by the system. Performs specific tasks when the operation mode is changed.
FPGA Reflexive Module		Field Programmable Gate Array (FPGA) based hardware subsystem of Situation Awareness architecture (SAWBB) for acceleration of robot reflexive behaviour.
Safety Module		Verification that actuator output is in line with the commanded output and that it satisfies safety-related position, velocity, current and/or torque constraints.
Real-Time Data Server		Real-time data server is a software module responsible for communicating sensor data from real-time (RT) bus to other software modules.. This excludes communication of RT modules with sensors and actuators which communicate with sensors and actuators directly, in order to preserve RT control behaviour.
Real-Time Network (RTN)		Sensor network for real-time, safety critical data transmission
General Purpose Network (GPN)		Network for robot control and interface to the cognitive modules
Demonstrator Specific Technology Components		
Mobile Robotic Gait Rehabilitation System	Pelvis Link	Mechanical interface between the mobile platform and the powered orthosis equipped with an appropriate actuation and sensing system.
	Powered Orthosis	Exoskeleton system to help the patient in moving his/her legs and receiving an appropriate rehabilitation therapy.
	Mobile Platform	The platform for the entire system, including Pelvis Link, Powered Orthosis, necessary computational, storage, and power supply modules, as well as motored wheels for movement
Reconnaissance robot for Investigation of Hazardous Environments	Vision System	Cameras of the 2nd demonstrator used for environment perception including human tracking
	Robot Arm	7DOF lightweight robot arm mounted on the Mobile Platform used for the object manipulation (for contaminated area sample drawing)
	Mobile Platform	Mobile platform of the 2nd demonstrator which consists of a variable drive system that is equipped with chains. It is used for mounting of the robot arm and sensors for environment perception as well as sensors for platform navigation and robot arm control. Containers for samples are also placed on mobile platform

Table of Contents

CORBYS DEFINITION OF TERMS III

EXECUTIVE SUMMARY 1

1 INTRODUCTION 4

1.1 DOCUMENT SCOPE 4
1.2 DOCUMENT STRUCTURE 4
1.3 ASSOCIATED DOCUMENTS 5

2 HUMAN SENSORY SYSTEM REALIZATION 6

2.1 HSS ARCHITECTURE 6
2.2 CHEST UNIT 11
2.3 IMU SENSOR UNIT 17
2.4 EMG SENSORS 22
2.5 HUMAN SENSORY SYSTEM CONTROLLER 23
2.6 OFFLINE CHARGING STATION FOR WIRELESS SENSORS 39

3 BRAIN COMPUTER INTERFACE (BCI) 41

3.1.1 EVALUATION OF EEG ACQUISITION SYSTEMS THAT COULD REDUCE THE NOISE LEVEL 43
3.2 ANALYSIS AND REMOVAL OF MOVEMENTS' ARTIFACTS DURING LOCOMOTION 52
3.3 DETECTION OF ATTENTION DURING ASSISTED PASSIVE LEG MOTION 65

4 SAFETY 72

4.1 CHEST UNIT 72
4.2 IMU UNIT 72
4.3 EMG UNITS 72
4.4 HSS CONTROLLER COMPUTER 72
4.5 OFFLINE CHARGER 72
4.6 SAFETY ANALYSIS: 73
4.7 EEG UNIT 76
4.8 BCI SOFTWARE 76
4.9 BCI SAFETY ANALYSIS: 76

5 REQUIREMENTS FROM D2.1 79

6 CONCLUSIONS AND FUTURE WORK 91

7 REFERENCES 93

Executive Summary

This deliverable document (D3.2) reports on work related to the development of Human Sensory System (HSS) and Brain Computer Interface (BCI) as performed in Work Package 3 "Sensing systems for assessing dynamic system environments including humans" of the CORBYS project.

Based on deliverable documents, D2.1 Requirements and Specification, and D2.2 Detailed Specifications of the System, this document describes the realisation of the Human Sensory System and the analysis of Brain Computer Interface processes related to development and integration of the BCI module in the CORBYS 1st demonstrator.

To meet challenges in physiological monitoring in robotics systems a human sensory system has been realized. Compared to available commercial sensor systems the CORBYS human sensory system has features that make it suitable for robotics environments. It is compact, easy to attach and remove and does not disturb or cause any discomfort for the user. The sensors provide relevant physiological measures and can coexist with robotic systems like gait rehabilitation robots. Data is provided on a standardized robotics software interface.

The sensors have been realized through development of a chest belt with sensors situated on the chest and back of the patient. Physiological parameters like heart rate with ECG, humidity, skin temperature are measured together with velocity and orientation. These parameters will be used by the cognitive modules of the CORBYS Demonstrator I, robot-assisted gait rehabilitation system, for assessing physical effort, identifying psyco-physiological states and for identifying intentions of the patient. Similarly the Human Sensory System may be used for providing physiological data for CORBYS Demonstrator II, the Reconnaissance Robot. The infrastructure for transmitting sensor data to the cognitive framework has been developed. Sensors are transmitting sensor data wirelessly with a predictable low latency to a computer. The computer is running controller software that is synchronizing and time-stamping sensor data before data is provided to the cognitive modules, therapist and engineering user interfaces through the general purpose network. The sensor modules are based on state of the art components that are highly integrated and optimized for long term wireless physiological monitoring. Effort has been put into compact integrated design and low power consumption enabling long term physiological monitoring.

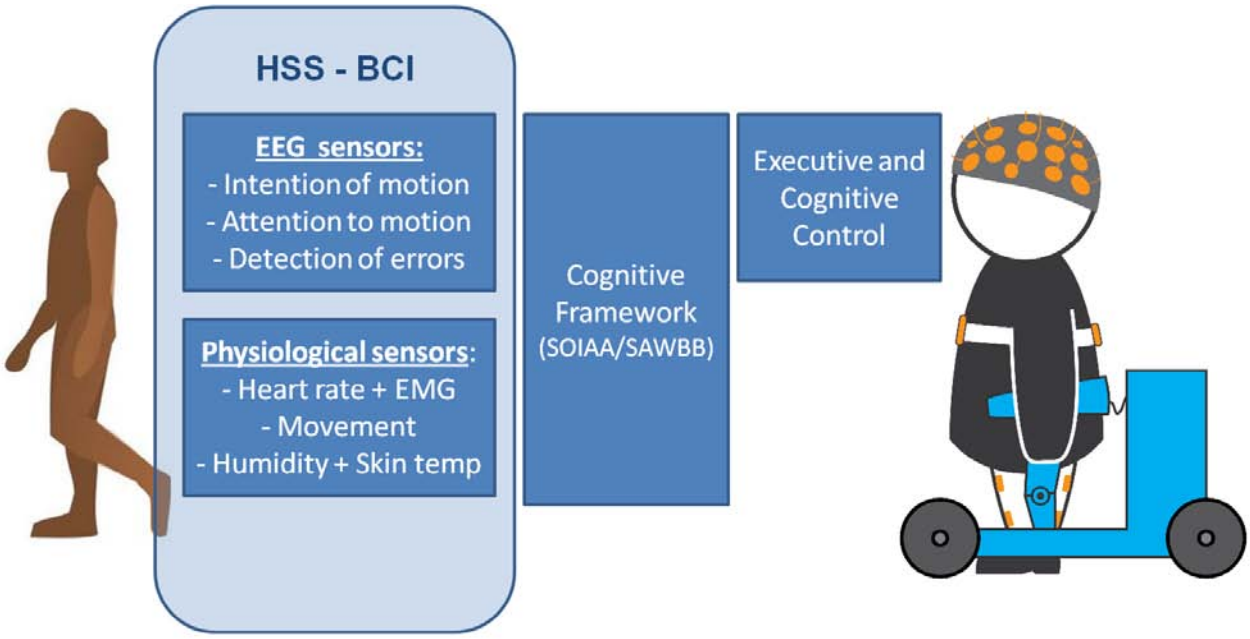

Figure 1: Human sensors interaction with other modules in CORBYS Demonstrator I

Figure 1 illustrates how the Human Sensory System (HSS) and Brain Computer Interface (BCI) interact with the cognitive framework and executive and cognitive control part of CORBYS Demonstrator I. The cognitive framework, composed of the Situation Awareness Blackboard (SAWBB) and the Self Organizing Information Anticipatory Architecture (SOIAA), endows robotic systems with cognitive capabilities and are responsible for identifying the current state of the system and maintaining a cognitive image of the environment (including representation of the humans interacting with the system) and generating high-level commands. The physiological data will be used as input via SAWBB to the reasoning sub-systems within the Situation Assessment architecture for observation and learning of patterns, identification of deviation from established reference points, and rectifications suggested to the human-in-the-loop (therapist in case of Demonstrator I). EEG data is largely utilized by SOIAA for detection of intention and attention of motion. Details of cognitive modules will be described in documents deliverables under WP4 and WP5.

This deliverable, D3.2, gives detailed information about development of Human Sensory System sensors and controller software. The main document contains an overall description of the system; however some implementation details for the sensor systems and test specifications are given in the project internal appendices.

To meet challenges in the integration of BCI – related algorithms for detection of cognitive processes in real time robotic applications (i.e. CORBYS first demonstrator), studies on the impact of different artifacts have been performed and documented in the current deliverable. Ocular, mechanical and electromagnetical contaminations on the EEG signal have been addressed through the execution of several experiments. Due to the result obtained, the TMSi system has been chosen as EEG system for the CORBYS demonstrator I. In addition, the Independent Component Analysis (ICA) has been showed to be a feasible technique to use in artifact removal within a simulation of the CORBYS rehabilitation scenario.
An initial analysis of passive lower limb movements with attention or non-attention to the motor task have been performed, in order to improve rehabilitation programs, where the movement repetitions could lead to a

lack of patient engagement compromising the adherence to the therapy. Results reported showed the feasibility to distinguish between the two conditions.

Dataset from human sensors (including BCI data) have been recorded, analysed and provided to the cognitive partners as an early integration activity. This have served the basis for which all data is handled, establishing protocols for sampling, handling data with different time scales, and interfaces for testing various information-theoretic tools.

The safety of the Human Sensory System and of the Brain Computer Interface is discussed and FMEA risk analysis is provided. There are no safety concerns for the Human Sensory System for the clinical testing in WP9.

The relevant requirements from D2.1 are analysed and compared to the current implementation. Most requirements of the Human Sensory System are fulfilled in this deliverable; the remaining requirements will be fulfilled in D3.4. Regarding BCI most requirements will be fulfilled in D3.3 and D3.4

The Human Sensory System will be extended in Deliverable D3.4 in month 26. The main addition will be EMG sensors to measure muscle activity, but improvements in the sensors and the controller will also be added. The Demonstrator I development will at that time be ready for early integration and hence the Human Sensory System will be enhanced to fit with the cognitive modules, and the engineering and therapist user interfaces. Options to simulate the Human Sensory System from recorded data will be added so to ease system integration.

The analysis Brain Computer Interface submodule will be advanced in D3.3 (month 38) and D3.4 (month 26). The main addition will include the design of BCI software architecture, addressing also network integration and synchronization issues, and the implementation of the decoding CORBYS – related decoding algorithms.

1 Introduction

The focus of CORBYS is on robotic systems that have a symbiotic relationship with humans. Such robotic systems have to cope with highly dynamic environments, as humans are demanding, curious and often act unpredictably. CORBYS will design and implement a cognitive robot control architecture that allows the integration of 1) high-level cognitive control modules, 2) a semantically-driven self-awareness module, and 3) a cognitive framework for anticipation of, and synergy with, human behaviour, based on biologically-inspired information-theoretic principles.

The CORBYS control architecture will be validated within the two CORBYS demonstrators. The first demonstrator is the novel mobile robot-assisted gait rehabilitation system CORBYS.

Further information about the design challenges of CORBYS can be found on the CORBYS web page [www.corbys.eu]. Additionally, general information about the field of Cognitive Robotics can be found on the EU Framework Program 7 web pages on Cognitive Systems and Robotics [http://cordis.europa.eu/fp7/ict/cognition/].

One of the main CORBYS objectives is development of advanced sensing module for assessing the physical and psychological state of human in robots environment. The physiological sensing devices in the CORBYS project consist of the Brain Computer Interface (BCI) and the Human Sensory System (HSS).

Non invasive Brain Computer Interface (using EEG) performs online detection of human cognitive information such as intention of leg motion, feedback error-related potential and attention states.

The Human Sensory System consists of a set of physiological sensors to measure patient effort and movement. The sensors are grouped into four categories, i.e., physiological sensors, movement sensors, environmental sensors and mechanical sensing technologies.

BCI and HSS are connected to controllers that convert and transmit data to the cognitive framework in the CORBYS system.

1.1 Document Scope

The present document corresponds to Deliverable 3.2 in the CORBYS project, and is the outcome of work in CORBYS Task 3-1 on Sensoring, data acquisition, fusion and interpretation as well as Task 3-5 Human-robot sharing of cognitive information.

1.2 Document Structure

This document is structured as follows: After a brief introduction, the Human Sensory System and BCI implementation are described. The next chapter focuses on safety followed by a chapter in which relevant requirements (as identified in WP2) are listed and discussed. The last section concludes the document and also presents a list of future work.

1.3 Associated Documents

The following documents give additional perspectives for the present work:

- D2.1 Requirements and Specification: State-of-the-Art, Prioritised End-User Requirements, Ethical Aspects
- D2.2 Detailed Specification of the System: System Architecture Specification with control and data flow, module interdependencies, user scenarios etc.
- D3.1 Sensor Network

2 Human Sensory System realization

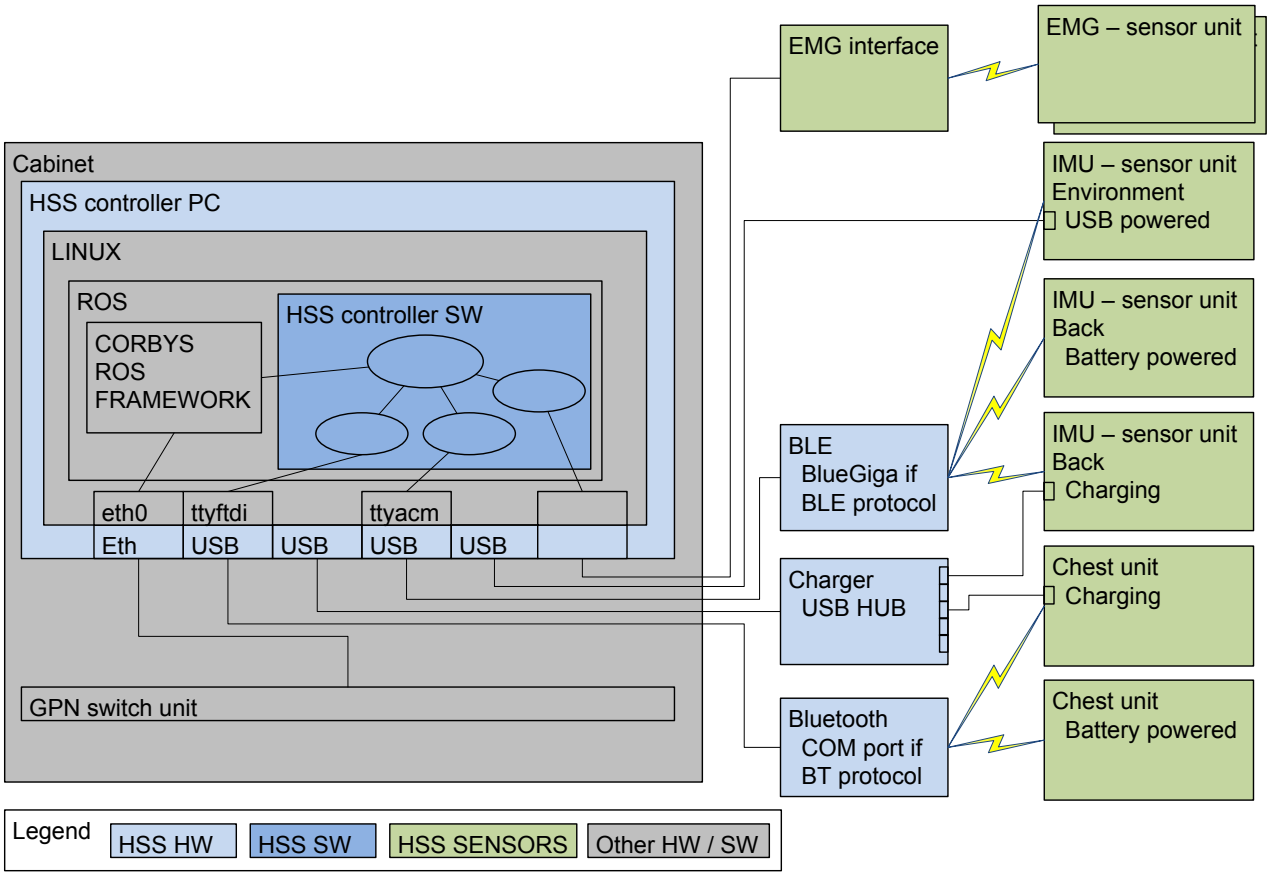

Figure 2: Human Sensory System overview

Figure 2 gives an overview of all HSS modules that will be presented in this chapter.

2.1 HSS architecture

The Human Sensory System (HSS) consists of a set of HSS Sensor Modules that interface with the HSS Controller, which in turn interfaces with the CORBYS network as illustrated in Figure 3. The HSS Sensor Modules are one or more sensors connected to a sensor controller handling communication. The HSS Controller handles all communication with the CORBYS Demonstrators via the CORBYS General Purpose Network. The module-based architecture facilitates the use of HSS modules in multiple Cognitive Robotics applications.

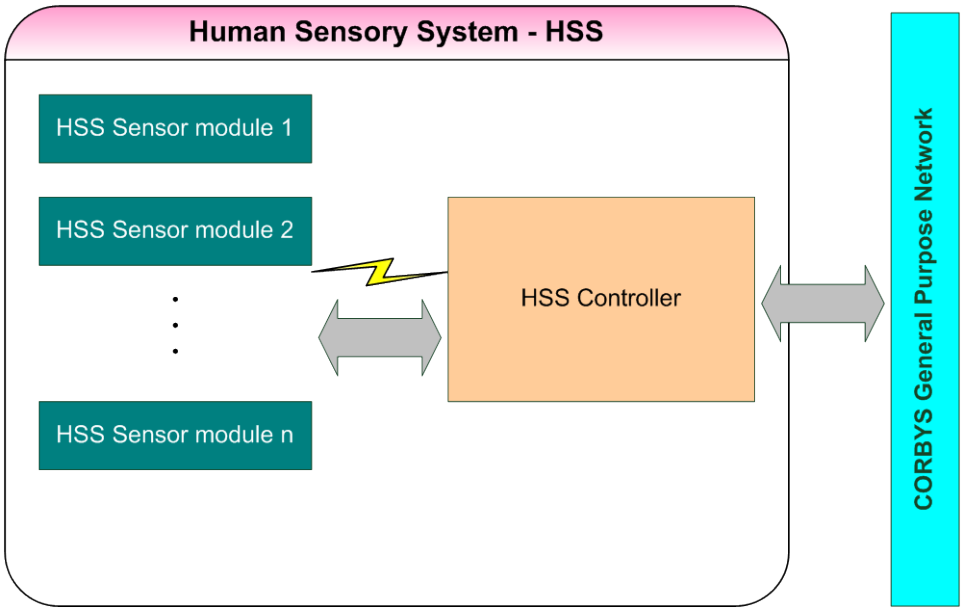

Figure 3: Human Sensory system architecture

2.1.1 Sensor Module architecture

Sensor modules differ in type and functionality. The simplest module can consist of a single sensor and a communication module transmitting raw data to the HSS controller. HSS Sensor Modules contain multiple sensors and a sensor controller handling multi-sensor interpretation as well as transmitting data.

The sensors are grouped into 4 main groups: physiological sensors, movement sensors, environmental sensors and mechanical sensing technologies. Mechanical sensors are not in the scope of HSS. Figure 4 shows the gait rehabilitation HSS Sensor Module measurement positions along with their use in the gait rehabilitation application.

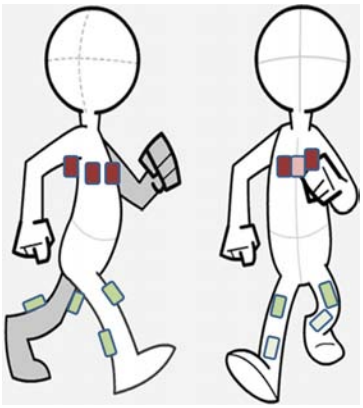

Figure 4: Measurement positioning of the gait rehabilitation HSS Sensor Module

Table 1 lists all the sensors in CORBYS Human Sensory System.

Sensor	Purpose	Gait rehabilitation measurement position
Physiological sensors		
Electromyography – EMG	Measuring the electrical activity produced by the skeletal muscles.	Measured on thigh and calf, both front and rear muscle, on both legs. A total of 8 sensors.
Heart rate and ECG signal	Used in the assessment of physical effort.	The heart rate is derived from the ECG signal measured on the patient chest. The full ECG signal is also provided.
Skin temperature	Monitor skin temperature.	Skin temperature is measured on the patient chest.
Humidity (sweat)	Used in the assessment of physical effort	The humidity is measured on the back of the patient.
Movement sensors		
Inertial Measurement Units – IMU	The IMU consists of a 3 axis accelerometer, a 3 axis gyroscope and optionally a magnetometer. The IMU is measuring velocity, orientation and gravitational forces. In CORBYS it is used for measuring patient balance and movement.	One IMU is located at the chest and one at the back of the patient. The IMU at the back also includes a magnetometer.
Environmental sensors		
Environment temperature	Exterior temperature, used in humidity/sweat calculations.	Located externally on the HSS Controller

Table 1. CORBYS HSS Sensors

These sensors are grouped into the following sensor modules:

- Chest unit – a unit connected to a belt around the patient chest measuring heart rate, ECG, skin temperature and IMU data. See Figure 5.
- IMU sensor unit connected to the same belt as chest unit, but at the back of the patient. The IMU sensor unit measures skin temperature, humidity and activity via the IMU. This IMU also includes a magnetometer. See Figure 5.
- Environment temperature, an IMU sensor unit is attached to the mobile platform and is used for environment humidity measurements.
- EMG sensors, 8 sensors all together. Two sensors are connected to each thigh and similarly two sensors to each calf for each leg of the patient.

Figure 5: Belt with Chest unit sensors and IMU sensors at back.

2.1.2 Communication links and timing issues

The Human Sensory System is linked to Demonstrator I via the General Purpose Network, a TCP/IP network. This network is defined in WP 3.

The various HSS sensors are connected to the HSS controller via Bluetooth wireless technology. The Chest unit uses standard Bluetooth communication via SPP protocol (Serial Port Profile).

The IMU sensor unit uses Bluetooth Smart[1] a part of the Bluetooth 4.0 specification (formerly named Bluetooth Low Energy) for communication; this is an emerging low-power, low latency communication protocol providing defined profiles for various sensor devices.

All computers on the General Purpose Network (GPN) will have synchronized clocks, the accuracy is expected to be in the range 1-5msec.

Testing made using Bluetooth communication between the Chest unit and a computer showed that the link introduced a delay variation in the range 0-250msec. To compensate for this a timestamp is added to each measurement. The chest unit has a local timer and a timestamp is added before sending to the computer. This solution has good accuracy for inter sample timing. In order to obtain an absolute accuracy, the local timer needs to be synchronized with the computer clock. The current synchronization algorithm does a single handshake during connection, this algorithm does not compensate for the delay in the messages. The result is an uncertainty in the absolute accuracy in the range 0-250ms. There are currently no specific requirements for the absolute accuracy, the minimum required accuracy will be investigated and added to D3.4. These requirements will be implemented in the final version of the HSS Controller.

[1] http://www.bluetooth.org/Technical/Specifications/adopted.htm

The delay variation for the Bluetooth Smart communication between IMU sensor unit and a computer has not been yet tested, however it is expected to be better than the delay variation measured for the Chest unit. The current implementation adds timestamp when sensor data arrives at the computer. The relative delay between samples will be low, however the absolute accuracy will not be better than the delay characteristics of the Bluetooth Smart link. This will be tested during setup of the system and test results will be presented in D3.4.

2.2 Chest Unit

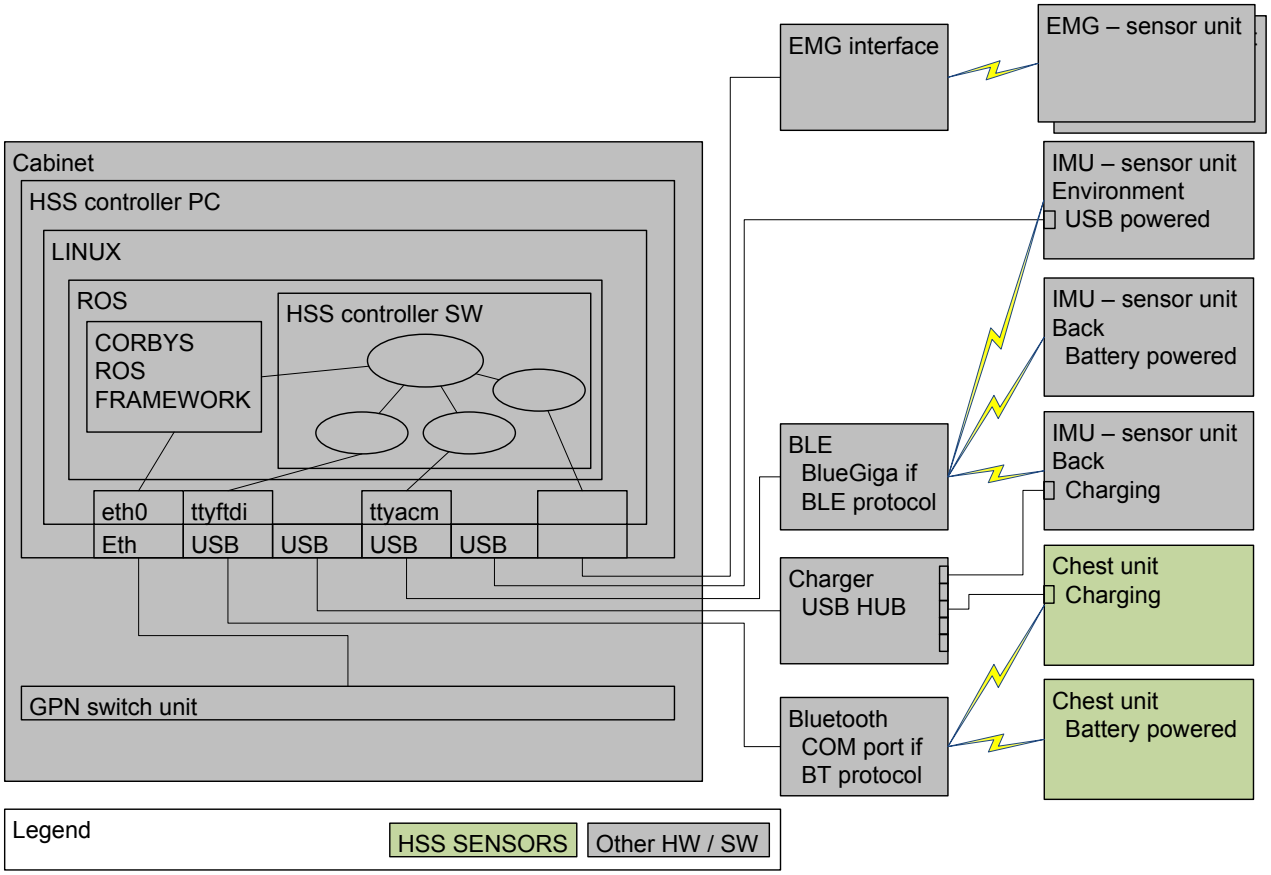

Figure 6: Chest unit in Human Sensory system

The Chest Unit shown in green in Figure 6 is used for measuring ECG, heart rate, temperature at the chest of the patient. In addition it can measure acceleration and rotation of the patient.

The Chest Unit and the belt are connected by a mechanical and electrical connector device. The majority of electronics, as well as radio and battery are to be hosted in the Chest Unit. The belt contains contact electrodes for heart rate measurements and ECG.

The Chest Unit is manufactured in a rugged plastic material, and is designed without any sharp edges. It is protected against splash water and entry of foreign objects, but it is not designed to be immersed in water, see Figure 7.

The Chest unit integrates both activity and physiological sensors in the same device. A 3-axis accelerometer is used to detect activity; and a 3-axis gyroscope used for measuring rotation. Both the accelerometer and gyroscope raw data are provided as part of the HSS dataset to the cognitive modules. Skin temperature is measured by an infrared (IR) sensor. Heart rate measurement is based on detection of electrical signals from the heart measured on the skin. Extraction of heart rate from the complex analogue signals is performed in the digital domain by the chest unit processor system. Power is provided by a rechargeable battery, and

components are selected for minimum power consumption. Wireless communication is using the Bluetooth SPP protocol stack.

Figure 7: Belt with Chest unit sensor.

Microcontroller software is based on the real-time kernel µC/OS-II, and optimized for low power consumption by putting microcontroller and radio into sleep mode when idle. Sensors are read at regular intervals, and data is transmitted using Bluetooth, avoiding requests from the client application. To ease sensor data analysis, a Java based monitoring application for recording and visualization of sensor data is developed and shown in Figure 8.

The main development of the Chest Belt and Chest Unit has been done by SINTEF in a project called ESUMS[2]. However, the embedded microcode has been enhanced to fit the usage in the CORBYS project providing more sensor data at a better timing accuracy to the cognitive system than required for use in the ESUMS project.

- Gyroscope functionality has been added.
- The sample rate has been increased from 300ms to 52ms better follow the movement of the patient.
- The wireless data rate has been doubled compared to previous versions.
- The resolution of the sample timestamps has been increased from 1seconds up to 4 milliseconds.

[2] ESUMS, http://www.sintefannualreport.com/2011/en/with-your-heart-in-his-hands/

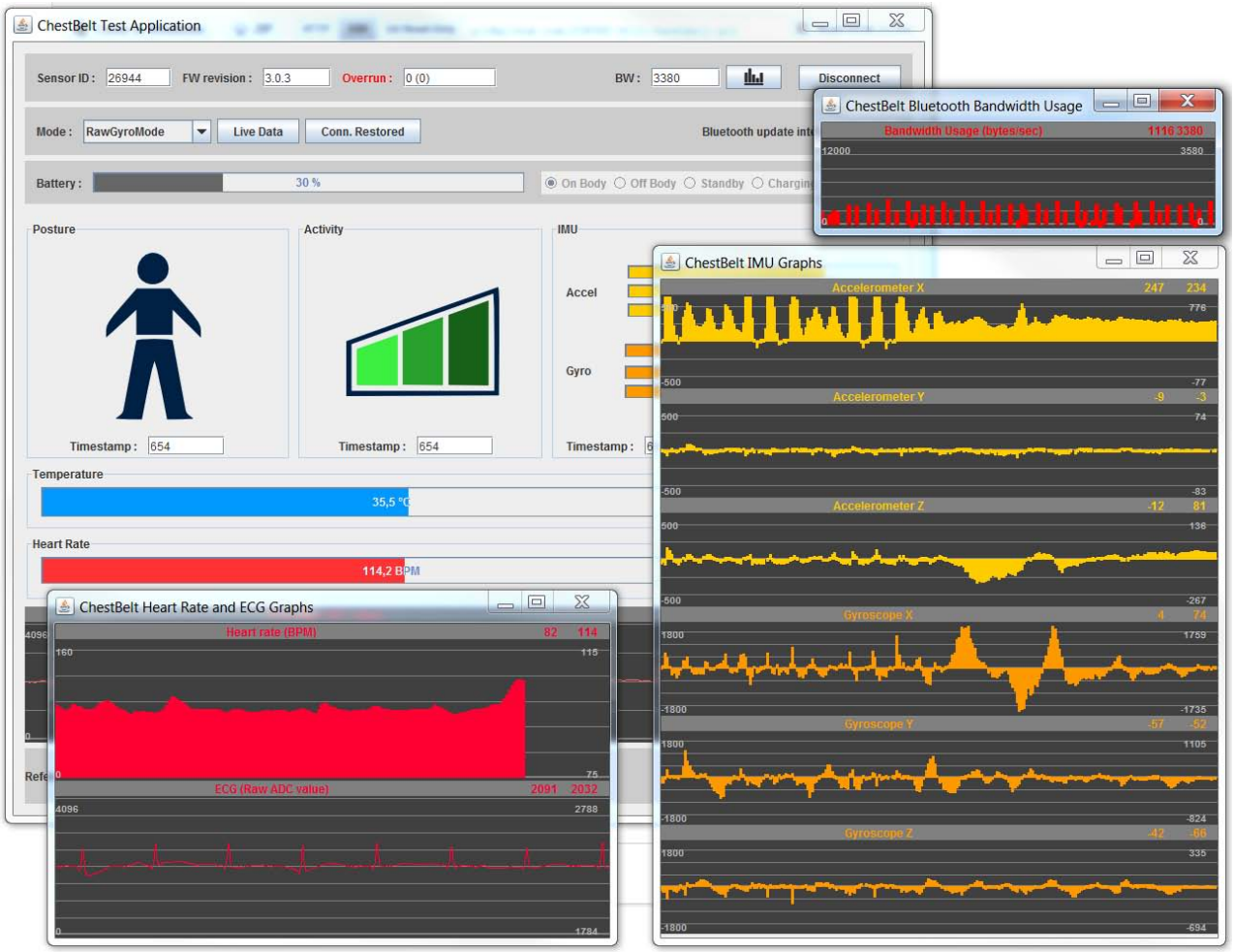

Figure 8 A screen dump of the Java application receiving sensor data from Chest unit.

2.2.1 Chest Unit Test

The Chest Unit has been thoroughly tested in lab by SINTEF and externally towards reference systems before use in the CORBYS project. Hence only the modified configuration is tested in the CORBYS project. This covers:

- Gyroscope
- Raw accelerometer data
- Time stamping
- Higher Bluetooth data-rates

2.2.1.1 Gyroscope

The gyroscope has been tested with respect to static rotation using a turntable. This has been used to verify scaling of the outputs and rotation axis. The combined message with gyroscope and accelerometer data introduced in CORBYS has been verified towards the Java application at the PC. Visual inspection of the graphs has been done as a check of data usefulness with respect to body movements.

2.2.1.2 Raw accelerometer data

Raw accelerometer data has been provided and tested before the use in CORBYS, but then at a lower rate of 300 milliseconds. The rate is increased to 52 milliseconds for CORBYS as requested by the cognitive partners to be able to detect gait movements. A regression test of the accelerometer functionality with activity and posture algorithms has been performed. The new combined message with gyroscope and accelerometer data has been tested towards the Java application at the PC. Visual inspection of the graphs has been done as a check of data usefulness with respect to body movements.

2.2.1.3 Timestamping

The enhanced timestamp resolution has been tested by analysing log files created at the computer side. The information has been compared to the known sample rate for the different sensors. No deviations have been found.

2.2.1.4 Bluetooth delay variation

Test made using Bluetooth communication between Chest unit and a computer showed that the link introduced a delay variation in the range 0-250msec. To compensate for this a timestamp is attached to each measurement. The chest unit has a local timer used to add timestamp before sending to the computer. This solution gives an accuracy of relative timing between samples. In order to have an absolute accuracy, the local timer needs to be synchronized with the computer clock. The current synchronization algorithm does a single handshake during connect. This algorithm does not compensate for the delay in the messages used. The result is an uncertainty in the absolute accuracy in the range 0-250ms.

Test datasets with sensor data from the Chest Unit have been recorded using the Java monitoring application. Based on these datasets the delay variation has been analysed.

The figure below shows delay variation for a person standing. This gives a static distance for the communication path. This is also expected to be the case for the demonstrator I where the patient is attached to the powered orthosis and the Bluetooth interface to the HSS controller is placed on the mobile platform cabinet. The delay variation is given in milliseconds (one line per 10 milliseconds). The graph is based on a dataset containing 1500 message packets send over a period of one minute.

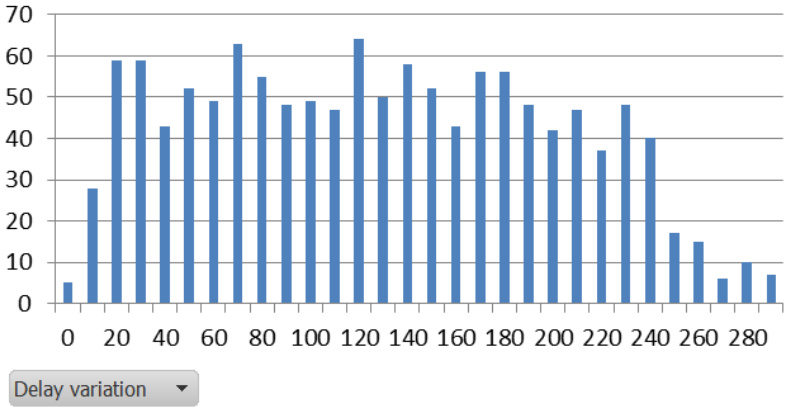

Figure 9 Test 1- Person standing
The graph shows the distribution of delay for 1500 packets. X-axis: Delay in milliseconds. Y-axis: Number of packets

The next figure shows a person walking in a corridor. The person is starting and stopping. The computer is not moved with the patient. Here some longer delays show up. This is probably due to some retransmissions. The graph is based on a dataset containing 2200 message-packets send over a period of two minutes.

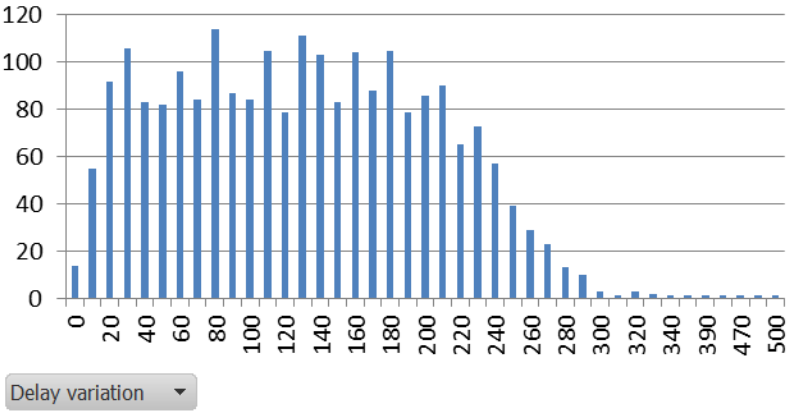

Figure 10 Test 4 - Person walking
The graph shows the distribution of delay for 2200 packets. X-axis: Delay in milliseconds. Y-axis: Number of packets

2.2.1.5 Bluetooth transfer rate

When enabling raw data at higher data rates there were a concern whether the data were above the practical Bluetooth transfer rate. From previous projects SINTEF had experienced large variations related to CPU load on the computer. Different brands of Bluetooth dongles had also shown different performance. We chose to use a dongle from TARGUS and a dongle from Roving. The TARGUS dongle has the Bluetooth protocol stack running on the computer while Roving has an external protocol stack running on a processor inside the dongle. Running an external protocol stack offloads the computer and makes the communication more robust with respect to CPU load on the computer.

A special test program was made generating a test sequence that could detect lost and duplicated data. The tests showed that it was possible to run at data rates of 7500 bytes/sec, but data loss was frequent. It also showed that the Roving dongle handled much higher data rates than the TARGUS dongle.

The goal to transfer 2000 bytes/sec was achieved by both dongles.

Test duration (sec)	Rate (bytes/sec)	Sequence length (bytes)	Device	Loss (sequence/sec)	Handshake	Comment
1580	**3750**	**15**	**Targus**	**0**	**No**	
46983	**3750**	**15**	**Targus**	**0,001**	**RTS**	
198	**5000**	**20**	**Targus**	**0,510**	**RTS**	

310	**5000**	**20**	**Targus**	**0,135**	**RTS**	
256	**5000**	**20**	**Targus**	**0,871**	**No**	
521	**5000**	**20**	**Targus**	**0,576**	**No**	
271	**7500**	**30**	**Targus**	**5,070**	**No**	
18388	**3750**	**15**	**Roving**	**0**	**RTS**	**Much other activity on computer**
68529	**5000**	**20**	**Roving**	**0**	**RTS**	**Much other activity on computer**
492	**5000**	**20**	**Roving**	**0**	**RTS**	
253	**7500**	**30**	**Roving**	**1,273**	**RTS**	

Table 2 Bluetooth bandwidth measurement results

2.3 IMU Sensor Unit

The IMU sensor is used in two settings in the CORBYS Demonstrator I system, connected to the Chest Belt on the back of the patient, and on the mobile platform for measuring environment humidity and temperature.

2.3.1 IMU Sensor Back unit

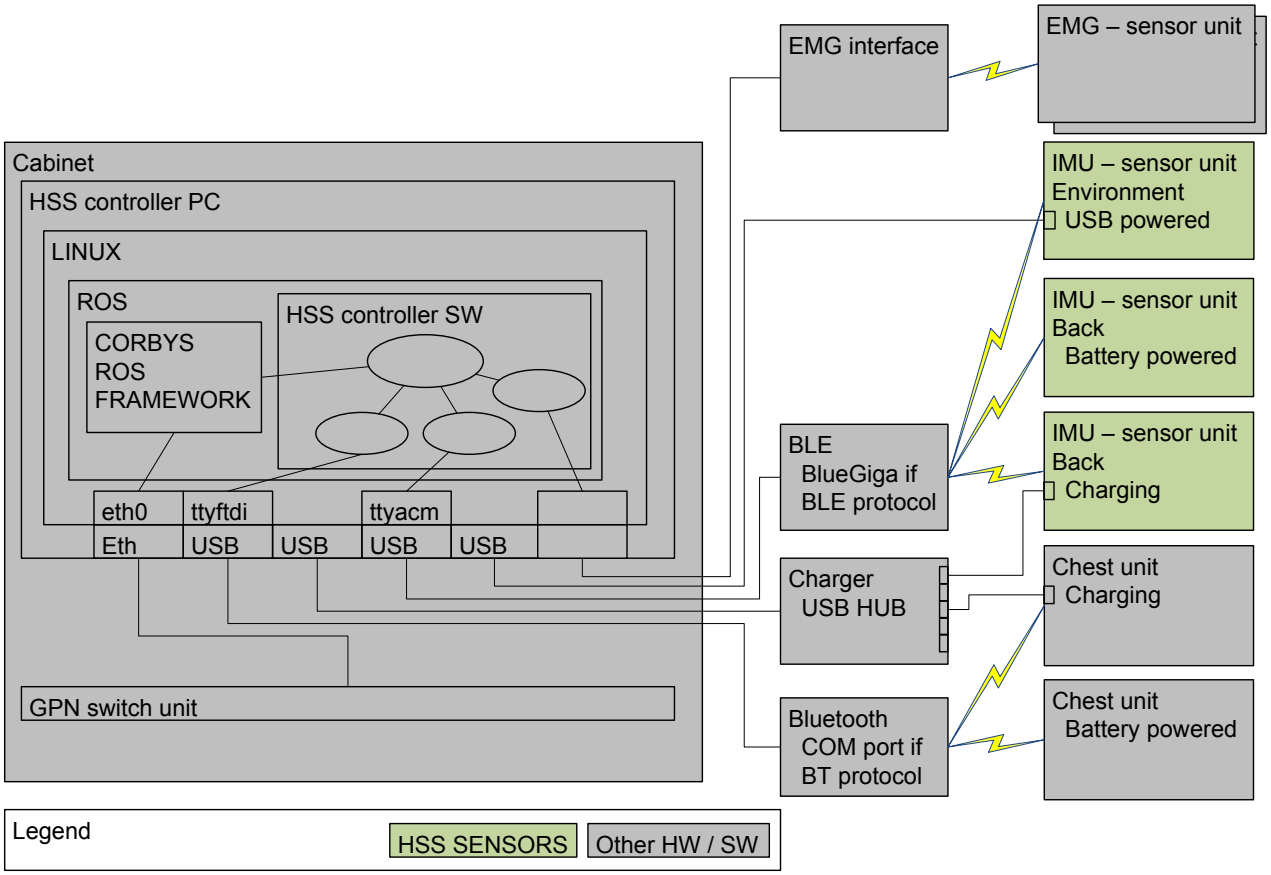

Figure 11: IMU sensor unit in Human Sensory system

The IMU sensor is used for humidity and IMU measurements on the patient back and for environment temperature measurements. The development for the IMU sensor was started in an internal SINTEF project called TRÅLE [Liverud et all, 2012]., however most of the firmware development and device manufacturing were done in the CORBYS project. The following sections give a technical description of the implementation of the sensor unit, including basic application and user information.

The IMU sensor unit shown in Figure 12 integrates both activity and physiological sensors in the same device. A combined 3-axis accelerometer and gyroscope, in addition to a magnetometer, form an inertial measurement unit (IMU). Skin temperature is measured by an infrared (IR) sensor. Additionally, two I^2C ports are available for external sensors. In CORBYS usage, a combined humidity/temperature sensor is fitted measuring the humidity at the patient back. Power is provided by a rechargeable battery, and components are selected for minimum power consumption. Wireless communication is by the new Bluetooth Smart

technology, previously called Bluetooth Low Energy. This is a feature of the Bluetooth 4.0 standard, providing low latency, low power short range communication. Profiles are defined for sensor values like temperature and heart rate; allowing Smartphones or other devices to receive data without proprietary drivers. The Bluetooth Smart technology is included in the Continua Health Alliance design guidelines[3].

Figure 12: The IMU sensor unit without and with enclosure, measuring 54x34x15 mm.

Microcontroller software is based on the real-time kernel µC/OS-II, and optimized for low power consumption by putting microcontroller and radio into sleep mode when idle. Sensors are read at regular intervals, and data transmitted using the Bluetooth Smart attribute indicate operation, avoiding requests from the client application. To ease sensor data analysis, a Java based monitoring application for recording and visualization of sensor data is developed and shown in Figure 13.

[3] http://www.continuaalliance.org/products/design-guidelines.html

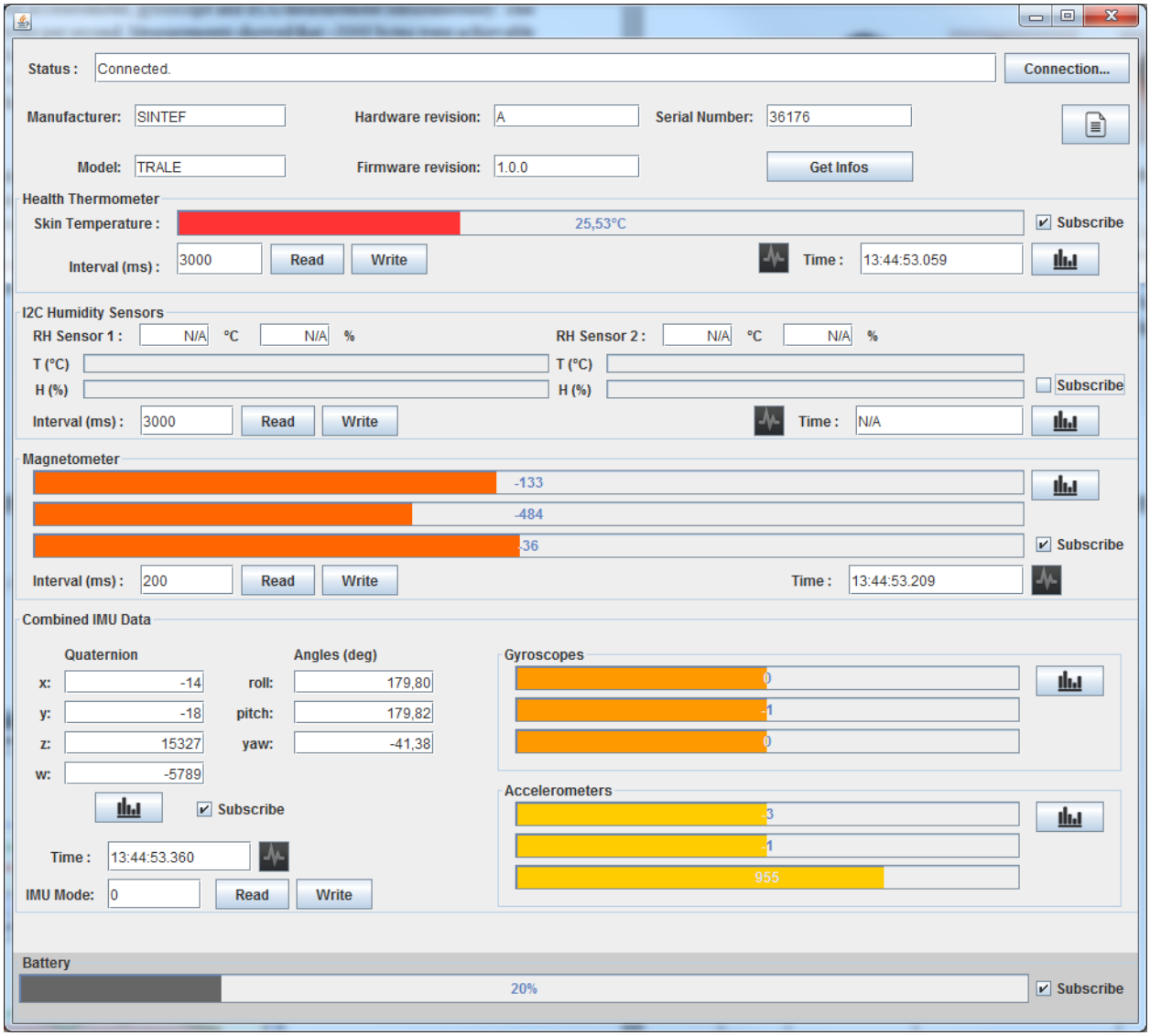

Figure 13: A screen dump of the Java application receiving sensor data from IMU sensor unit.

2.3.2 IMU Environment humidity and temperature sensor unit

A special version of the IMU is used for measuring environment temperature and humidity. These measurements are needed as a reference value for calculating the humidity at the patient.

The unit is mounted on the mobile unit and connected to the HSS controller using a USB cable. The external sensor, voltage regulator and the IMU unit is embedded into a small box.

- The external sensor is the same type that is used for IMU located on the patient's back.
- Voltage regulator is used for providing power from the USB plug to the external sensor and the IMU environment unit. The IMU unit will not have any battery to avoid procedures for charging the unit. The unit will be operating as long as the HSS controller computer is running.
- All parts are integrated into a single box to avoid cabling between multiple boxes.

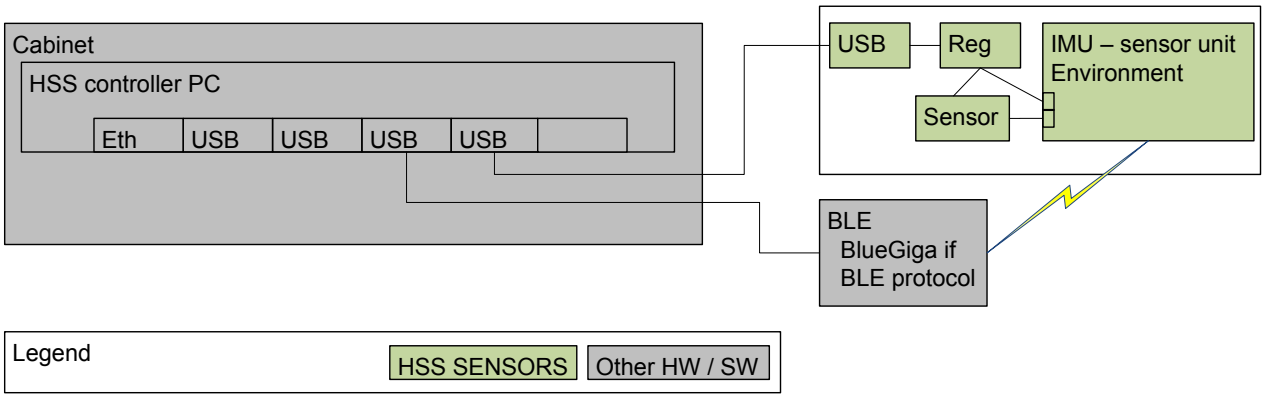

Figure 14: IMU environment sensor unit internals

The wireless interface is the same as for IMU back sensor unit. The IMU unit may be enabled providing movement information for the mobile platform.

2.3.3 IMU Sensor Unit Test

The IMU sensor is currently in an internal design verification test where all features are tested against specifications. The planned tests are listed in Table 3

ID	*Module*	*Test description*
B1	Battery	From completely empty battery, charge battery. Measure charging time. Record charging curve from console printout
B2	Battery	From fully charged battery, measure usage time for measuring IR temperature and dual humidity sensor before battery empty. Record data using IMU Sensor Unit Java app and console
B3	Battery	From fully charged battery, measure usage time for measuring all sensors before battery empty. Record data using IMU Sensor Unit Java app and console

L1	LED	Test led at power on, off, charging, low battery – may change
BU1	Button	Push button for 3 seconds to switch on, similarly 3 seconds to switch off
BU2	Button	Short push to make unit start advertising
P1	Power usage	Measure standby current before and after running unit with all sensors (multimeter, average of 200 samples)
P2	Power usage	Measure current usage not transmitting any data
P3	Power usage	Measure current usage transmitting IR temperature and dual humidity sensors
P4	Power usage	Measure current transmitting data from all sensors
P5	Power usage	Test that the unit is automatically switched off after 5 minutes when not connected on Bluetooth.
H1	Humidity sensor	Compare humidity sensor readouts for humidity and temperature at low, medium and high humidity and compare results with Sensirion development kit[4] results. 1 second update rate.
IR1	Skin temperature	Compare IR temperature readout at 1 seconds readout interval with values from ESUMS Chest Belt, high, low and medium temperature.
M1	Magnetometer	Compare readout with other device - reference device to be specified
A1	Accelerometer	Test against g in x,y,z directions
G1	Gyroscope	Mount unit at stepper motor and compare readout with stepper-motor speed at various speeds
C1	Communication	Test max distance before communication lost
C2	Communication	Communication performance tested and presented at pHealth 2012 [Liverud et all, 2012].

Table 3. IMU sensor Unit design verification test

Tests have so far uncovered that battery charging and discharging does not work fully as intended and needs to be corrected. This will probably be corrected by an embedded firmware update for the IMU Sensor Unit. Full tests results will be provided in D3.4

[4] http://www.sensirion.com/en/products/humidity-temperature/humidity-sensor-sht21/

2.4 EMG sensors

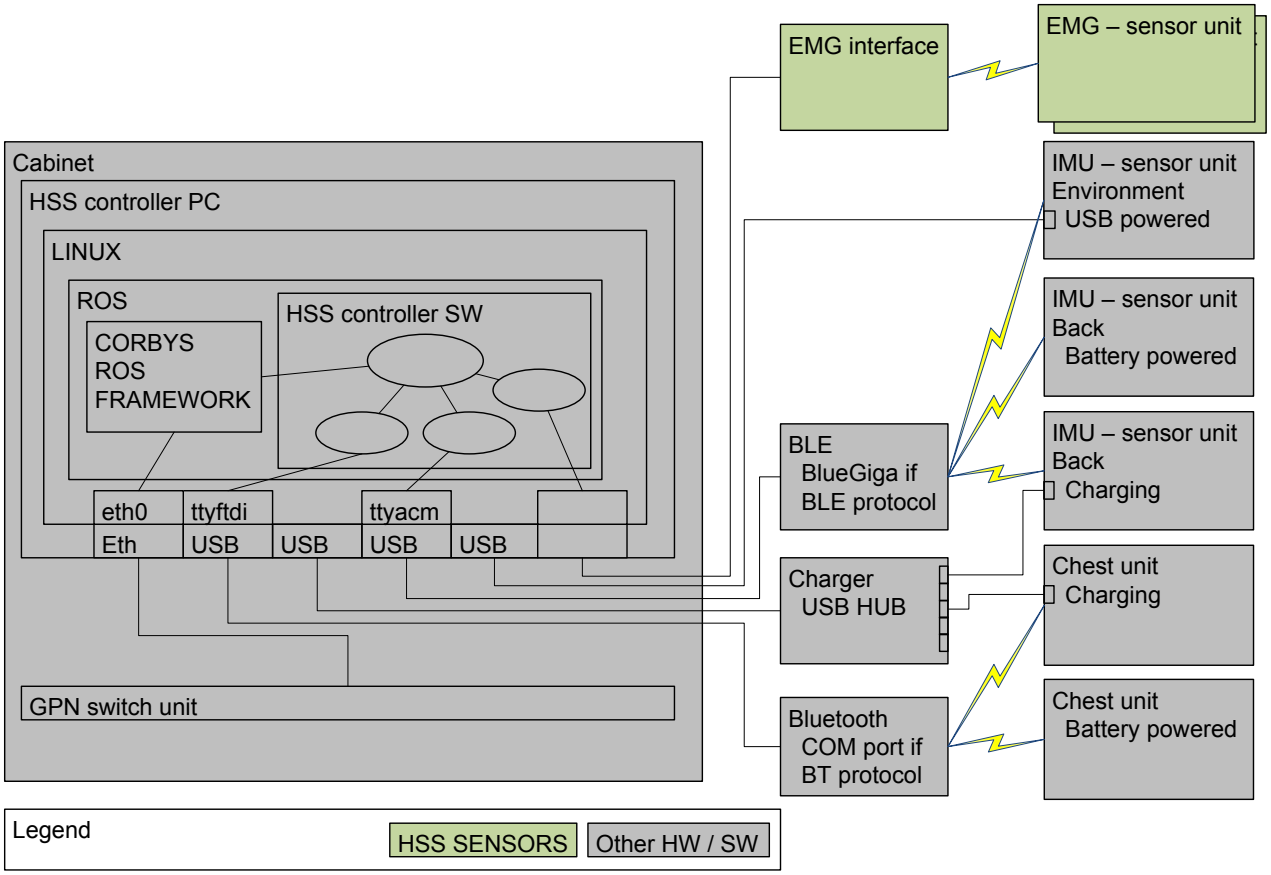

Figure 15: EMG sensors in Human Sensory System

The purpose of the EMG sensors is to measure the muscle activity of the patient. EMG will be measured on the thigh and calf of each leg. The CORBYS EMG system will be presented in D3.4 in month 26.

2.5 Human Sensory System controller

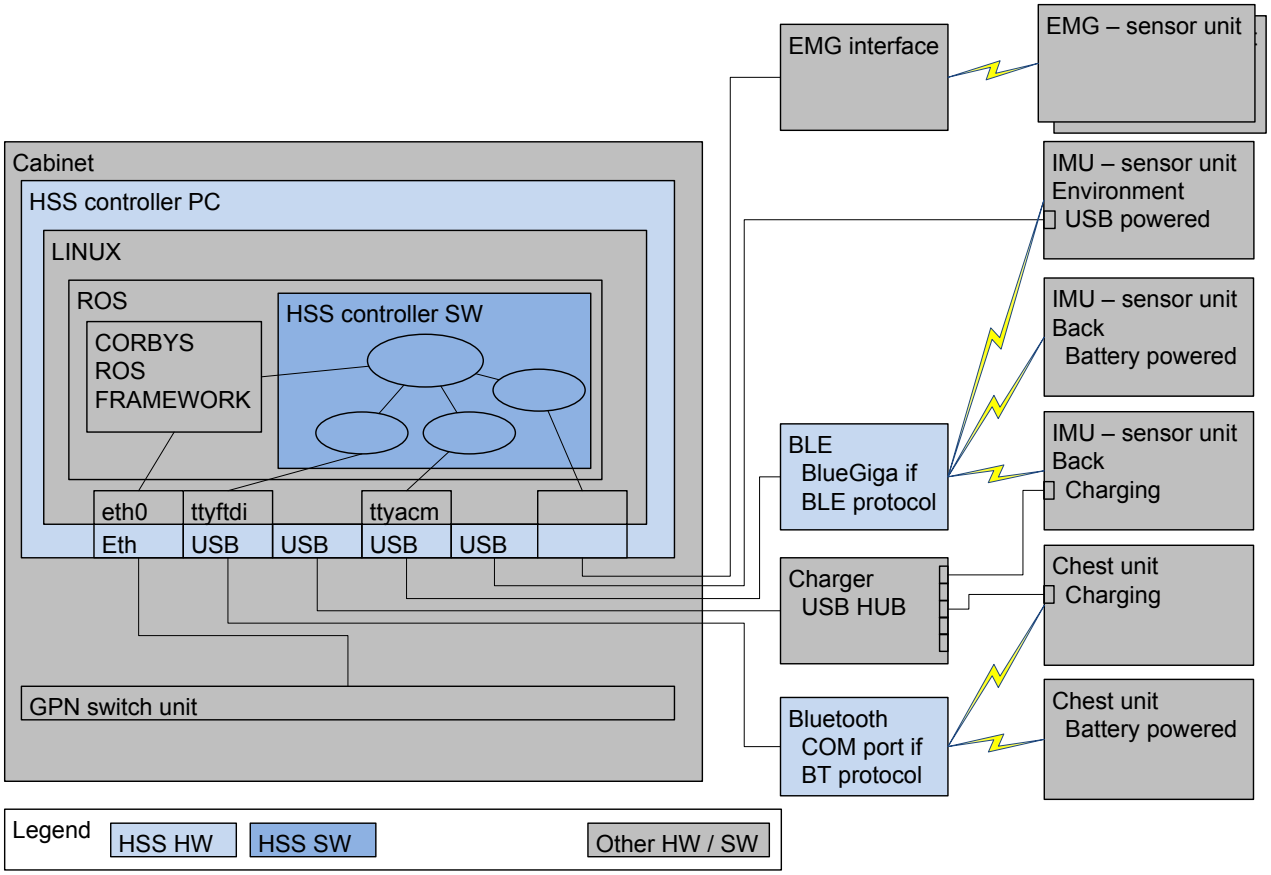

Figure 16: HSS controller in Human Sensory System

2.5.1 HSS Controller Hardware

The HSS controller software will be running on an industrial ruggedized Intel Atom based computer mounted in the Carrier Frame of Demonstrator I. At this point the HSS Controller Software is developed and tested in a VirtualBox virtual machine with a hard drive of 16GB and 2GB of allocated RAM.

2.5.2 CORBYS GPN and Robot Operating System (ROS)

The HSS Controller is one module of the overall CORBYS System (as described in deliverable D2.2). The integration between the different CORBYS modules is done through the CORBYS General Purpose Network (GPN). The CORBYS GPN is a standard TCP/IP network over Ethernet. To ease the integration of the different module the CORBYS system uses the Robot Operating System (ROS)[5] framework. The ROS framework runs on top of the operating system and TCP/IP network and provides standard ways to describe and publish both services and data in a distributed network.

ROS (Robot Operating System) provides libraries and tools to help software developers create robot applications. It provides hardware abstraction, device drivers, libraries, visualizers, message-passing, package management, and more. ROS is licensed under an open source, BSD license.

ROS facilitates communication between processes running on the same or on different machines. The communication between processes can take place either by a blackboard-style paradigm with publishers and subscribers, called Topics or in a server-client mode, called Services.

A ROS node is a process that performs computation and runs in a separate process, using a socket (IP address and port). Nodes are combined together into a graph and communicate with one another using streaming topics, remote procedure call (RPC) services, and the Parameter Server. These nodes are meant to operate at a fine-grained scale; a robot control system will usually comprise many nodes. For example, one node controls a laser range-finder, one node controls the robot's wheel motors, one node performs localization, one node performs path planning, one node provide a graphical view of the system, and so on.

The use of nodes in ROS provides several benefits to the overall system. There is additional fault tolerance as crashes are isolated to individual nodes. Code complexity is reduced in comparison to monolithic systems. Implementation details are also well hidden as the nodes expose a minimal API to the rest of the graph and alternate implementations, even in other programming languages, can easily be substituted.

The ROS nodes of the CORBYS system are all running Ubuntu Linux version 10.04LTS 32bits and the Electric version of ROS. These choices are expected to provide a stable platform for the development and use of the CORBYS system. A set of common CORBYS ROS messages and topics have been defined and allow for the integration between the HSS Controller and the cognitive modules.

2.5.3 HSS Controller setup and operating system

Figure 17 details the installation steps for setting up the HSS controller. The first step is a standard installation of Ubuntu Linux. A single user account is setup on the HSS Controller:

Login: hsscontroller - Password: corbys

The next installation step installs some required packages and security updates from Ubuntu repositories.

[5] http://www.ros.org/wiki/

```
################################################################################
# This script describes the steps to setup the HSS Controller.
################################################################################

# Install Ubuntu 10.04 LTS from the iso image
# Install all updates
# Install packets for git, svn, ssh, Java and Maven2 (for hss controller JAVA debug UI)

sudo apt-get install subversion default-jdk eclipse openssh-server maven2 git-core

################################################################################
# Install ROS
################################################################################
sudo sh -c 'echo "deb http://packages.ros.org/ros/ubuntu lucid main" > \
/etc/apt/sources.list.d/ros-latest.list'
wget http://packages.ros.org/ros.key -O - | sudo apt-key add -
sudo apt-get update
sudo apt-get install ros-electric-desktop-full
echo "source /opt/ros/electric/setup.bash" >> ~/.bashrc
. ~/.bashrc
mkdir ~/ros_workspace
echo "export ROS_PACKAGE_PATH=~/ros_workspace:\$ROS_PACKAGE_PATH" >> ~/.bashrc
echo "export ROS_WORKSPACE=~/ros_workspace" >> ~/.bashrc
. ~/.bashrc
echo $ROS_PACKAGE_PATH

################################################################################
# Install QT 4.8.1
################################################################################
# Download "QtSdk-online-linux-x86-v1.2.1.run" from QT web page
mv /home/hsscontroller/Downloads/QtSdk-online-linux-x86-v1.2.1.run /opt/
cd /opt
chmod u+x QtSdk-online-linux-x86-v1.2.1.run
./QtSdk-online-linux-x86-v1.2.1.run

################################################################################
# Install QWT
################################################################################
# Download "qwt-6.0.1.zip" from qwt web page
cd /opt/
cp /home/hsscontroller/Downloads/qwt-6.0.1.zip .
unzip qwt-6.0.1.zip
cd qwt-6.0.1/
qmake
make
sudo make install
sudo su
# The following is required for the CORBYS_GUI to run
echo "/usr/local/qwt-6.0.1/lib" > /etc/ld.so.conf.d/qwt.conf
ldconfig

################################################################################
# Checkout CORBYS SVN CODE
################################################################################
svn checkout https://corbys.eu/svn/CORBYS
```

Figure 17 HSS Controller Installation Script

2.5.4 HSS Controller Software

This section describes the drivers and software parts of the HSS controller which makes the link between the sensor units and the CORBYS general purpose network. Figure 18 presents a high level view of the architecture of the HSS Controller software. The HSS software is composed of a set of driver components (on the left hand side of Figure 18) which manage the connection with individual sensors and of a front-end component which provides the interface of the HSS controller on the CORBYS GPN. The interface of the HSS controller is made of 3 ROS topics which have been defined in collaboration with other CORBYS modules. The Config_Data topic is a common topic for all modules and allows distributing the configuration of the CORBYS system to all its modules. The Heart_Beat topic is also used by all modules to publish status information at regular intervals. Finally the Sensor_Data_HSS topic is specific to the HSS Controller and used to publish the sensor data.

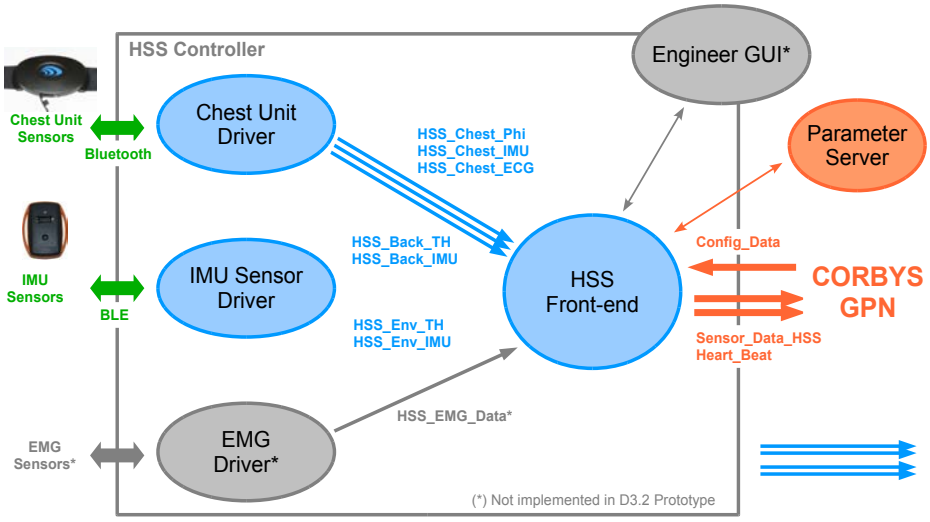

Figure 18 Architecture of the HSS Controller Software

Each component described in Figure 18 runs in its own process (ROS node) in the HSS controller in order to avoid having the failure of one component bring down the whole HSS controller. The communication between the drivers and the front-end component uses a set of ROS topics which publish the data received by the drivers. These ROS topics are internal to the HSS controller and should not be used by other CORBYS nodes. The HSS front-end receives the data from all drivers, performs some sanity checking on the data and forwards sensor data to the CORBYS Sensor_Data_HSS topic.

The following sub-sections describe the components of the HSS controller software.

2.5.5 Chest Unit Driver

Figure 19 presents the interfaces of the Chest Unit driver. In the initialization phase the driver needs to discover the chest units within range and read their battery status. Once a session is initialized the driver is connected to only one chest unit, collects the sensor data and publishes it on three separate ROS topics. These three topics were designed to bundle together the data with common update rates:

- 3 seconds for skin temperature, heart rate, posture and activity data. The battery status has been added to this message even if its actual update rate is around 30 seconds.
- 52ms for the IMU data (accelerometers and gyroscopes).

- 32ms for 8 samples chunks of ECG data which has an update rate of 4ms. At this stage chunk of 8 samples seems to be a good trade-off between bandwidth and latency. It might be adjusted if required by the nodes using the data.

On the sensor side the chest units are connected to the HSS controller via Bluetooth using the Serial Port Profile (SPP). The SPP is supported by recent Linux kernel modules but turned out to be unstable in Ubuntu 10.04LTS. To avoid any instability the HSS controller is setup to use an external Bluetooth adapter which implements its own Bluetooth stack as well as the SPP. The chosen adapter is a BlueSMiRF Bluetooth modem which is based on a Roving Networks Bluetooth module[6]. The HSS controller communicates with the Bluetooth using a standard serial interface.

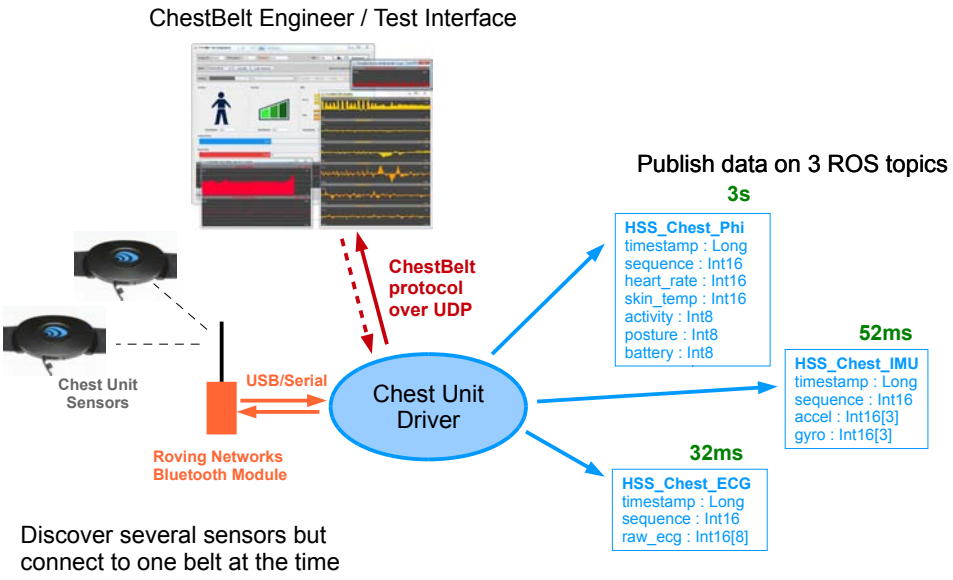

Figure 19 Interface of the Chest Unit Driver

For testing and debugging purposes, a graphical user interface can be connected to the Chest Unit driver. This graphical interface communicates with the driver over UDP which allows executing it either locally on the HSS Controller or remotely on a separate computer. This interface mainly displays and logs the data coming from the sensor. It might also be used to send commands to the sensor for debugging purposes. This functionality will be disabled in the deployed HSS Controller in order to avoid conflicting commands reaching the sensors.

[6] https://www.sparkfun.com/products/158

Figure 20 presents the architecture of the Chest Unit driver and shows the three main part of the driver: the operating system part, the Chest Unit driver and the testing GUI respectively.

On the operating system side (bottom of Figure 20), the Bluetooth module is connected to the HSS Controller via a FTDI USB to TTL serial chip. The Linux kernel includes a driver for the FTDI chip and recognizes it is a standard serial port. By default the device is automatically mounted and provided with a device handle named /dev/ttyUSBX where X varies. In order for the Chest Unit driver to always be able to connect to the right device we have used the Linux UDEV service in order to automatically create a symbolic link with a fixed name whenever the specific FTDI chip is connected. Figure 20 presents the UDEV rule added to create a link from /dev/bluesmirf to the appropriate device. This rule includes the serial number of the FTDI chip used with the Bluetooth module. This serial number should be changed to match the actual chip being used on the HSS Controller. The /dev/bluesmirf can be used as a standard serial port with an 115200 baud rate, 8 data bits, 1 stop bit and no parity (8N1). Hardware flow control is supported all the way from the computer to the FTDI chip, Bluetooth module and Bluetooth SPP.

The Chest Unit driver itself consists of four main components (blue in Figure 20):

- The Roving Network AT / Serial driver. This component manages all the communications with the serial device. It uses AT commands to interact with the Bluetooth stack of the module when no sensor is connected, and it decodes serial packets coming from the sensor once a connection has been established. It provides a simple API for discovering and connecting to Bluetooth devices, and allows sending and receiving packets to the Chest Unit.

- The Chest Unit Driver encodes and decodes serial packets according the Chest Unit protocol. It provides an API to configure the Chest Unit and receive the data from its different sensors.

- The ROS Publisher uses the Chest Unit driver to subscribe to the sensor data and forward the data on to the HSS Controller internal ROS topics.

- The UDP GUI Server is implemented for debugging purposes. It forwards the data exchanged on the serial port to a UDP socket. A test application can be connected to display the sensor data.

All these components are modelled using the ThingML languages[7] which allow automatically generating C/C++ implementations for Linux and ROS packages.

[7] http://www.thingml.org

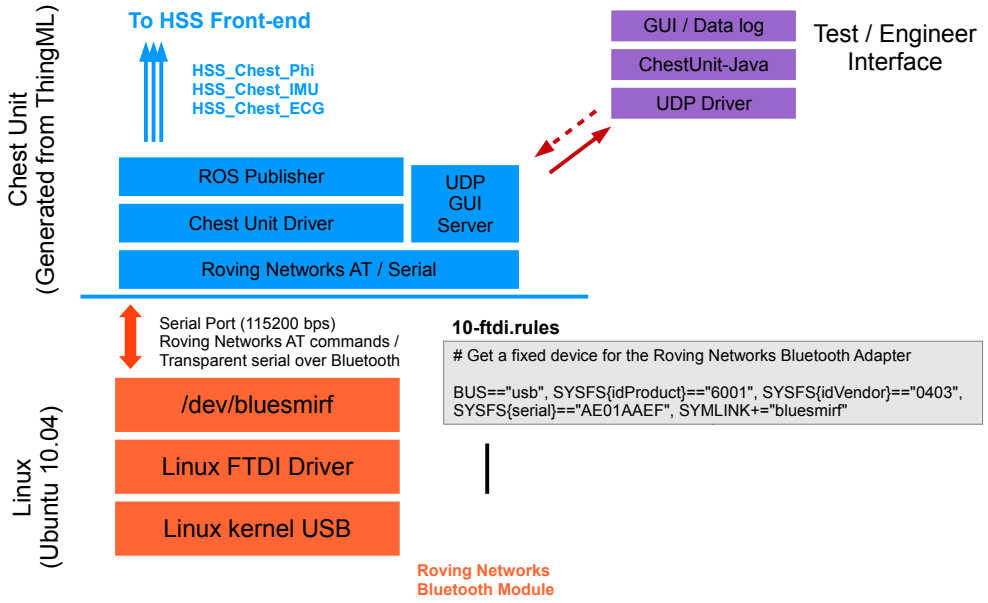

Figure 20 Architecture of the Chest Unit Driver

The test and engineer interface on the top right corner of Figure 20 is a Java application which implements its own driver and GUI for the Chest Unit sensors. It can be connected locally or remotely to the HSS Controller Chest Unit module in order to visualize the low level communications with the sensors. Since the debug application implements its own driver for the Chest Unit, this allows comparison of the data provided by the debug application and the data forwarded on the ROS topic, which in turn enables validation of the implementation of the HSS Controller driver.

2.5.6 IMU Sensors Driver

The structure and design of the IMU sensor driver is similar to the Chest Unit driver. Figure 21presents an overview its architecture.

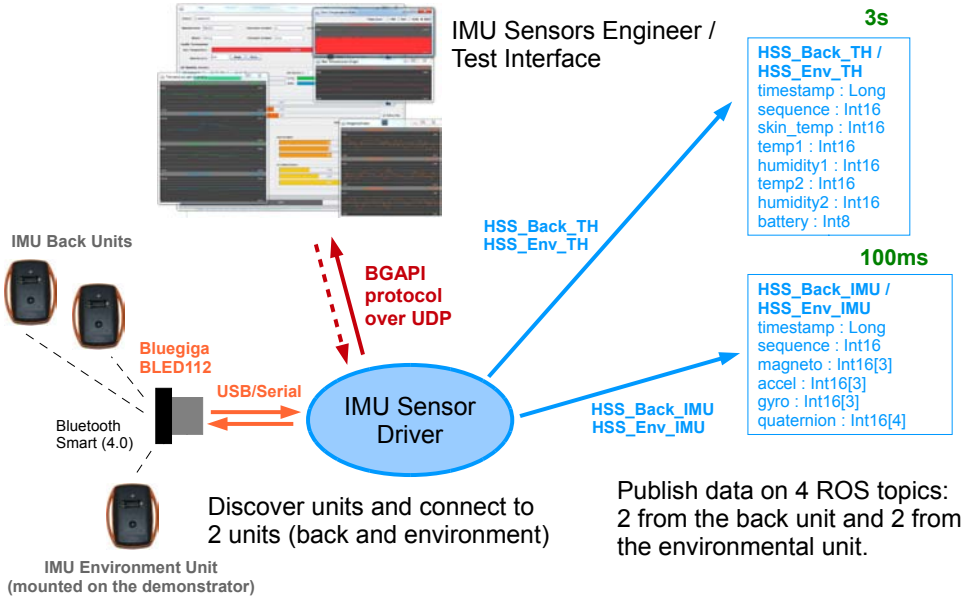

Figure 21 Interface of the IMU Sensor Driver

The IMU Unit sensors use the Bluetooth Smart 4.0 protocol for which no support is available in Linux. To communicate with the sensors, the HSS Controller uses an external Bluetooth Smart 4.0 module which implements the protocol stack and provides and API over a USB virtual serial port. The chosen module is a Bluegiga BLED112 USB dongle[8].

The IMU Sensor driver connects to two different IMU sensors. One is mounted on the back of the chest belt of the patient, and the other is mounted on the CORBYS demonstrator mobile platform and used as an environmental sensor. The environment device is a single unit which has an address that can be hard coded in the HSS Controller. The back unit is one of several units available for training sessions and needs to be discovered and configured in the initialization phase of each training session. At least two units need to be available in order to be able charge one while the other is being used on a patient.

The IMU Sensor driver outputs data on 4 different topics: 2 topics for the environment unit and 2 for the back unit. The topic messages have been designed to group together data which have common update rates:

- 3 seconds for the temperature and humidity measurements and the battery status. The temp2 and humidity2 value are currently not populated in the CORBYS demonstrator but provided for future

[8] http://www.bluegiga.com/BLED112_Bluetooth_low_energy_dongle

applications. The skin temperature for the environment unit is not meaningful in the context of the demonstrator since the sensor is mounted on the chassis of the demonstrator.

- 100 ms for the IMU data. This value might be adjusted in order to cope with the Bluetooth Smart bandwidth limitations. The current implementation provides all IMU data (raw accelerometer, gyros and magnetometer data as well and fused attitude data from the accelerometers and gyros as a quaternion).

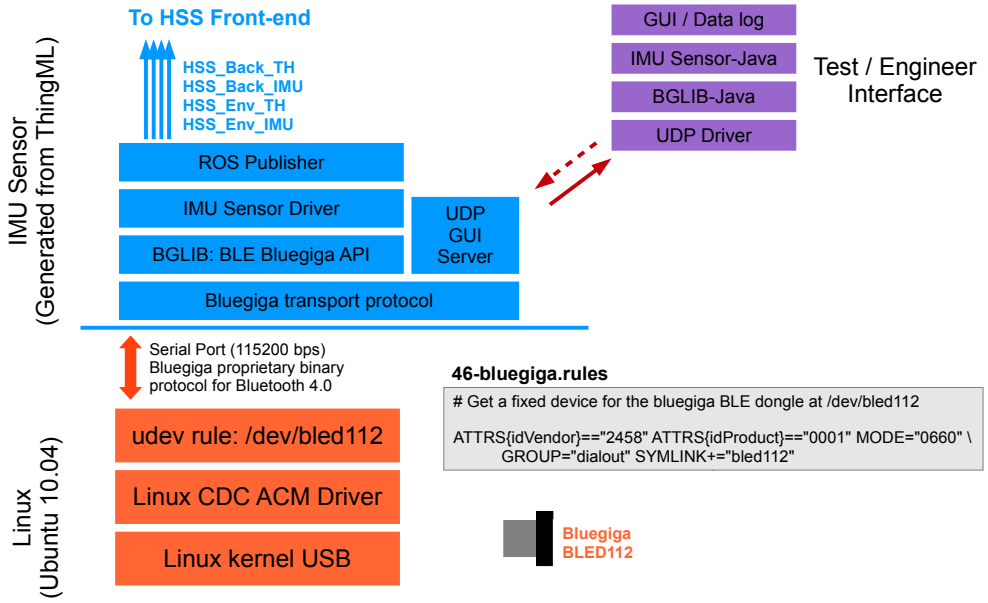

Figure 22 Architecture of the IMU Sensors Driver

Figure 22 presents the structure of the IMU sensor driver. The bottom part of the figure represents the operating system drivers which link to the BLED112 dongle. The BLED112 dongle implements an USB CDC ACM driver which is recognized by the Linux kernel as a virtual serial port and automatically mounted as a /dev/ttyACMX device (X varies depending on the number of devices plugged to the computer). In order to get a fixed device inode, the HSS controller uses a custom UDEV rule which creates a /dev/bled112 symbolic link for the BLED112 dongle. The UDEV rule is generic for all BLED112 dongles and assumes that only one is plugged to the HSS Controller. In case several dongles need to be used specific rules which include the serial numbers of the dongles should be created. The /dev/bled112 devices is a standard virtual serial port with a 115200 baud rate, 8 data bits, 1 stop bit and no parity (8N1). The BLED112 dongle uses a proprietary packet based protocol over this serial link.

The implementation of the IMU Sensor driver is composed of four layers and a UDP GUI server which is used for diagnosis and debugging purposes. These five components are modelled using the ThingML languages and the C/C++ and ROS implementation code is automatically generated:

- The Bluegiga transport protocol manages the connection with the /dev/bled112 device and sends and receives packets conforming to the Bluegiga proprietary protocol.

- The BGLIB layer provides an API to interact with the Bluetooth Smart stack of the BLED112 dongle. API commands are transformed to packets to be transmitted to the dongle and incoming packets coming from the dongle are decoded and forwarded as messages (or callbacks) the layer above.

- The IMU Sensor driver uses the Bluetooth Smart API provided by the BGLIB layer and implements the specific services provided that the IMU Sensor Unit. It provides a specific API to the layer above which allow connecting to IMU Sensor units, subscribing to the different sensors it contains and collecting sensor data.

- The ROS publisher is the top layer of the stack. It subscribes to data from the two IMU Units to use for a training session and forwards the sensor data on the HSS Controller as ROS topics.

The test and engineer interface on the top right corner of Figure 22 is a Java application which implements its own driver and GUI for the IMU Unit sensors. It can be connected locally or remotely to the HSS Controller IMU Sensor driver in order to visualize the low level communications with the BLED112 dongle. Since the debug application implements its own driver for the Bluegiga protocol and IMU Sensor, comparing the data provided by the debug application and the data forwarded on the ROS topic allow validating the implementation of the HSS Controller driver.

2.5.7 EMG Sensors Driver

Not implemented as part of D3.2. Once the EMG sensor will be selected a specific driver will be implemented to provide the sensor data internal HSS ROS topics (in the same way as other sensors).

2.5.8 HSS Controller Front-End and ROS Interface

The role of the HSS front-end is to collect all the data coming from the sensors and provide this data on the CORBYS general purpose network using the SensorData_HSS ROS topic. The sensor data on this topic is represented using a common CORBYS format which is used by all CORBYS modules.

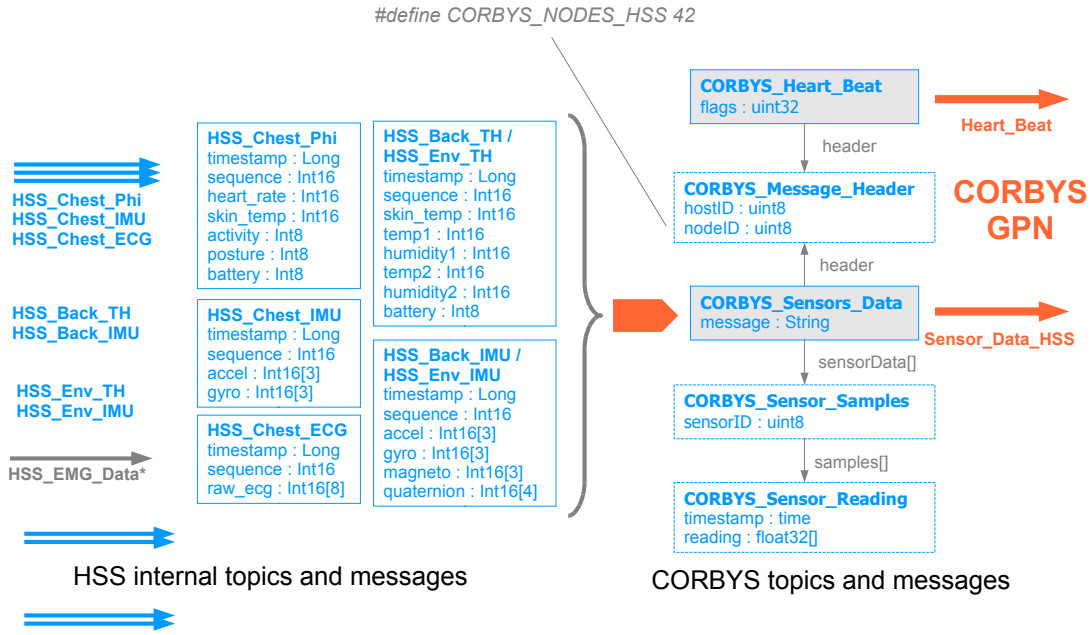

Figure 23 From the Internal topics to the CORBYS topics

Figure 23 presents the ROS messages used by the HSS Controller front-end. The left hand side of the figure presents the ROS messages provided by the sensor drivers. These messages are specific to each individual sensor and use the data types provided by the sensor (no scaling or any other form of processing is done in the sensor driver nodes). The right hand side of the figure presents the structure of the ROS messages exchanged on the CORBYS GPN.

The CORBYS_Sensor_Data message is a generic structure which is designed to represent data coming from all the different sensors. Each message is composed of a header which provides the origin of the data, and a set of sensor samples. Each sensor sample corresponds to a specific sensor ID and can contain a set of sensor readings. Each reading has a timestamp and a set of sensor data represented as 32bit floating point numbers. This structure allows representing in a single message data coming from different sensors as well as several sets of readings for a single sensor.

2.5.8.1 HSS Controller data interface

The HSS Controller main functionality is to collect the data from the different sensors and publish it on the Sensor_Data_HSS topic. The front-end receives the raw data from the sensors, the data needs to be processed, scaled and converted to a set of 32bit floats which can be provided to the CORBYS topic.

Other CORBYS nodes should not subscribe to the HSS internal topics but only to the HSS_Sensor_Data topic.

Several alternatives can be used to define the sensor IDs on the Sensor_Data_HSS topic:

- One Sensor ID per individual sensor value. This option leads to a large number of sensors (about 24 without the EEG sensors). Since many sensors are sampled at the same rate this requires to duplicate many timestamps in the output messages.
- One Sensor ID per physical sensor unit. This option allows reducing the number of sensors to the minimum, but is impractical because the sensors of a single unit have different sampling rates, which means that not all data can be populated for each update.
- One Sensor ID per HSS internal topic. This is the solution which was chosen because it minimizes the required bandwidth on the CORBYS network (no duplication of timestamps and no missing data).

Message	SensorID	HSS Sensor Data Reading Format (float32[])	Size	Rate(ms)
HSS_Chest_Phi	0xA1 (161)	[heart_rate, skin_temp, activity*, posture*, battery]	5	3000
HSS_Chest_IMU	0xA2 (162)	[accel_x, accel_y, accel_z, gyro_x, gyro_y, gyro_z]	6	52
HSS_Chest_ECG	0xA3 (163)	[ecg1, ecg2, ecg3, …, ecg8]	8	32
HSS_Back_TH	0xA4 (164)	[skin_temp, temp1, humidity1, temp2*, humidity2*, battery]	6	3000
HSS_Back_IMU	0xA5 (165)	[ax, ay, az, gx, gy, gz, mx, my, mz, qw, qx, qy, qz]	13	100
HSS_Env_TH	0xA6 (166)	[skin_temp*, temp1, humidity1, temp2*, humidity2*, battery]	6	3000
HSS_Env_IMU*	0xA7 (167)	[ax, ay, az, gx, gy, gz, mx, my, mz, qw, qx, qy, qz]	13	100
HSS_EMG_*	0xAx*	?	?	?

Figure 24 Data format on the CORBYS Sensor_Data_HSS topic

Figure 24 presents how the data from the internal sensor topics is provided in CORBYS_Sensor_Samples as well as the sampling rate of each sensor. Variables marked with a * are currently not populated or populated with a non specified value, and hence should not be used at this point.

The amount of data generated by the HSS controller sensors will use some bandwidth on the CORBYS GPN. As an early estimation of the required bandwidth: given the size if the messages and their sampling rate the required bandwidths are 2.53kByes/s to transmit the sensor data and 3.32kBytes/s when taking headers and timestamps into account. The overhead of the ROS framework might require some additional bandwidth; however these numbers seem reasonable and should not pose any problem to the CORBYS GPN.

Subscribers to the Sensor_Data_HSS topic should use the IDs provided in Figure 24 (and the corresponding macros in the CORBYS_Common source folder) to decode the data according to the specified sensor reading format.

Name	Internal Topic	Internal Type	Scaling	Unit	Mininum	Maximum	Resolution	Accuracy	Notes
heart_rate	HSS_Chest_Phi	Int16	0,1	BPM	25	230	0,1	1	
skin_temp	HSS_Chest_Phi	Int16	0,01	°C	20	40	?	0,1	
activity*	HSS_Chest_Phi	UInt8	?	?	?	?	?	?	Enumerated values
posture*	HSS_Chest_Phi	UInt8	?	?	?	?	?	?	Enumerated values
battery	HSS_Chest_Phi	UInt8	1	%	0	100	1	1	
accel_x	HSS_Chest_IMU	Int16	?	m/s²	?	?	?	?	
accel_y	HSS_Chest_IMU	Int16	?	m/s²	?	?	?	?	
accel_z	HSS_Chest_IMU	Int16	?	m/s²	?	?	?	?	
gyro_x	HSS_Chest_IMU	Int16	?	deg/s	?	?	?	?	
gyro_y	HSS_Chest_IMU	Int16	?	deg/s	?	?	?	?	
gyro_z	HSS_Chest_IMU	Int16	?	deg/s	?	?	?	?	
ecg[1..8]	HSS_Chest_ECG	Int16	?	mV	?	?	?	?	
skin_temp	HSS_Back_TH	Int16	0,01	°C	20	40	?	0,1	
temp1	HSS_Back_TH	Int16	0,01	°C	10	50	?	0,1	
humidity1	HSS_Back_TH	Int16	0,01	%	0	100	0,1	5	
temp2*	HSS_Back_TH	Int16	?	?	?	?	?	?	No Sensor
humidity2*	HSS_Back_TH	Int16	?	?	?	?	?	?	No Sensor
battery	HSS_Back_TH	UInt8	1	%	0	100	1	1	
skin_temp*	HSS_Env_TH	Int16	0,01	°C	20	40	?	0,1	No Meaning
temp1	HSS_Env_TH	Int16	0,01	°C	-10	50	?	0,1	
humidity1	HSS_Env_TH	Int16	0,01	%	0	100	0,1	5	
temp2*	HSS_Env_TH	Int16	?	?	?	?	?	?	No Sensor
humidity2*	HSS_Env_TH	Int16	?	?	?	?	?	?	No Sensor
battery	HSS_Env_TH	UInt8	1	%	0	100	1	1	
ax	HSS_[Back|Env]_IMU	Int16	?	m/s²	?	?	?	?	
ay	HSS_[Back|Env]_IMU	Int16	?	m/s²	?	?	?	?	
az	HSS_[Back|Env]_IMU	Int16	?	m/s²	?	?	?	?	
gx	HSS_[Back|Env]_IMU	Int16	?	deg/s	?	?	?	?	
gy	HSS_[Back|Env]_IMU	Int16	?	deg/s	?	?	?	?	
gz	HSS_[Back|Env]_IMU	Int16	?	deg/s	?	?	?	?	
mx	HSS_[Back|Env]_IMU	Int16	?	nT/m	?	?	?	?	
my	HSS_[Back|Env]_IMU	Int16	?	nT/m	?	?	?	?	
mz	HSS_[Back|Env]_IMU	Int16	?	nT/m	?	?	?	?	
qw	HSS_[Back|Env]_IMU	Int16	?	?	?	?	?	?	
qx	HSS_[Back|Env]_IMU	Int16	?	?	?	?	?	?	
qy	HSS_[Back|Env]_IMU	Int16	?	?	?	?	?	?	
qz	HSS_[Back|Env]_IMU	Int16	?	?	?	?	?	?	

Figure 25 HSS Controller sensor data specification

Figure 25 details the scaling applied to the raw data, the minimum and maximum value and the unit for all the individual sensor data published by the HSS Controller. As an indication the table also provides the resolution and accuracy of each sensor. The missing information in this table as well as the specification of the EEG data will be added in deliverable 3.4.

In the event of missing sensor data or invalid sensor data the HSS front-end will not output the corresponding data on the Sensor_Data_HSS topic. A common strategy for handling these cases should be defined for all CORBYS Sensor data topics. Solutions such as outputting zero data, or NaN (Not-a-Number) values in

combination with some flags could be used to keep populating the topics at the expected rate while clearly marking the data as abnormal.

2.5.8.2 HSS Controller status and flags

In addition to the Sensor_Data_HSS topic, the HSS Controller has to publish heartbeat messages on the general CORBYS Heart_Beat topic. These heartbeats are processed by the CORBYS functionality supervisor node in order to check the health of all CORBYS nodes. Heartbeat messages include a 32bit flag which can be use to indicate the status of the node. At this point no common format for these flags has been defined yet, but the HSS Controller will use the flag value to indicate the status of each individual driver node, and the presence of valid data at the expected rate for the different sensors.

2.5.9 HSS Controller Engineer GUI(s)

The CORBYS GUI developed as part of the CORBYS ROS framework provides a highly customizable interface which covers the visualization of all the sensor data produced by the HSS Controller. No additional GUI is expected to be developed to display the HSS Controller sensor data. However a specific GUI module will be developed in order to display the set of available sensor units and initialize training sessions by choosing the sensors to be used by the patient. This HSS Controller specific GUI will also display information about the state and status of the HSS Controller (based on the heart beat messages sent by the HSS Controller). According to the CORBYS ROS framework, the interactions between the GUI and the HSS Controller will be implemented via the central ROS parameter server. The exact parameters to be used will be defined and documented in D3.4.

2.5.10 HSS Controller Initialization

The HSS Controller has two main modes: A standby mode in which sensors are discovered and the state of their battery is monitored. In this mode no data is produced on the CORBYS ROS topic, the list of available sensors, their serial number and battery status are just populated in the ROS parameter server. The second mode is a "training session" mode in which the HSS Controller is connected to the sensors and continuously transfers data on the CORBY ROS topics. On startup the HSS Controller automatically goes to standby mode. The following sub-section briefly describe the initialization steps of the HSS Controller at startup and when transitioning to the "training session" mode.

2.5.10.1HSS Controller startup

On startup the HSS Controller automatically starts the sensor drivers and the HSS front-end as system daemons. The drivers start in standby mode and scan for available sensors to collect their serial numbers, status and battery levels. The front-end also starts in standby mode and monitors the executions status of the sensor drivers. All nodes wait for the CORBYS ROS core and parameter server to be available. Once the parameter server is available, the HSS front-end populates it with the list of available sensors and their characteristics. The HSS Controller stays in this mode until a session is initialized.

2.5.10.2Training session initialization

In order to start a training session and publish sensor data on the CORBYS ROS topic the HSS controller needs to go through a number of steps:

- Discovery of the sensor within range (and battery status). This is continuously done in the standby mode and the set of available sensor is kept updated in the ROS parameter server.

- Selection of the desired sensors and connection. The user of the demonstrator has to choose among the available sensors the ones to use for the training session. At this point the sensor should be set up on the patient and the selection should be populated in the ROS parameter server using the HSS Controller GUI. Once the selection of the sensors has been made, the drivers attempt to connect to these sensors.

- Log all versions of software, hardware and firmware. The first step after connecting to the sensor is to query the sensors for their versions and status in order to populate the parameter server with complete information about the sensors being used and confirm that the connection is properly established.

- Synchronization of the clocks of the sensors with the HSS Controller. In order to get accurate time information the wireless sensors need to be synchronized with the HSS Controller clock (which is itself synchronized with other CORBYS nodes). Experiments will be made in order to evaluate if a time synchronization "over the air" allows for a sufficient accuracy. In case wireless transmission delays are too unpredictable, the clock synchronization could be done using serial communication with the sensor on the charging station. In that case the synchronization would have to be made before the sensors are installed on the patient.

- Configuration of the sensors and subscription to the data. At this stage the sensor drivers will configure the sensors according the required CORBYS update rates and start collecting data from the sensors.

- Start forwarding data on the CORBYS GPN. After all sensors have been configured and the driver has stated forwarding data on the HSS internal topics, the front-end will start forwarding the data on the CORBYS topic. At this stage the HSS Controller is still in initialization mode and the subscriber to the sensor data should use the incoming data only for initialization checks.

- Basic checks of the selection and positioning of the sensors. The CORBYS GUI should be used to visualize the data coming from the HSS Controller and confirm that all sensors are providing sensible data and that all sensors are properly mounted. In particular:

    - ECG Signal should be visualized to confirm that the electrodes are properly placed. A drop of water can be used to moisten the electrodes and the belt size should be adjusted for a good contact between the electrodes and the skin.

    - Chest IMU and Back IMU data should be checked to confirm the correct orientation of the Sensors.

    - Skin temperature should be checked for both the Chest and Back sensors to make sure that no obstacles block the IR sensors.

    - Specific checks will be required for the EMG sensors.

- Switch to training mode. After the sensor mounting and connection has been confirmed by the user, the HSS controller switches to the training session mode in which the data can be exploited by subscribers.

At the end of a training session the HSS controller stops forwarding sensor data, disconnects from the sensor and goes back the standby mode.

2.5.11 HSS Controller Test

The HSS controller is designed to allow testing its components in isolations and to ease the testing of its integration in the CORBYS demonstrator. This section provides a short description of the different testing phases for the HSS Controller. The specification of the tests and results will be provided in D3.4.

2.5.11.1Unit tests of the driver modules

All the HSS Controller sensor drivers are independent processes connected to the sensors on one side and outputting sensor data on the HSS Controller internal ROS topics. For each sensor a testing application can be connected at the lowest level of the driver. The debugging GUI implements it own version of the sensor driver. Inconsistencies and faults can be detected by logging the sensor data produced by the HSS Controller driver and comparing it to the data produced by the debugging GUIs.

2.5.11.2Unit tests of HSS Front-End

The front-end of the HSS controller front-end can be tested in isolation of the sensor drivers by using ROS bags in order to capture data sequences on the internal HSS ROS topic and playing these data to the HSS Controller front-end. The output data of the front-end can be compared to the data played on the internal topics in order to detect potential malfunctions.

2.5.11.3Robustness tests

An important aspect of the HSS controller is its robustness with respect to potential failures. Special attention will be made at testing the ability of the HSS Controller to detect failures and recover from them. Testing will include scenarios with a high occurrence probability such as:

- Loss of connection with a sensor.
- Crash of a driver and/or of the radio adapter.
- Poor wireless connection leading to packet loss and/or high latency.
- Failure of a sensor and/or abnormal sensor values.

2.5.11.4QoS and extra-functional properties tests

Specific tests will be performed to evaluate typical data latency and time stamping offset in order to ensure that the CORBYS requirements are met. The time stamping offset mostly depends on the time synchronization between the HSS Controller and the sensor devices. Latency can be introduces at every stage of the sensor data processing and distribution. It is expected that the main source of latency is the wireless communications between the sensor units and the HSS controller but latency introduced by the HSS internal communication though ROS topics, the processing time of the drivers and front-end as well as distribution of the data on the CORBYS ROS topic will be evaluated.

2.5.11.5Integration tests

To test the integration of data from the HSS controller with the reset of the CORBYS demonstrator, a set of front-end datasets will be provided as ROS bags which can be replayed to simulate the presence of the HSS Controller on the ROS network. Multiple data sets will be provided for the different phases of the execution of the HSS controller.

Also, to test the HSS controller front-end ROS module integration with the CORBYS demonstrator, a set of datasets will be provided as ROS bags which can be played to simulate the presence of the HSS sensor modules for the HSS controller front-end. This enables usage of the HSS controller front-end without having the HSS sensor modules present.

An aggregated dataset containing data from HSS, BCI and hardware sensors should be made. This will give synchronized data from all modules for a training session.

2.6 Offline charging station for wireless sensors

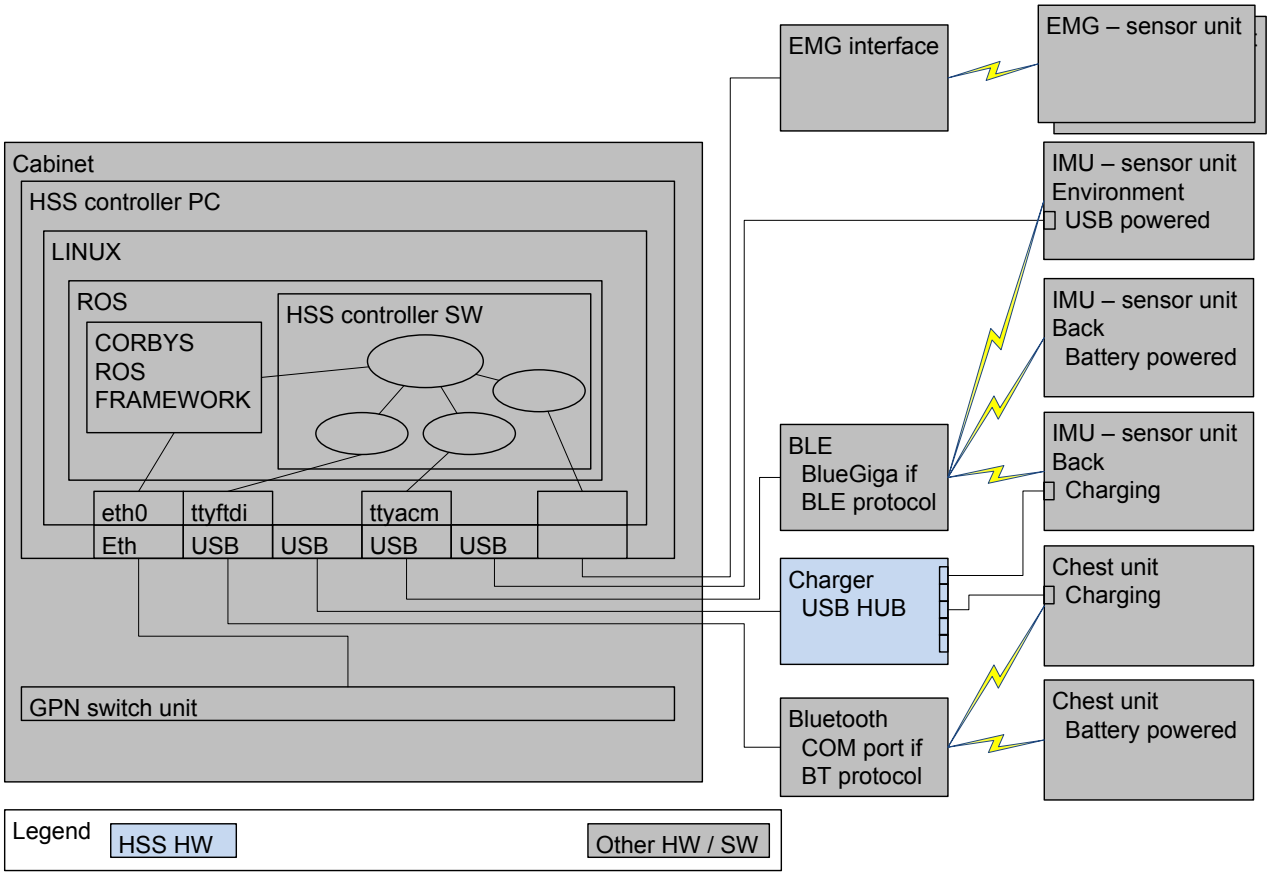

Figure 26: HSS controller in Human Sensory system

The chest unit and the IMU sensor need to be charged regularly. There will be two sets of sensors available, one set in use while the other set is charging. Charging is done in the offline charging station. The charging time is less than 2 hours and the following operational time is more than 2 hours (exact numbers will be provided in D3.4). The charge level can be monitored over Bluetooth and shown at the therapist GUI. During the training session only the charge level for the sensors in use are shown. Between training sessions the charge level for all sensors can be shown.

Location of the charger will be decided when the EMG system is specified in D3.4, the goal is to have a common location for charging of all sensors.

There are three alternatives for powering the charger:

- The HUB is powered from the HSS controller computer USB interface. Location has to be on the mobile platform.
- The HUB is powered from an external 24VDC power supply. Location has to be on the mobile platform.

- The HUB is powered from an external 220VAC power supply. Location has to be on a table somewhere near CORBYS Demonstrator I.

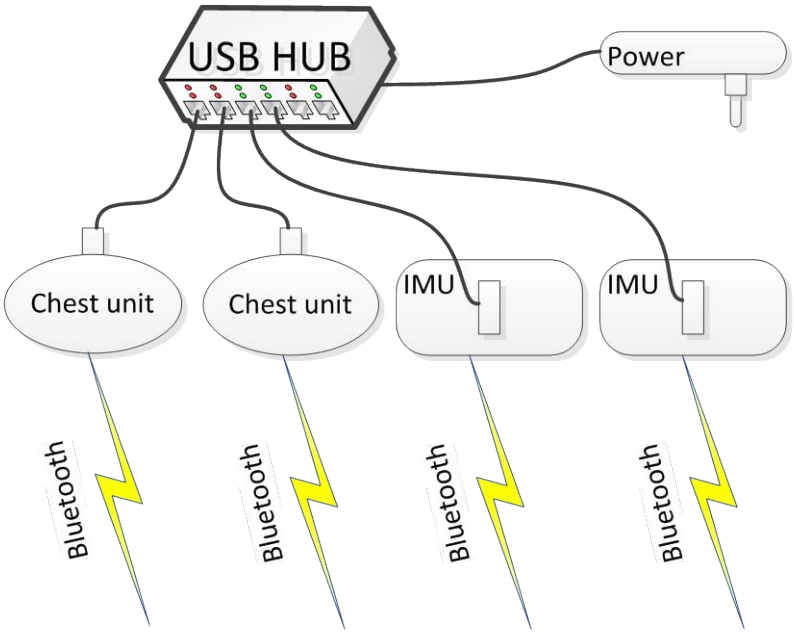

Figure 27 HSS - offline charging station

3 Brain Computer Interface (BCI)

CORBYS project focuses on a robotic system that have a symbiotic relationship with humans. One of Its objective concerns the development of a perception system for assessing the physical and mental state of the environment including humans. The perception system includes multimodal physiological sensing devices such as the Brain Computer Interface (BCI) and the Human Sensory System (HSS) that are important for human motor control and learning.

The Non invasive Brain Computer Interface (using EEG) will detect human cognitive information (in real-time) used by the robot cognitive control architecture for perception of the human mental state. In particular BCI will decode cognitive processes such as intention of leg motion, feedback error-related potential and attention states.

In the CORBYS gait rehabilitation system scenario, the subject will be walking assisted by a robotic device. In this context the EEG data will be affected by typical artifacts such as EOG and EMG, but also electromagnetic artefacts, due to the mobile platform (i.e. motors used for the powered orthosis and for the mobile platform's wings) and mechanical artefacts associated with head movements and locomotion. In section 3.2, Analysis and removal of movements' artifacts during locomotion, ocular and mechanical artefacts and their removal process based on Independent Component Analysis (ICA) technique are addressed. Section 3.1, Evaluation of EEG acquisition systems that could reduce the noise level, focuses on the study of the electromagnetic noise (i.e. noise due to the DC motors) and their impact in the CORBYS demonstrator. The EEG system that showed to be less affected by electrical noise contamination will be chosen for the CORBYS gait rehabilitation system.

In robotic related rehabilitation programs it has been suggested that human cognitive processes, such as motor intention, attention, and higher level motivational states play an important role in the success of the therapy [Tee et al, 2008]. In this context the BCI module will online detect cognitive processes of interest for the CORBYS gait rehabilitation system such as intention of leg motion, feedback error-related potential and attention states. Section 3.3, Detection of attention during assisted passive leg motion, reports the progress in designing a BCI system to decode passive lower limb movements with attention and non-attention to the motor task.

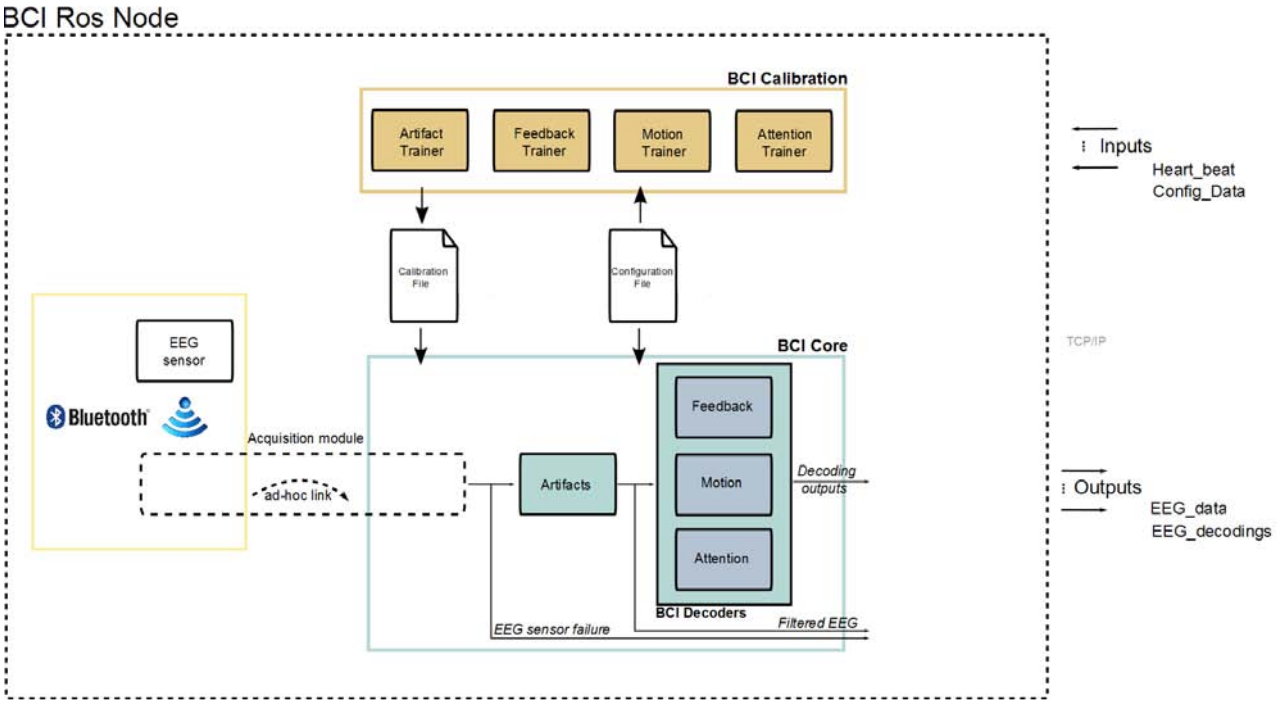

Figure 28 Brain Computer Interface submodule overview

Figure 28 presents an overview of the BCI submodule. It will be integrated in the architecture of the 1st CORBYS demonstrator as a ROS Node (task 6.1 - Architecture decomposition and definition).The inputs required from the BCI (i.e. configuration parameters and system state, D2.2) will be read from the ROS Parameter Server; its outputs will be sent from the BCI ROS Node using a ROS Topic (Sensors_Data_EEG). The ROS Message sent will include EEG data and BCI decoding outputs from those decoders enables in the current demonstrator state. Further information will be reported in D3.4.

3.1.1 Evaluation of EEG acquisition systems that could reduce the noise level

3.1.2 Introduction

EEG systems take an important place in BCI applications as they provide an excellent way to describe brain signals with good time resolution and lower cost than other brain activity acquisition systems. A key parameter of studies of EEG systems is the signal-to-noise ratio, (SNR), as it provides a measurement of the signal quality. In the EEG context, this parameter is affected by a significant number of internal and external sources which influence the recorded signal, independent of the system used for recording. Sensor-scalp contact (i.e. to guarantee low contact impedance between the electrode and scalp) and the capability to automatically remove or reduce noise sources are also important aspect of the acquisition system that determines the quality of the recording. There are several studies in literature about EEG acquisition technologies, such as those with focus on classical gel-based electrodes and novel water-based electrodes applied in specific brain-computer-interface [Searle and Kirkup, 2010; Matteucci et al, 2007]. Research teams have also developed working prototypes of dry EEG sensors and demonstrated that the signal obtained can be largely comparable to wet electrodes [Popescu, 2007].

Among those existing sources of noise that can affect the EEG signals, the electromagnetic noise caused by external devices such as motors, and the power supply are those that could have a significant impact on the use of BCI in CORBYS scenario. This deliverable focuses on a technical evaluation of the quality of EEG recordings of two commercial systems to find adequate equipment for the CORBYS scenario. This is because in CORBYS, the EEG system will be forced to work close to a robot in movement, which is a source of electromagnetic activity and noise and might affect the EEG readings. This document reports the evaluation of two commercial EEG systems in scenarios similar to the CORBYS 1st demonstrator. The first one is the Porti amplifier, a multichannel device of TMSi (Twente Medical System International BV, Netherlands) with passive electrodes of water solution. The second one is g.USBAmp, a biosignal amplifier produced by g.Tec (Graz, Austria), with active electrodes of gel solution.

The first section describes the technical specifications of these two commercial EEG systems. The second section presents an analysis of both EEG systems in two different experiments. The objective of the experiments was to study the possible effect of electromagnetic noise in the EEG signals caused by electric motors in two different scenarios: the first experiment was developed under a controlled situation, where a DC brush motor was used as proposed by related partner developing mobile platform (i.e. there will be the motors used for the powered orthosis and for the wings in the mobile platform); the second experiment involved a less-controlled scenario, where the source of electromagnetic noise was caused by a generic AC motor.

Figure 29 Commercial EEG systems. On the left: passive electrode (water solution) and Porti-16 of TMSi. On the right: active electrode (gel solution) and g.USBamp of g.Tec.

3.1.3 EEG Systems: Evaluation of technical specifications

The electroencephalogram (EEG) is an acquisition system that measures electrical brain activity through electrodes placed on the surface of scalp. These sensors measure neural activity by electrical potentials (voltage) over time between a signal electrode and a reference one. Every EEG system includes three acquisition blocks: the electrodes, the wires (interface sensor-amplifier) and the amplifier (filtering, amplifying and signal conversion).

- *Electrodes*

The brain activity is acquired by electrodes which build an interface between the scalp skin and the metal of the wire. The electrode is a metallic sensor that converts the local differences of the concentration of charged ions into an electrical potential signal. However, the measurement of the electrical activity of target physiological processes can contain a number of undesired components, for example 50 Hz-mains interference, electrode-offset-potential, drift in offset potential or fluctuations caused by mechanical influences such as movements.

An EEG sensor is tested concerning its technical specifications, such as (active, passive), level of noise, DC behaviour and variability, frequency response, impedance and its stability, weight, wearability and sensor material. However the main challenge to EEG electrodes is to get a good low impedance contact to the skin (for comparison about different electrode technologies refer to CORBYS Deliverable D2.1- Section 15 State of the Art in Non Invasive Brain Computer Interface). The other point need to be concerned is whether the contact of the electrode is affect by the locomotion of the human. From the technical specifications, there is not a clear reason to state which of these electrodes is better suited for this purpose.

- *Wires*

Both devices have shielded wires which send the EEG signals that are measured at the electrode into the amplifier. The main advantage of the shielded cable is that movements of the cable and environmental noise do not influence the signals in the cable. Thus, this source of noise does not affect the recorded EEG signals in the CORBYS scenario. In TMSi equipment, the cables are covered with active shielding, so that the signal is immune to the cable movement artifacts and to mains interference (i.e. 50 or 60 Hz coupling). Thus, the inner

wire of the input cable is not affected by any capacitive coupling, which means that there will be no artifact when the cables are moving. On the other hand, g.Tec provides no information about the specific cable shielding used for their systems. In CORBYS, it is expected to find artifacts from wire movements due to the user locomotion and thus, the TMSi wires seem to be more appropriate as the movement of the cables will be difficult to avoid (notice that this statement is mainly due to the lack of information about the g.Tec wires).

- *Amplifier*

The amplifier includes the following functions: filtering, amplifying and signal conversion. The next table resumes the technical specifications of the commercial amplifiers related to the signal quality such as input impedance, the common-mode rejection ratio (CMRR).

Table 4 Technical specifications of the Porti-16 and g.USBamp amplifiers.

	Porti-16	g.USBamp
Input referred noise	<2 µVpp (@ Fs = 128 Hz)	< 0.3 µV RMS (0.1-10Hz)
Input impedance	$>10^{12}\,\Omega$	$>10^{10}\,\Omega$
CMRR	>100 dB	>100 dB
Connector	Micro coax, active shielding	1 mm 2-pin touch-proof
Special features	Active guarded shielded leads and electrodes	50-60Hz selectable hardware notch filter

One of the most relevant amplifier parameters is the input impedance as it alleviates the need of a low impedance contact to the skin. High input impedance in an amplifier can decrease the dependency of the electrode contact impedance, on the contrary low input impedance causes load of bio-signal source and it results in damaging of the signal. The input impedance in the Porti-16 is of two orders of magnitude higher than in the g.USBamp. The need of low contact impedance can be mitigated partly by the high input impedance of the amplifier and the shielding of the electrode wires or connectors as with the TMSi equipment as well as by using local impedance adapters as the active electrodes of g.Tec electrodes. CMRR is a measure of the ability of a test instrument to reject interference that is common to both of its measurement inputs, which is equal in both amplifiers. Mains interference (i.e. 50-60 Hz) can be prevented with active guarded shielded leads and electrodes, also it is possible to reject this interference using a notch filter of main frequency (i.e. 50 Hz) by hardware (as g.USBamp) or by software as well.

From a theoretical point of view, the high input impedance of the amplifiers could be a technical parameter that makes the TMSi amplifier more appropriate for CORBYS (as both amplifiers have very similar characteristics). However, this decision needs to be confirmed by the experimental evaluation as there are many other aspects that mediate in the EEG recordings.

3.1.4 Evaluation scenarios

This section addresses the influence of electrical motor noise in the EEG recordings of both EEG acquisition systems in two different experiments. The first experiment was developed under a controlled situation, where a DC brush motor was used as proposed by related partner developing mobile platform; the second experiment involved a less-controlled scenario, where the source of electromagnetic noise was caused by a

generic AC motor.

Data recording

Both experiments used the same data recording setup. Three subjects participated in both experiments. EEG signals were recorded simultaneously from g.Tec and TMSi systems. Data acquired from g.Tec system was recorded from 10 active electrodes placed F3, Fz, F4, C3, Cz, C4, P3, Pz, P4 and Oz (according to the 10/10 system). Ground and reference electrodes were placed on FPz and on the right earlobe respectively. Data acquired from TMSi equipment was recorded from 10 water electrodes placed next to g.Tec electrodes at the following locations: AFF3, AFFz, AFF4, FOC3, FOCz, FOC4, OCP3, OCPz, OCP4 and POOz (according to the 10/5 system), see Figure 30.

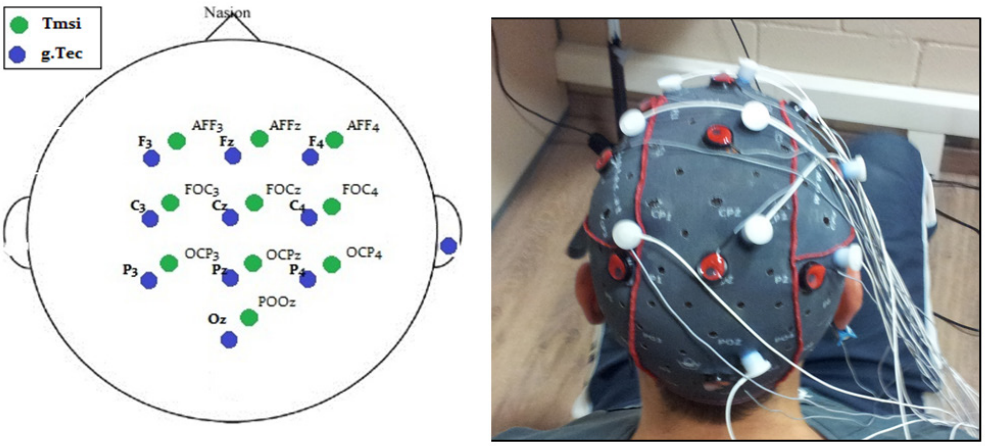

Figure 30 On the Left: EEG montage of gel electrodes in blue (g.Tec) and water electrodes in green (TMSi). On the right: picture of real montage gel electrodes (red) and water electrodes (white).

Electrodes were placed over a g.Tec cap according to the extended 10/5 international system. For both EEG systems, data were digitized at a sampling rate of 256 Hz, band-pass filtered at 0.5-60 Hz and recorded simultaneously with the same computer using BBT proprietary software.

Experiment 1: Noise influence of a DC brush motor

In this section, both EEG systems are exposed to electromagnetic (capacitive or inductive) noise from a DC brush motor, as these types of motors were as specified in D2.2.

Experimental protocol

Experiments were carried out in a real scenario environment with ambient light and without any particular restriction on the background noise and luminance. Subjects were seated in a comfortable chair approximately 100 cm from a LCD monitor, which displayed the tasks instructions. A DC brush motor (i.e. PITTMAN

GM9236E 349-R1 12 VCD 500 CPR) was used to analyze its influence in EEG recording. Motor was working with constant velocity at 17 motor revolutions per second (RPS), and it was located at two different positions from the subject's head respectively: distance_1 = 0.5 m. and distance_2 = 1 m.

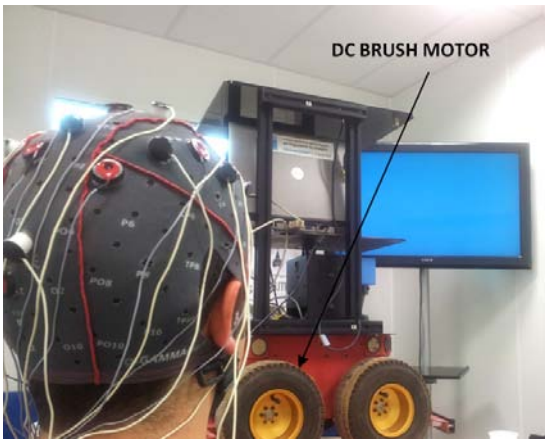

Figure 31 Subject during experimental procedure, EEG was recorded during relaxing task with noise influence produced of DC brush motor.

The experimental design is shown in Figure 32 with three conditions (distance_1, distance_2 and motor off). Each condition was recorded for 60 trials, where after each condition the subject has 2 minutes of rest. Each trial was composed of a 3 seconds resting time and 5 seconds baseline executing task. The subject was asked to avoid blinking during the baseline condition.

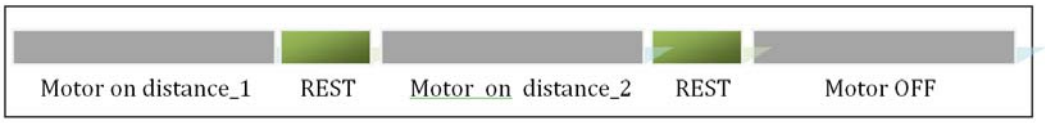

Figure 32 Time diagram of protocol in the experimental procedure.

Data processing and results

For each trial, the EEG data from the baseline were visually inspected, and one-second epochs were discarded if a physiological artifact was identified. EEG power spectrum was calculated by a sliding window periodogram of one second with 30 ms of overlapping and then averaged. To compute the periodogram a 1s hamming window was used with a resolution of 0.25 Hz (1024 points using zero-padding) and power-line is notch-filtered at 50 Hz.

For each condition the power spectrum density (PSD) was averaged across channels and then averaged across subjects. Figure 33 shows the PSDs for each condition and amplifier. The only visible difference is around 56 Hz where it seems to be an artifact as, up to our knowledge, this abnormal activity cannot be attributed to any known neural activity. This artifact appears in all three conditions of the g.Tec system (even when the motor is OFF), and it appears only in one condition of the TMSi system (i.e. motor ON). This suggests that the nature

of the artifact is not due to the DC motor. The rest of the PSD is very similar in three conditions and thus there is no other apparent effect of artifacts on the EEG. This result is confirmed by the Figure 34, which shows PSDs resulted from both EEG systems in the 3 conditions recorded.

Figure 35 shows the ratio between the PSDs of motor ON and motor OFF conditions for each subject (this ratio eliminates the effect of the different gains of the amplifiers and allows the comparison). The results show that there is not apparent difference below 20 Hz (that is the range where the difference should be due to the RPS of the motor – about 17 Hz). Greater difference is present in the range 20-50 Hz; it can't be attributed to the DC motors since in the analysis performed in Figure 33 and Figure 346 this is not visible. Artifacts above 50 Hz are not due to the motor activity.

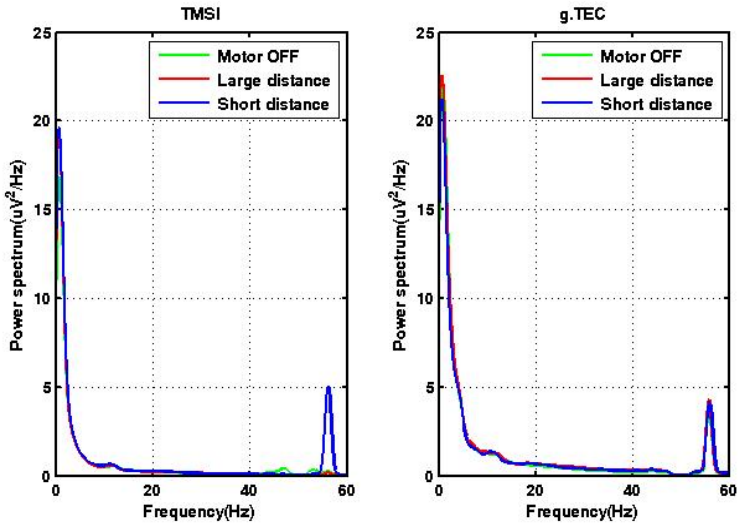

Figure 33 Average power spectrum density for every conditions: motor OFF, large distance, short distance using TMSi system (left) and g.Tec one (right).

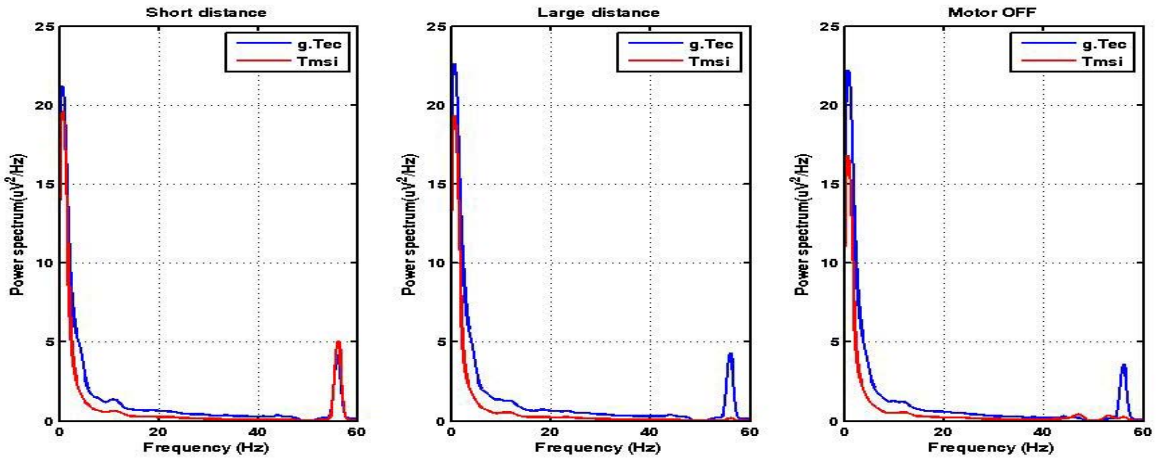

Figure 34 Average power spectrum densities for three conditions recording: motor on located 0.5 m far subject's head, motor on located 1 m far subject's head and motor.

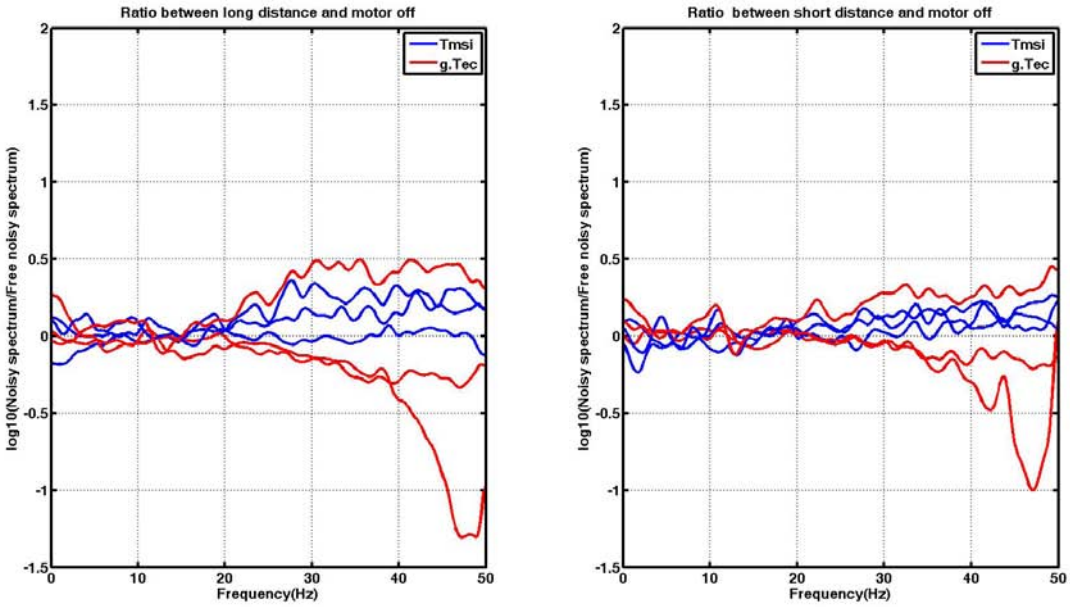

Figure 35 Ratio between power spectrum of noise conditions and motor OFF for TMSi (blue) and g.USBamp (red) systems of each subject. Noise condition is considered motor located 1 m (left) and 0.5 m (right) from subject's head.

Experiment 2: Noise influence of an AC electrical engine

Experiments were carried in a real scenario environment with ambient light, without any particular restriction on the background noise and luminance. Subjects were seated in a comfortable chair approximately 60 cm from a LCD monitor, which displayed the tasks instructions. Close to the subject there is an electric mini-bike activated by remote control by the subject. From an electrical point of view, this device behaves as a solenoid which works in different frequencies depending on the speed bike and for the experimentation the slowest speed motor was used.

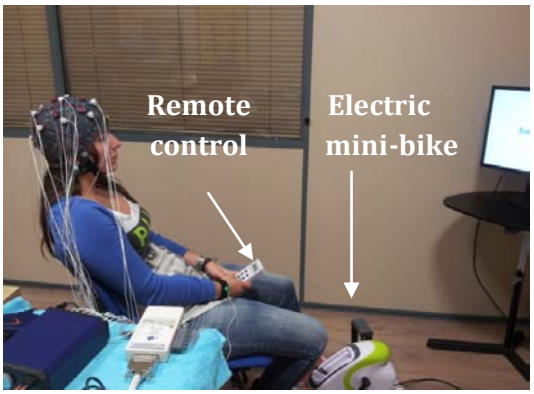

Figure 36 Subject during experimental procedure, EEG was recorded during relaxing task with noise influence produced by an electric mini-bike.

The experimental design is shown in Figure 37 with two conditions (motor ON and motor OFF). A trial was composed of a rest time of 3 seconds and baseline task of 5 seconds. The subject was asked to avoid blinking during baseline period. A total of 60 trials were recorded (30 trial of each condition).

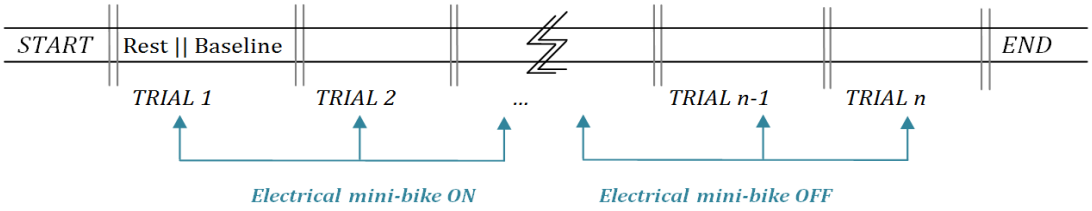

Figure 37 Time diagram of protocol in the experimental procedure.

Data processing and results

Artifact filtering was performed by visual inspection of the baseline recordings in both conditions. Epochs of one second were discarded if a physiological artifact was identified. EEG power spectrum was calculated by a sliding window periodogram of one second with 30 ms of overlapping and then averaging. To compute the periodogram a hamming window was used with a resolution of 0.25 Hz (1024 points using zero-padding) and power-line notch-filtered at 50 Hz and bandpass filtered between 0.5 and 60 Hz.

Figure 38 shows EEG signal affected by noise (i.e. 20 Hz sinusoidal contamination).

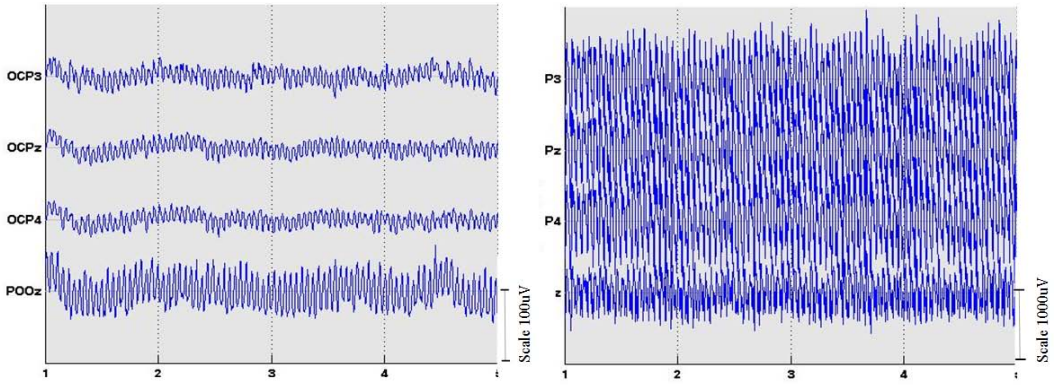

Figure 38 Example of four EEG channels contaminated by electric mini-bike recorded using TMSi (left - with scale of 100 uV) and g.Tec (right- with scale of 1000 uV) system, over a time window of 4 seconds.

Figure 39 shows power spectrum averaged across channels of EEG recorded for both systems for Subject 2. A peak at 20 Hz and at its fundamental harmonic frequencies (i.e. 40 Hz, 60 Hz, etc.) reflects the electric noise contamination.

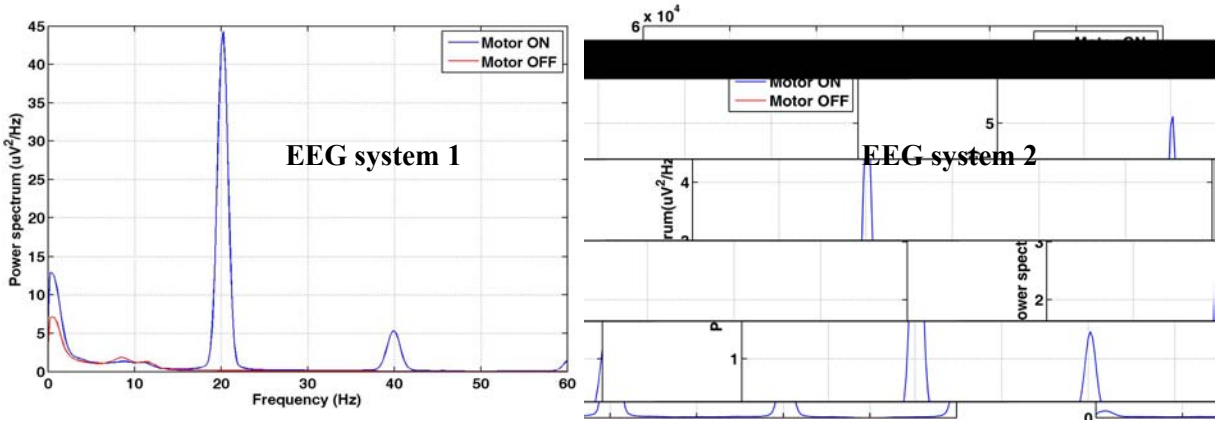

Figure 39 EEG spectrum recording during motor ON (blue) and motor OFF (red) conditios, averaged across 10 channels registered with TMSi (left) and g.Tec (right) system for subject 2.

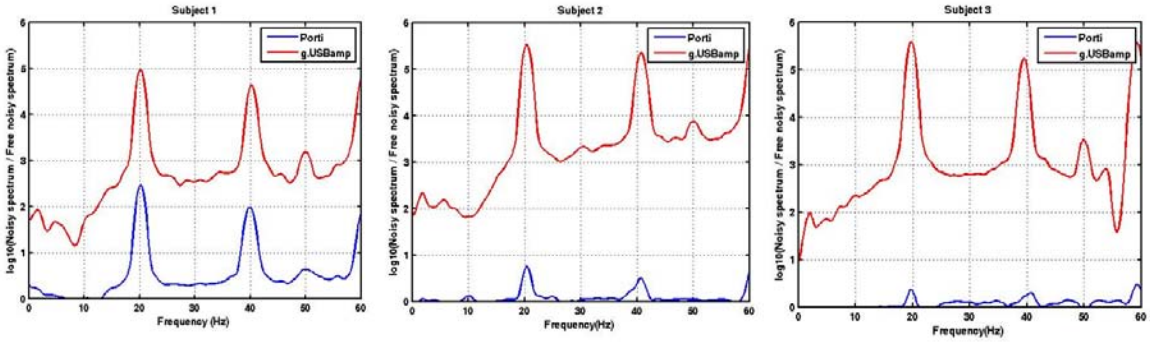

Figure 40 Ratio between power spectrum of noisy and free noise one for Porti (blue) and g.USBamp (red) sytem of each subject.

Since both amplifiers have different gain across frequency it is not possible to compare their EEG or corresponding PSD. To avoid this phenomenon, the ratio between the power spectrums of both conditions is used, this is presented in Figure 40 for all subjects. Notice that the level in Noise condition in g.USBamp is more than two orders of magnitude greater than in the TMSi system for frequencies between 0.5-60Hz and for all the subjects. For both systems the ratio frequency spectra show a peak at 20 Hz and at its fundamental harmonic frequencies (i.e. 40 Hz, 60 Hz, etc.), although in case of g.Tec noise data is spread over all frequencies while it is not the case for the TMSi system.

3.1.5 Discussion

Two commercial EEG systems are presented in this document. Results show that TMSi equipment was less affected by electrical noise than g.Tec system. There could be two reasons result in this effect: differences in technical characteristics in the electrodes or the differences in the technical features of the amplifiers. While the electrodes could affect the data quality due to the impedance between sensor and scalp, the amplifier could alleviate deficiency regards signal quality. In summary the TMSi system has a better performance in the presence of motor activity and unknown sources of electrical noise, which is the best replication that has been devised to emulate the working conditions of the CORBYS experimentation.

3.2 Analysis and removal of movements' artifacts during locomotion

3.2.1 Introduction

Wide range of artifacts can occur in EEG recordings. One possible categorization of artifacts is based on their origin: technical (originated from outside the human body, such as the 50/60 Hz power-line noise, changes in electrode impedances, etc) and physiological (originated from a variety of bodily activities, such as potentials introduced by eye or body movements, muscular activity, cardiac activity, etc.). While some of these artifacts are easily identified, others may have similar characteristics to the neural activity and therefore difficult to recognize and to eliminate. The presence of artifacts in EEG signal has an impact on the analysis and could lead to unreliable results if they interfere with the neural process under study. This is the reason why one important part of biomedical signal processing is to understand the noise and the artifacts in order to minimize their impact either in the analysis or in the development of the technology.

The two physiological artifacts being mostly studied are the eye movements (EOG) and in the body movement (EMG). EOG artifacts are due to electrical eye activity propagated throughout the body and recorded at the scalp surface [Schlögl et al, 2007]. They are generally high-amplitude patterns in the brain signal caused by the blinking of the eyes, or low-amplitude patterns caused by movements such as rolling the eyes [Anderer and Roberts, 1999]. The EOG amplitude is attenuated approximately with the square of the distance [Croft and Barry, 2000], and thus contaminates mostly the frontal EEG channels. The EOG activity spans a wide frequency range, being maximal at frequencies below 4Hz. The EMG artefacts are generated in the muscles of the face, neck and on the scalp, and are caused by movement, chewing, swallowing, muscle twitches, anxiety, tremor or general muscle tension [Van de Velde et al, 1998]. The EMG activity also spans a broad frequency range distribution, and even weak muscle contractions produce an EMG activity that can mimic or obscure the EEG activity over the entire scalp [Goncharova et al, 2003].

In the CORBYS gait rehabilitation system scenario, the subject will walk with assistance of a robotic device. In this context, the EEG data will be affected by typical artifacts such as EOG and EMG, but also electromagnetic artifacts due to the mobile platform and mechanical artifacts associated with head movements and locomotion. The study of the impact of the electromagnetic noise (i.e. noise due to the DC motors) is addressed in the section 3.1, Evaluation of EEG acquisition system that could reduce the noise, of this deliverable.
Several research groups have studied the EEG artifacts during human locomotion. For instance [Gwin et al, 2010] studied the brain activity during walking and running on a treadmill in a controlled scenario. The results showed that during the walking condition the artifacts slightly contaminate the EEG signals in an event-related analysis, while during the running conditions the EEG signals are strongly affected by movement artifacts.

This deliverable addresses the mechanical artifacts and their removal process based on Independent Component Analysis (ICA) technique. In the present study two experiments were conducted, the first one addresses lateral head movement, and the second one studied the walking movement with a 'walker' device. The relevance for the CORBYS project is due to the presence of linear and angular head movement during locomotion [Hirasaki et al, 1999]; the second one emulates the walking condition of the 1st CORBYS demonstrator. Although in the clinical EEG the artifacts are addressed with generalist filters, in the brain

computer interface technology community they are addressed with filter design for each user / application. This is the reason why this study analyzes both average and individual artifacts.

3.2.2 Methods

A. Subjects

Data were collected from 4 healthy subjects, 3 women and one man (23.25 ± 3.59 years). None of them had a history of a neurological, psychiatric disorder or was under chronic medication. The group included 3 rights and one left hand-dominant people. The participants were duly informed about the experiment before they signed the consent form.

B. Data Collection

EEG was recorded using two g.Tec amplifiers with 32 active electrodes. The electrodes were placed at FP1, FP2, AF3, AF4, F7, F3, Fz, F4, F8, FC3, FC1, FCz, FC2, FC4, T7, C3, C1, Cz, C2, C4, T8, CP3, CPz, CP4, P7, P3, Pz, P4, P8, O1, Oz and O2 according to the international 10/10 system (Figure 41a). The ground electrode was placed on FPz and the reference on the left earlobe. EEG signals were sampled at 256 Hz, bandpass filtered (0.5 – 60 Hz) with a Butterworth filter of order 4 and power notch filtered at 50 Hz.

Vertical and horizontal EOG were acquired with the ground electrode on the right mastoid and the reference electrode on the left mastoid (Fig.1b). EOG signals were recorded with the gUSBamp amplifier from g.Tec at a sampling frequency of 256 Hz, bandpass filtered (0.5 – 60 Hz) with a Butterworth filter of order 4 and power notch filtered at 50 Hz.

Two unipolar EMG electrodes were placed on both left and right sternocleidomastoid muscle as they are activated with the head rotation movements [Costa et all, 1990] (see Figure 41c). The ground electrode was placed on the left forearm and the reference electrode was placed on the right forearm. EMG signals were registered with the gUSBamp amplifier from g.Tec at a sampling frequency of 256 Hz, bandpass filtered (0.5 – 100 Hz) with a Butterworth filter of order 4 and power notch filtered at 50 Hz.

a) b) c)

Figure 41 ***a)*** **Scalp electrode position according to the American EEG Society, 1994,** ***b)*** **subject wearing an EEG cap with 32 active electrodes,** ***c)*** **superficial muscular electrodes (EMG) on the right-sternocleidomastoid muscle.**

The data recording was carried out with three g.Tec amplifiers (two of them for the EEG and the other one for the EMG and EOG) synchronized. The experiment was executed using the proprietary *Bit&Brain Technologies (BBT) software.*

C. Experimental Procedure

The experimental procedure comprised a baseline recording and two experiments. It lasted about 30 minutes.

Baseline
Subjects were seated in a comfortable position with eyes open and were asked to try to minimize movements and blinking for an interval of 5 minutes.

Experiment I
The subjects were in a standing position in front of a fixation cross placed in the center of a wall, 2 meters away from them (0° - initial position, straight ahead) and four targets located at an angle of ±25° and ±45° with the 0° (Figure 42a). The experiment consisted of successive trials of four different conditions that correspond to movements to align the head with the targets (i.e. target -25°, target +25°, target -45° and target +45°) and return to the initial position. Each trial started with a 3 seconds interval of time where the subjects relaxed in the initial position and minimized movements and blinking, followed by a variable (depending on the velocity of the subject head movement) execution interval where the subjects moved the head from the initial position to the target specified and move it back, and then finished with a 2 seconds rest time where subjects were allowed to minimally move and blink. The experiment had 10 trials for each condition with a rest period of 30 seconds between conditions. This experiment lasted approximately 12 minutes.

Experiment II
The subjects were in a standing position with a table on wheels emulating the walking device with the instrumentation located above (Figure 42b). The reaching point was set to 5 meters away from the start position. The experiment consisted in trials of one condition where the subjects walked from the starting point to the reference point. Each trial started with a 3 seconds interval of time where the subjects relaxed, followed by a variable duration between 10-15 seconds (depending on the velocity of the subject in reaching the reference point) execution interval where the subjects were walking until the reaching point, and then it finished with a 5 seconds rest period. The experiment comprised 22 trials and lasted approximately 9 minutes.

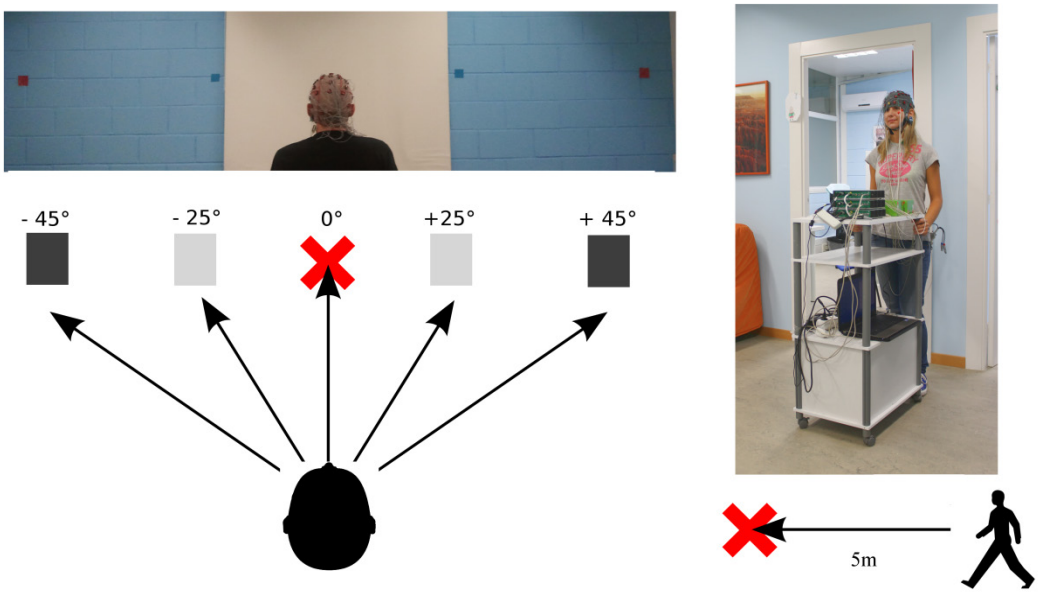

Figure 42 ***a)*** **Experimental setup and protocol of Experiment I: to look at the targets subjects need to turn the head ±25° and ±45°.** ***b)*** **Experimental setup and protocol of Experiment II: subjects were asked to walk pushing ahead a table on wheels emulating a walking device.**

D. Data Processing

Power spectral density (PSD) was obtained using Welch's method. For each trial the PSD was estimated on every 1s in the band 1 - 40 Hz with 0,25Hz resolution and then averaged across trials.

For each subject, the EEG data was filtered by Independent Component Analysis (ICA) algorithm (FastICA based on [Hyvärinen et Oja, 2000]) to eliminate the components from blinking and EMG artifacts. FastICA algorithm is based on a fixed-point iterative method that maximizes the non-Gaussianity as a measure of statistical independence [Hyvärinen et Oja, 2000]. The assumption is that the number of sources is the same as the number of electrodes (i.e 32). Each component was reprojected back to the sensor space, time-frequency representations of these reprojections with the associated spatial maps were visually inspected to assess whether the component was artifacted. The components free from artifacts were reprojected back to the sensor space to obtain an artifact free EEG.

For source localization, Standardised Low Resolution Brain Electromagnetic Tomography (sLORETA) [Pascual-Marqui, 2002] was employed. sLORETA is a linear method to compute from EEG data a statistical map that gives the location of neural generators within the brain. The source localization was used to assess whether the filtered EEG is free of artifacts as follows: the source activity of the pre filtered and post filtered EEG was computed and checked whatever it corresponds to the motor cortex. Notice that if the artifacts do not contaminate the EEG, then the motor cortex will be one of the neural generators. This strategy was used only in the first experiment, as the walking behaviour does not involve the motor cortex in a large extent since the majority of the behaviour is solved in the spinal cord.

3.2.3 Results

The channels located in central areas were selected for further analysis as they are the location where the legs movements are better observed [Pfurtscheller and Lopes da Silva, 1999]. The following nine channels were chosen: FC1, FCz, FC4, C1, Cz, C2, CP3, CPz and CP4.

Experiment I

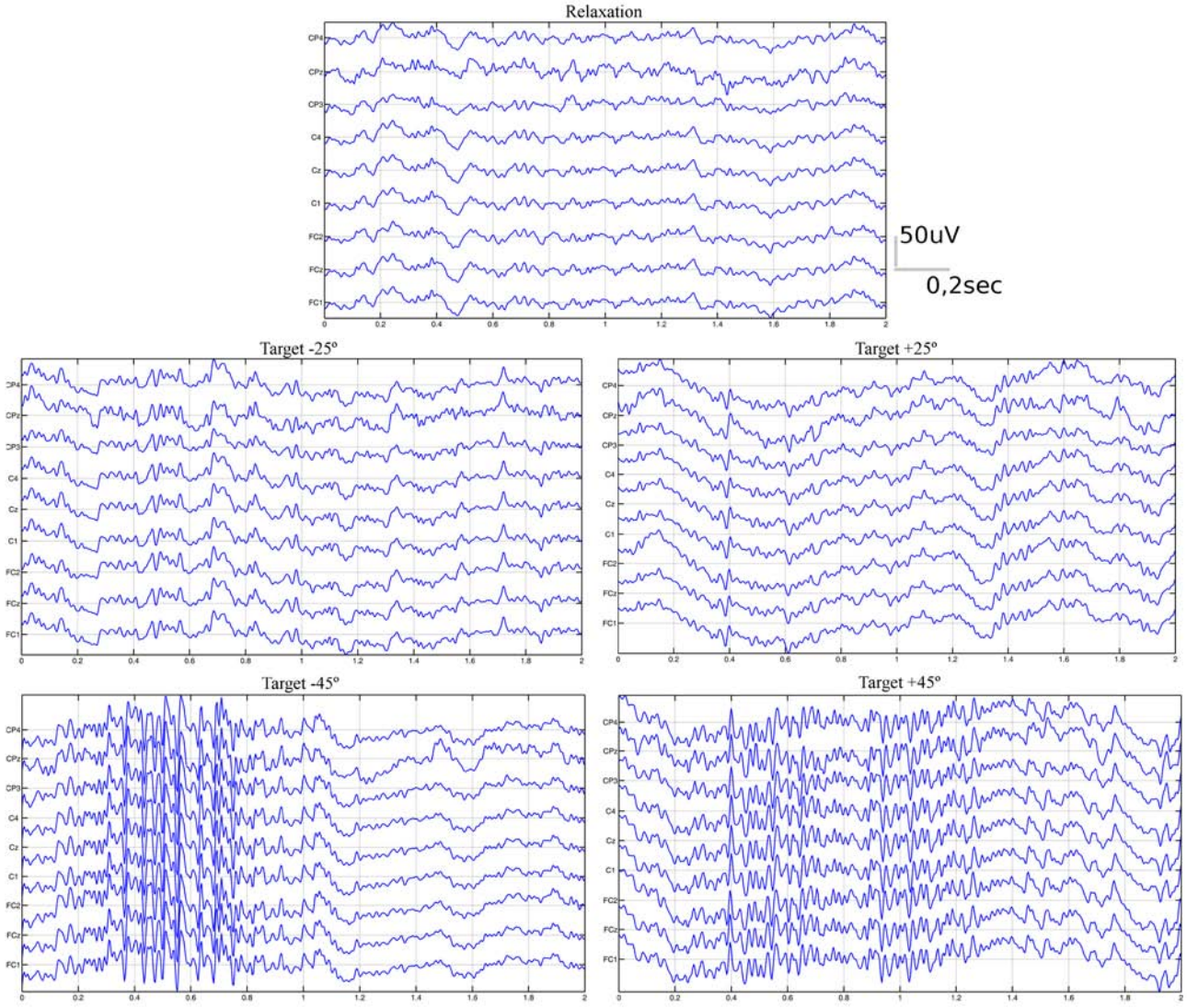

Figure 43 This figure displays for subject 3 two epochs of EEG signal recorded during relaxation (*top*), target -25° (*middle left*), target +25° (*middle right*), target -45° (*bottom left*) and target +45° (*bottom right*).

Figure 43 presents the EEG signal recorded during relaxation and target ±25° and ±45°, where the EEG is contaminated by the EMG artifact generated from the head movement. The influence of the artifacts in the frequency domain is that the power is higher when the angular movement is higher, and this effect is more prominent at high frequencies (10 – 40 Hz). Figure 44 displays the result for one subject and Figure 45 the

results of the mean of all the subjects. Notice that the spectra shows a peak in the alpha band (8 -13 Hz) that is largest in the centro-parietal location (i.e. CP3, CPz and CP4) in the not motion state, and this activity desynchronizes in the motion condition as it is the typical response in a motor behaviour [Pfurtscheller and Lopes da Silva, 1999].

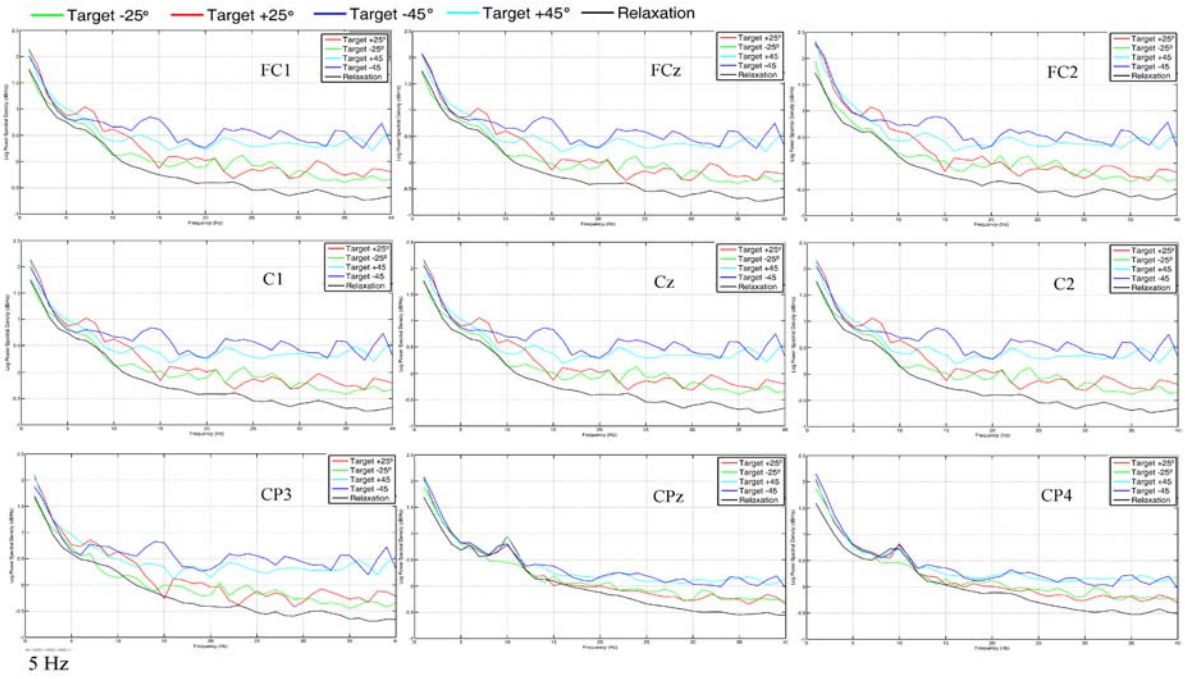

Figure 44 This figure displays for subject 3 the logarithmic power spectral density of the EEG signal recorded during relaxation (black), target -25° (green), target +25° (red), target -45° (blue) and target +45° (cyan).

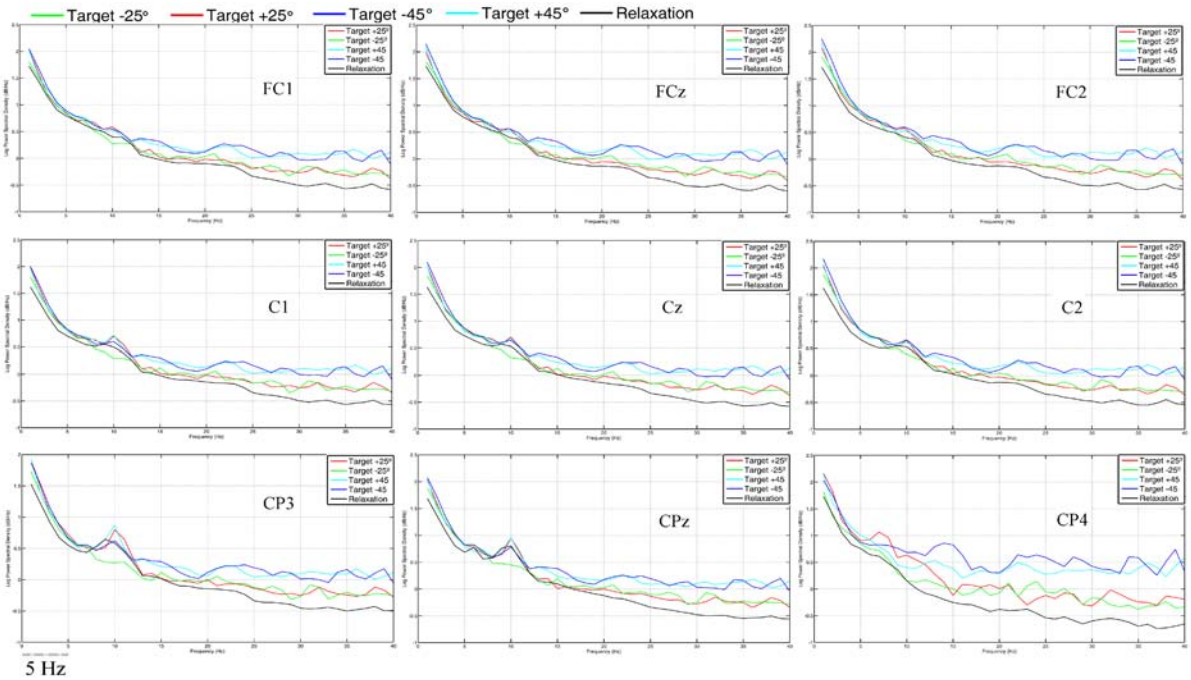

Figure 45 Average logarithmic power spectral density of the EEG signal recorded during relaxation (black), target -25° (green), target +25° (red), target -45° (blue) and target +45° (cyan).

For each subject, the ICA decomposition was computed on the EEG concatenated of the five conditions (i.e. 0º, targets ±25° and ±45°), where the size of the EEG data satisfies the condition of the minimum amount of data needed to obtain ICA good performance [Groppe et al, 2009].The ICA algorithm decomposed the EEG into spatially-fixed and temporally independent components (ICs). The components that contained artifacts were eliminated and then the remaining components were reprojected back to the sensor space [Jung et al, 1998].

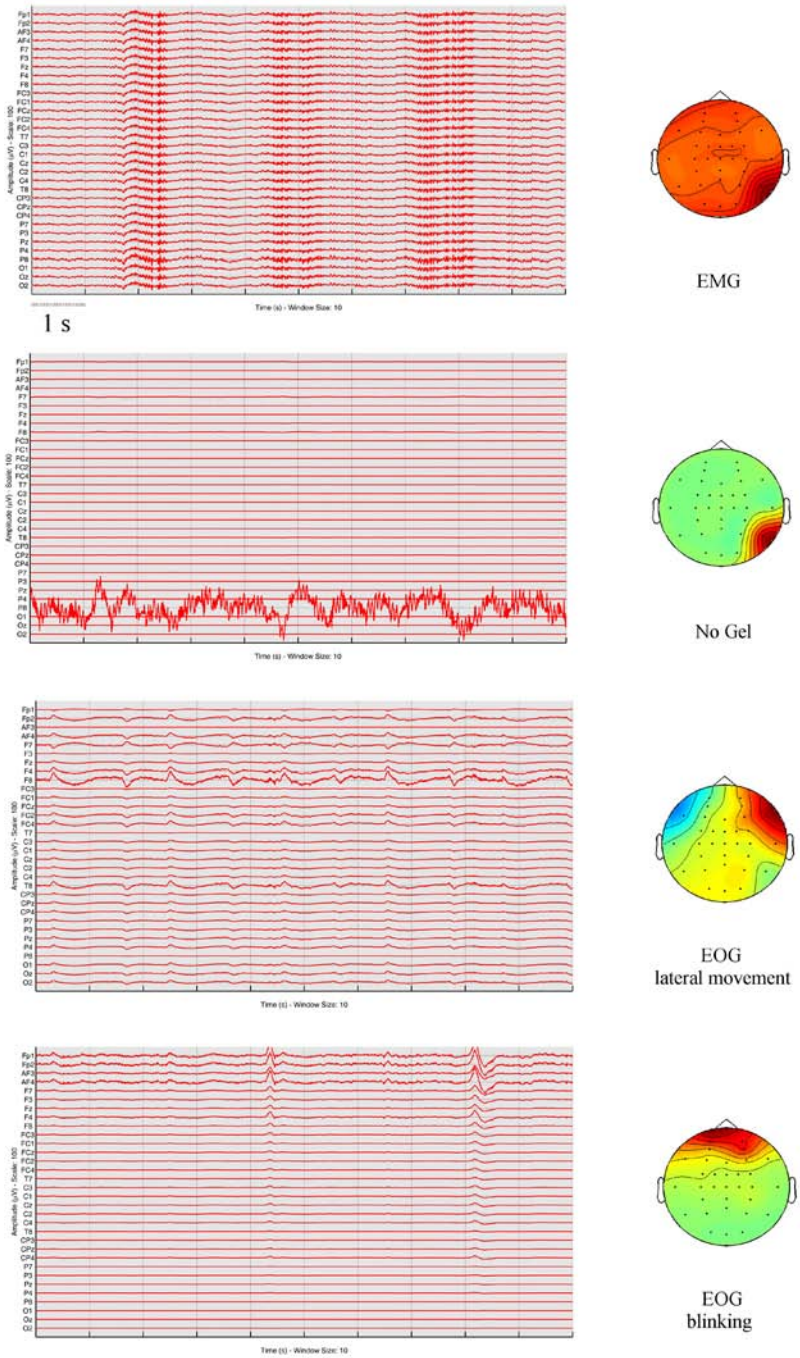

Figure 46 This figure shows for subject 3 scalp maps (right), and the component reprojected back to the sensor space (left) of the four ICs that contain artifacts: muscular activity, electrode without gel, eye blinking and eye lateral movement.

For one subject the Figure 46 shows several components eliminated and some EEG trials without artifacts reconstructed through reprojection (Figure 47). Notice how the presence of the main artifacts due to the head movement is mitigated, although in the last two conditions some EMG is still present.

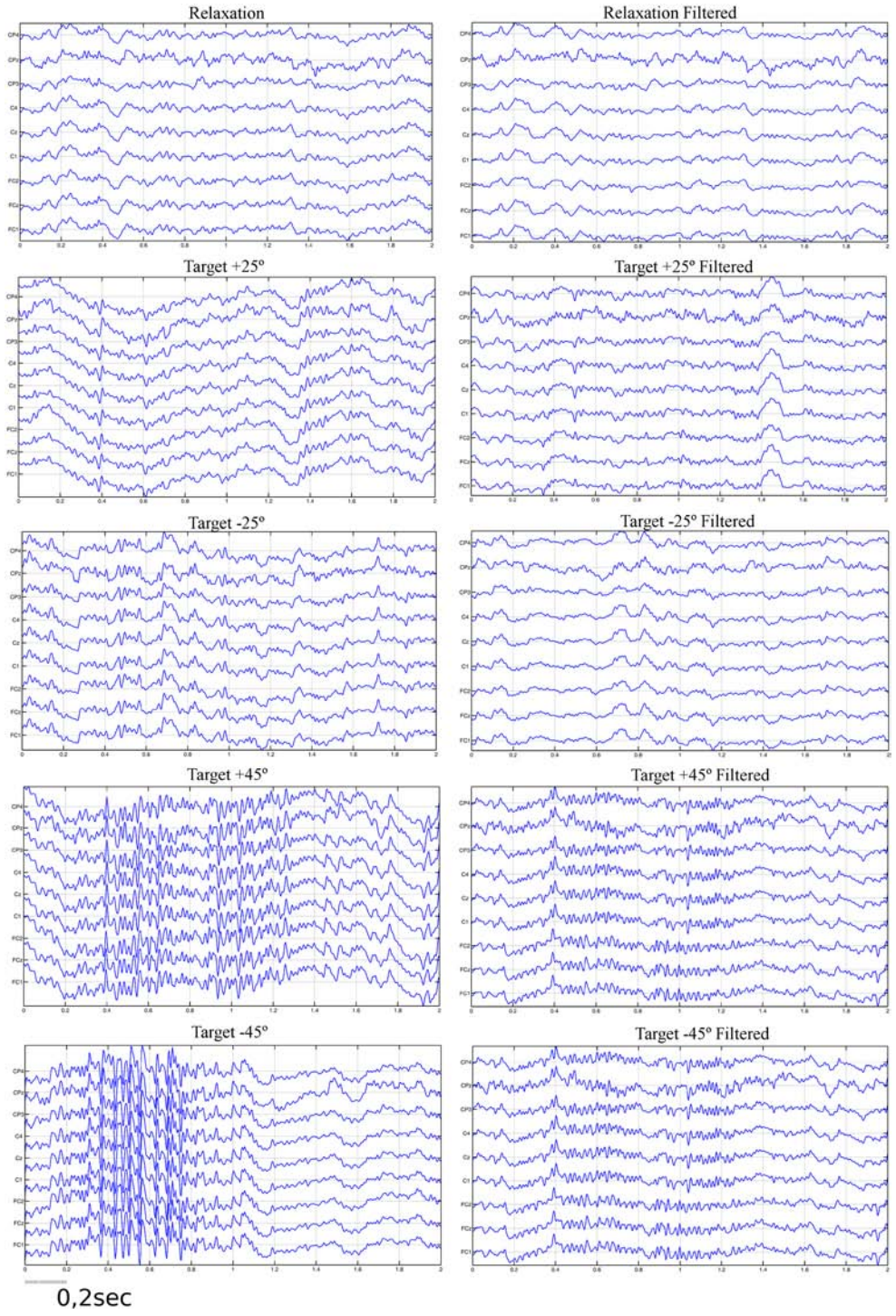

Figure 47 This figure shows for subject 3 two seconds portion of EEG signal (*left*), recorded during relaxation, target +25°, target -25°, target +45° and target -45°. The same EEG free of artifacts (*right*). The components eliminated are displayed in Figure 46.

The source localization of each trial was computed by sLORETA. EEG data were converted to cross spectrum using default frequencies, delta (1.5–6 Hz), theta (6.5–8 Hz), lower alpha (8.5–10 Hz), upper alpha (10.5–12 Hz), lower beta (12.5–18 Hz), beta (18.5–21 Hz), upper beta (21.5–30 Hz) and all bands (1.5–30 Hz). Figure 48 (a)–(d) presents localization results for the raw EEG (*left*) and EEG filtered (*right*) recorded during target +25° (a), target -25° (b), target +45° (c) and target -45° (d) for subject 3. The source localization from the raw EEG filtered in the upper alpha is in BA 37, 19, 39, 21 for all conditions respectively (see Table 5), where this neural generators are not apparently related to motor behaviour .Notice that in this case the artifacts act as noise for the sLORETA which is not able to locate activity on the motor cortex. The source localization from the EEG free of artifacts and filtered in the upper alpha/mu shows a prominent activity in the Brodmann area BA4 (primary motor cortex on the precentral gyrus). These results are consistent with previous description of motor cortex activation associated with motor execution and imagery [Dyson et al, 2010; Hanakawa et al, 2003; Pfurtscheller and Lopes da Silva, 1999]. This result shows that after the filtering, the primary motor cortex is one of the most relevant sources of the EEG (Table 5).

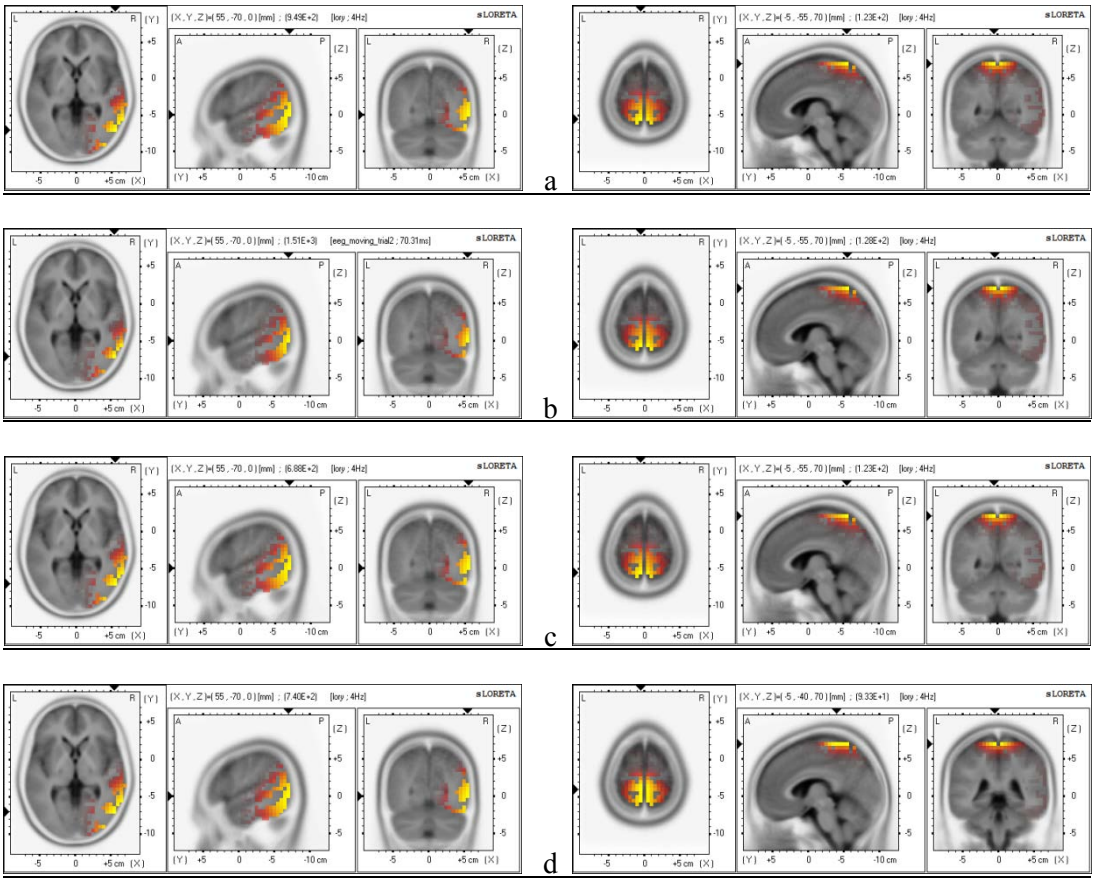

Figure 48 Source localisation results for raw EEG (left) and EEG data filtered (right) recorded during target +25° (a), target -25° (b), target +45° (c) and target -45° (d) for subject 3. EEG filtered shows activation in Brodmann area 4 in the upper alpha/mu band (10.5–12 Hz).

Brodmann Area (BA) - Best Match	Raw EEG	EEG filtered
Target +25º (a)	BA : 37, 19, 39, 21	BA : 7, 5, 4, 3
Target -25º (b)	BA : 37, 19, 39, 21	BA : 7, 5 , 4, 3
Target +45º (c)	BA : 37, 19 , 39, 21	BA : 7, 5 , 4, 3
Target -45º (d)	BA : 37, 19 , 39, 21	BA : 4, 3 , 5, 6

Table 5 The 4 Brodmann area localized trough sLORETA that show prominent activity in the raw EEG and in the EEG filtered.

Experiment II

Fig 49 displays the EEG signal recorded during relaxation and walking for subject 4. Notice that the locomotion creates a movement artifact that is more visible at low frequencies.

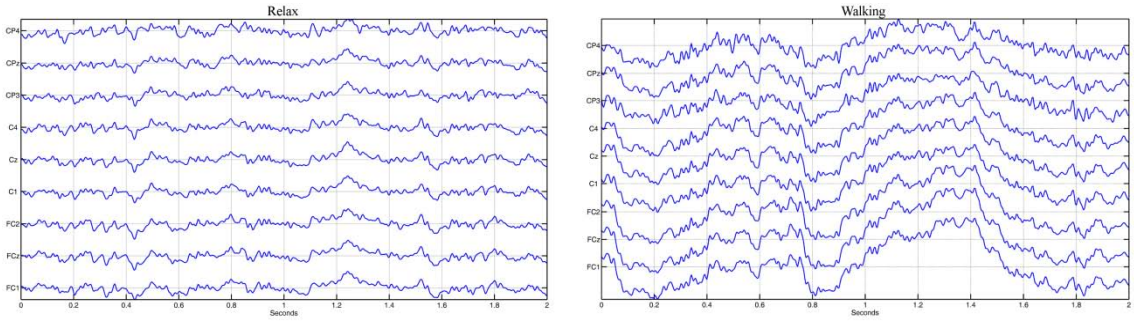

Figure 49 2 seconds portion of EEG signal recorded during relaxation (left) and walking (right) for subject 4.

Figure 50 presents the power spectral densities for subject 4 of the EEG signal recorded during walking and relaxation. The walking condition has a greater PSD at low frequency range (i.e. up to 4 Hz) reflecting the effect of the low frequency movement as it is observed in Figure 49. This artifact is also present in high frequency (30 – 40 Hz) and more prominent over central and parietal areas. Notice also that the walking creates a desynchronization in the alpha/mu rhythms in the central areas and synchronization around beta bands.

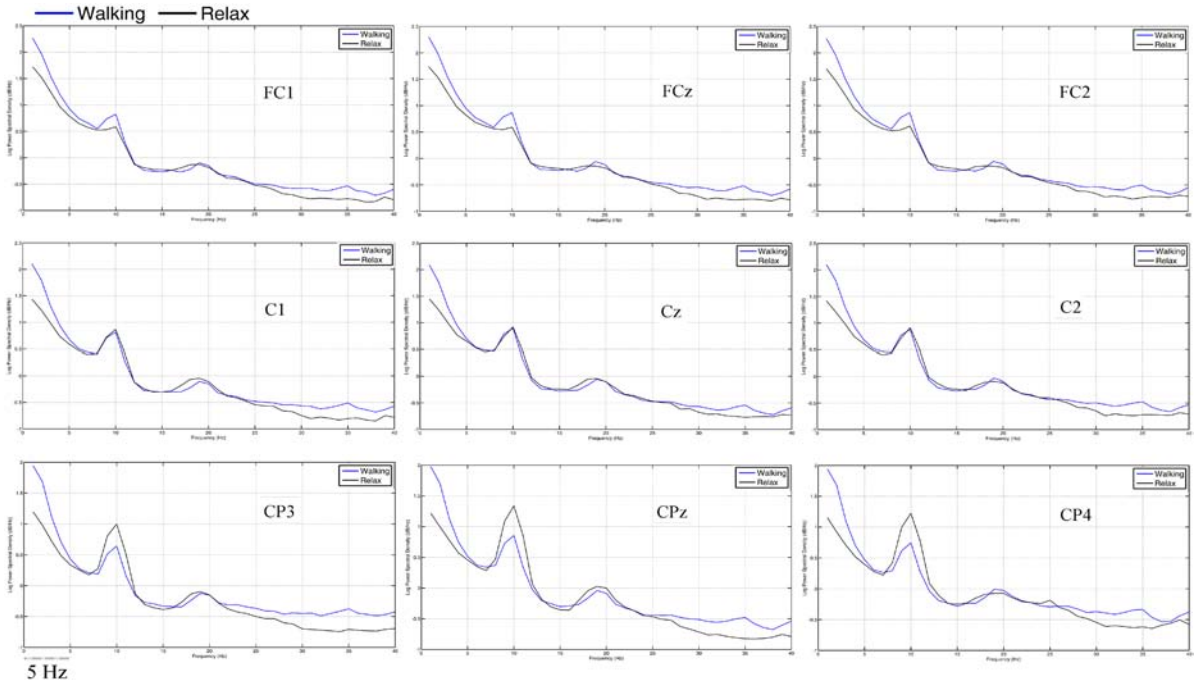

Figure 50 Logarithmic power spectral density of the EEG signal recorded during relaxation (black) and walking (blue) for subject 4

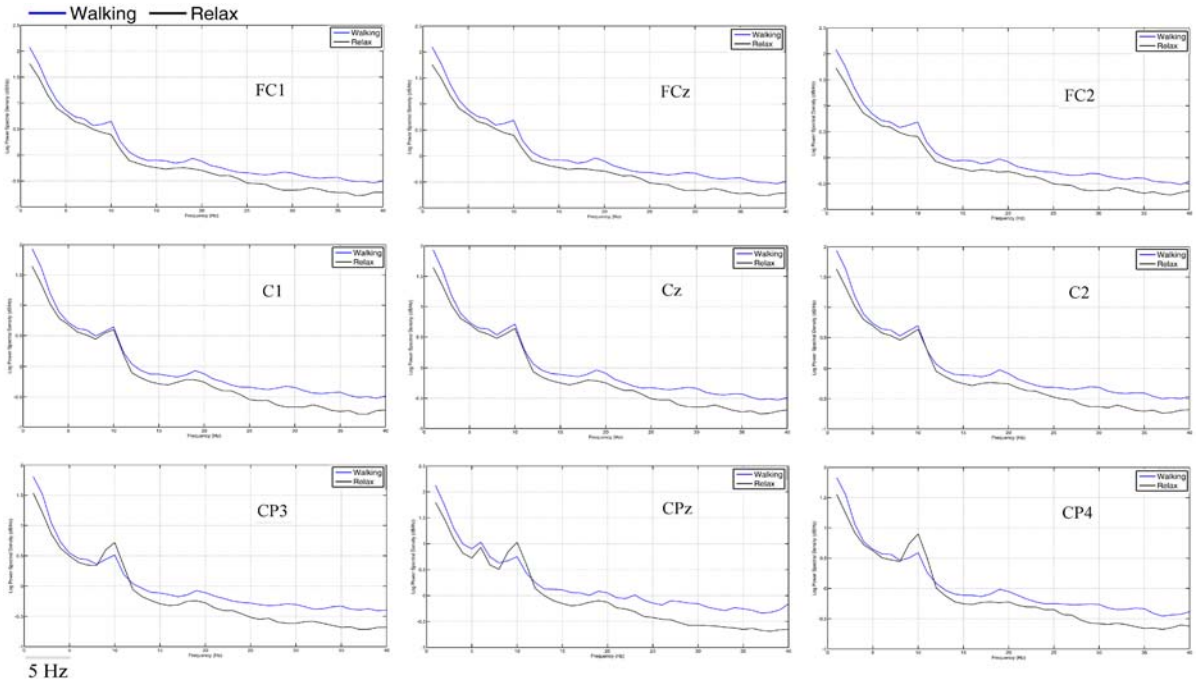

Figure 51 Average logarithmic power spectral density of the EEG signal recorded during relaxation (black) and walking (blue).

Figure 51 presents the average (i.e. all 4 subjects of the experiment) logarithmic power spectral density for EEG signal recorded during walking and relaxation. The spectral landscape is similar for all the channel locations, peaking at low frequency and decreasing smoothly as the frequency is higher. The spectra show a

peak in the alpha band (8-13 Hz) that is largest in the centro-parietal locations (i.e. CP3, CPz and CP4). Individual PSD displays sharper spectral peaks than the average one.

As in the previous experiment ICA decomposition was computed on the walking dataset separately for each subject. The ICA components were selected by visual inspection and depending on the subject, the components chosen varied between 7 and 8. Figure 52 presents some EEG trials without artifacts reconstructed through reprojection.

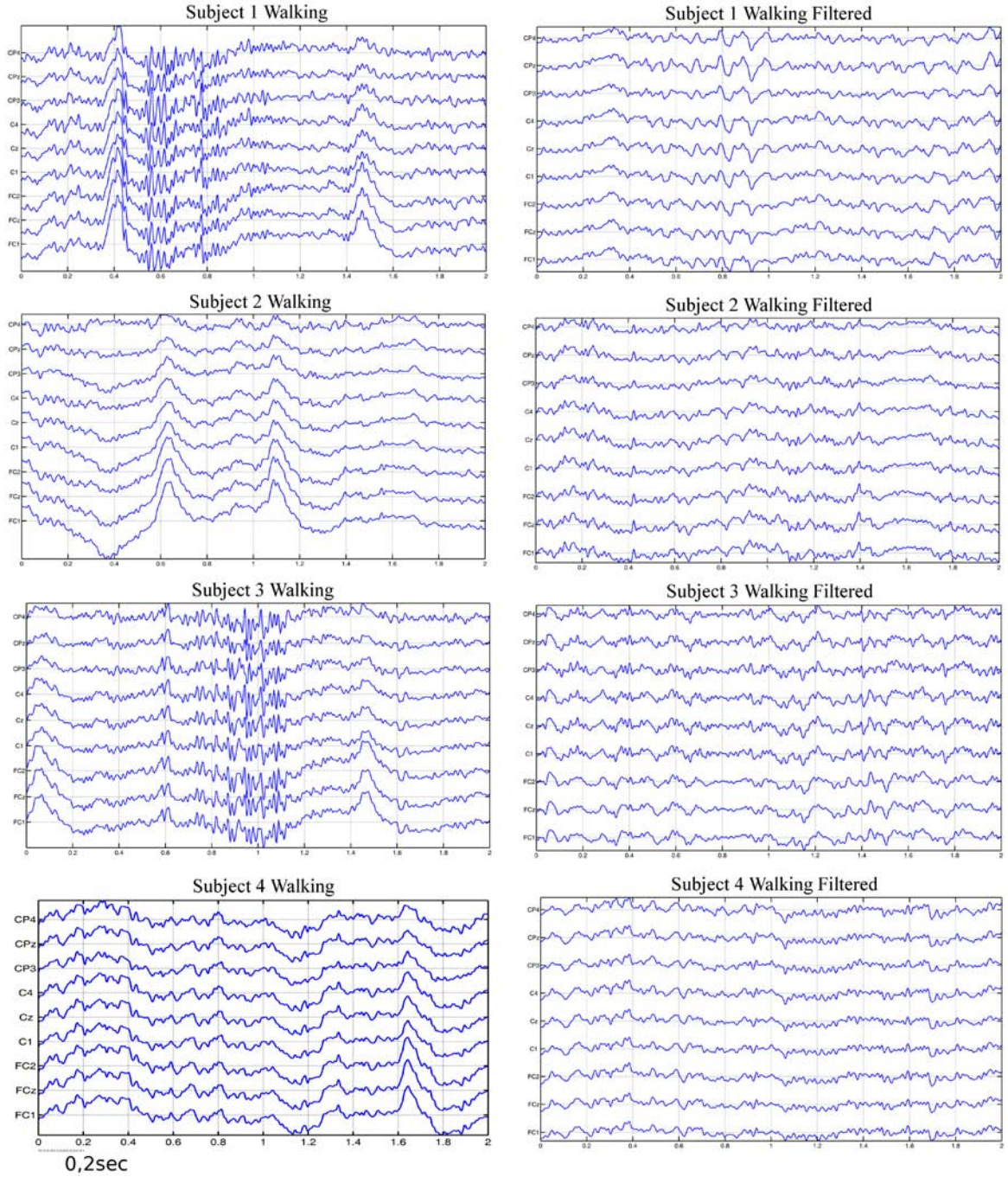

Figure 52 2 seconds portion of raw EEG (*left*) and EEG filtered (right), recorded during walking for all subjects. The filtered signal is obtained by removing the selected ICA components identified as artifacts.

3.2.4 Discussion

This deliverable reports on the analysis which describe temporal and spectrual characteristics of the main contamination introduced in the EEG by locomotion and head movements. These artifacts are likely to be present in the CORBYS 1st demonstrator. The results indicate that artifactual components can conceal or mimic EEG alpha and beta rhythms over the entire scalp as previously described for EMG contamination [Goncharova et al, 2003] and are also relevant at low frequencies.

Independent Component Analysis technique was applied to remove the artifact contamination generated as it appears to be an effective method for removing artifacts from EEG data [Jung et al, 1998]. The results suggest the feasibility of the use of this technique for artifact removal in CORBYS. The key issue for a BCI system is to what extent the artifacts components interferes with its goal. Notice that decoder-specific analysis is extremely important in order to study the feasibility of removing gait-related artifacts allowing correct interpretation of cognitive related process. In addition to this work, in the section 3.3, Detection of attention during assisted passive leg motion, of this deliverable, the ICA method was used to filter eye blinking and muscular artifacts. Results obtained indicate that ICA does not interfere with the attention decoding process, on the contrary, it improves its performances.

3.3 Detection of attention during assisted passive leg motion

3.3.1 Introduction

Neurological disorders or brain injuries such as brain stroke or spinal cord injury can cause problems in patient's movement, as the Central Nervous System (CNS) or the efferent channels from the CNS are compromised. Brain Computer Interfaces (BCI) is a technology that addresses this problem by creating a new channel to bypass the injury and recover the communication between the non affected CNS and the limb muscles. The principle is to measure the brain activity to extract some meaningful information to move the limbs by, for instance, functional electrical stimulation (FES) [Pfurtscheller et al. 2005] or by robotic exoskeletons [Pons 2008].

The electrophysiology of the motor skills is usually characterized by the event related synchronization/desynchronization (ERS/ERD), which refers to the increase or decrease in synchrony of the neural population of a determined area of the brain cortex [Pfurtscheller et Lopes da Silva 1999]. This technique has been used to quantify changes in EEG signal by calculating the increase or decrease of spectral power during a mental process compared to the brain activity during a reference time or baseline. There are associated techniques to visualize [Graimann et al. 2002] and compute [Gómez et al. 2012] neural changes in motor areas of the brain. For instance, the movement of a limb has been characterized by this method and thus it is known that neural population of the central brain cortex area (motor cortex) desynchronize in alpha and beta bands (7-13 Hz and 15-30 Hz. respectively).

Rehabilitation programs for patients with these injuries are usually based on the execution of repetitive movements to regain muscle control or to delay the loss of mobility due to the disease. One limitation in these rehabilitation therapies is that excessive repetitive movements could lead to a lack of patient engagement, compromising the adherence to the therapy. In this direction, it is well known that cognitive processes such as attention mediate in the rehabilitation and play an important role in the success of the therapy [Tee et al. 2008]. The possibility to monitor the patient attention could be a key issue in rehabilitation because it directly measures the cognitive process and indirectly the adherence to the therapy. To date, very few works have addressed the characterization of attention during the execution of motor tasks. An fMRI study has shown that the degree of attention to the motor task modulates brain activity in sensory-motor areas in such a way that focused attention produces higher activations of the motor brain rhythms [Johansen-Berg et Matthews 2002]. This result has been confirmed in the EEG domain for passive upper limb mobilization [Antelis et al. 2012]. In addition, the last paper shows that it is possible to build an offline classifier to distinguish between two conditions: passive movement with/without attention to the motor task. The present work builds in this direction by extending the previous research to the lower limbs.

The CORBYS project proposes a robot-assisted gait rehabilitation system. The objective of this deliverable is to report the progress developed by Bit&Brain Technologies (BBT) to design a BCI system to decode passive lower limb movements with attention or non-attention to the motor task. To study the viability of this decoder an experimental setup was built, where passive leg movements were performed by a mini stationary bike device while the subject was paying attention to the movement or executing a distractive task from the leg motion. The study spanned the electrophysiology and the development of an off-line classifier to differentiate between both conditions.

3.3.2 Methods

A) Experiment

4 right-footed and one left-footed healthy subjects participated in the experiment aged 20 to 28 years (mean 24.4 and standard deviation 3.28). They all signed an informed consent. Volunteers were seated in a comfortable chair in front of a computer screen. Their feet were held to the pedals of a mini stationary bike that is motor assisted to actively move the user's legs.

a) b)

Figure 53 *a)* Mini-bike and *b)* Experimental setup

The subjects were seated in a comfortable position, far enough from the mini stationary bike to allow a smooth passive movement of the legs and to avoid possible contact between the feet and the floor or furniture. The feet where held to the pedals by an elastic strip. Subjects were instructed to completely relax the limbs and to avoid voluntary leg movements during the experiment. The mini-bike and the experimental setup are displayed in Figure 53.

The experiment consisted of trials of two conditions (with attention or distraction to the motor task). In the first condition, subjects focused their attention to the legs during the execution time, while in the second one the subjects were instructed to perform mental algebraic computations as a distractor to the passive leg movement [Johansen-Berg et Matthews 2002, Antelis et al. 2012]. The algebraic computations were subtractions starting from a 3-digits voluntarily selected number and subtracting a one-digit figure voluntarily selected. Each trial started with a 5 seconds interval of time where the subjects relaxed minimizing movements and blinking while they were informed of the condition (attention or distraction) they had to

perform (the bike is stopped); followed by a 5 seconds execution time where the subject was mentally performing the task (bike is on); and it finished with a 5 seconds rest time where subjects were allowed to perform minimal movements and blinking (bike is stopped). Figure 54 shows the structure of one trial. The experiment consisted in 3 series of 30 trials, with 15 trials of each condition, presented in random order. There was a rest period of 1 minute between series. The experiment lasted 25 minutes.

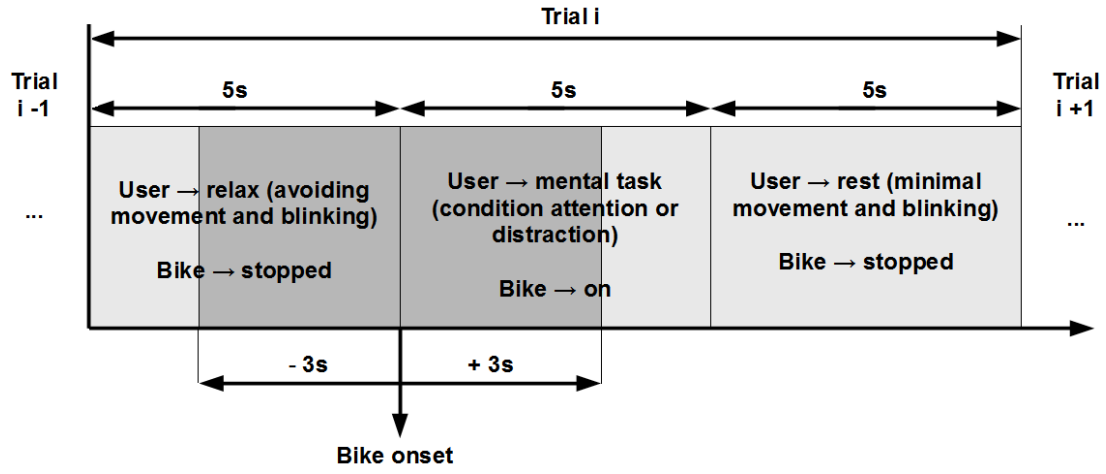

Figure 54. Example of a trial (darker grey: data processed)

B) Data recording and mini-bike

1) EEG system: EEG data was recorded by a TMSi amplifier with 16 electrodes according to the 10/10 system (FC3, FC1, FCz, FC2, FC4, C3, C1, Cz, C2, C4, CP3, CP1, CPz, CP2, CP4, Pz). Ground was located in FPz and the reference on the right earlobe. Notice that the large majority of electrodes were situated close to Cz as it is usually the sensor where the leg motor cortical activation is observed [Graimann et Pfurtscheller 2006]. The EEG signal was acquired with a sampling rate of 256 Hz, power-line notch-filtered (50 or 60 Hz) and bandpass-filtered from 0.5 Hz to 60 Hz. The acquisition and experimental software was property of Bit&Brain Technologies.
2) Mini-bike: A mini stationary bike (YF612 Tecnovita by BH) was used to move the user's legs. The angular velocity of the pedals was $\omega \sim 2\pi$ rad/s. The activation of the mini-bike was manually controlled by the supervisor of the experiment.

C) Data processing

For each subject, the EEG data was filtered by an Independent Component Analysis (ICA) algorithm (FastICA based on [Hyvärinen et Oja 2000]) to eliminate the components from blinking, EMG artifacts and electrical noise from the mini-bike. Each component was reprojected back to the sensor space, and time and time-frequency representations of these reprojections with the associated spatial filter were visually inspected to assess whether the component was artifacted. The components free from artifacts were reprojected back to the sensor space to obtain an artifact free EEG. This EEG was filtered and then, for each trial, the [-3s,3s] interval with respect to the mini-bike onset was extracted (see Figure 54). These new trials were again visually

inspected to assure they are artifact-free. Then, for each trial, the across-trials average was subtracted for each condition in order to remove the evoked potential caused by either the beep sound from the mini-bike device when it was activated and/or the sudden start of the motion.

The ERD/ERS during the motion process was obtained by (Pj-Ppas)/Pbas*100, where Pj is the power of each time-frequency bin of the j-trial from the onset of the mini-bike (0s) to +3s and Pbas means power of the baseline (-3s to 0s). Power spectra were computed by the Welch method with a sliding window of 128 samples with 120 samples of overlapping between consecutive windows. ERD/ERS is represented as a time-frequency plot where time varies from -3s to +3s and frequency from 0 Hz to 50 Hz. Significant ERD/ERS was computed by a bootstrap algorithm with a significance level of 0.05 [Graimann et Pfurtscheller 2006] (Figure 55).

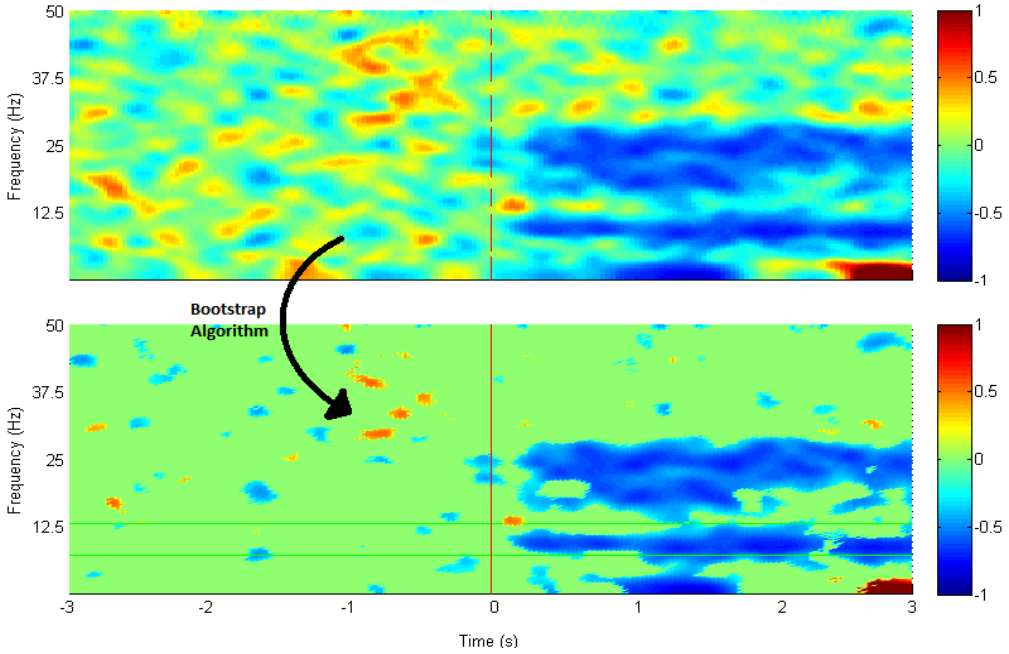

Figure 55 Example of bootstrap algorithm in a ERD/ERS time frequency map

D) Feature extraction and classification

A classifier was built to detect each condition (i.e. if the subject is paying attention or not to the leg movement task). The features extracted were the spectral power of channels (with significant desynchronization) located in the motor cortex area in alpha and beta bands (individually selected by visual inspection of the ERD/ERS from the most discriminant electrode). Welch method was used to compute the spectral power with a sliding window of 128 samples and a 120 samples overlapping. Features were concatenated, z-score normalized and used to train a linear discriminant analysis (LDA) classifier. A 10-fold cross validation procedure was performed to assess the generalization properties of the classifier.

3.3.3 Results

Figure 56 displays the ERD/ERS maps for the 5 subjects that participated in the experiment. Subjects 3, 4 and 5 showed a higher desynchronization during attention to the motion than in the other condition. This

desynchronization was more prominent in both bands (alpha and beta) for subjects 3 and 5, and in the beta band for subject 4. For Subject 2 the results are the contrary (i.e. higher activity in the distraction task) which could be due to the way that this subject performed the mental task. For subject 1 is difficult to visually identify the differences as it seems that the desynchronization in alpha is lower but the beta is higher in the attention condition than in the other, so more elaborated tools to quantify this desynchronization might need to be applied [Gómez et al. 2012]. In summary, in all the cases individually is possible to visually detect differences between the two mental states.

Figure 56 ERD/ERS maps for the five subjects from top row (Subject 1) to bottom row (Subject 5) for both conditions. First column: Passive Motion + Attention. Second Column: Passive Motion + Distraction. Black dashed line: individualized alpha band. Red dashed line: individualized beta band.

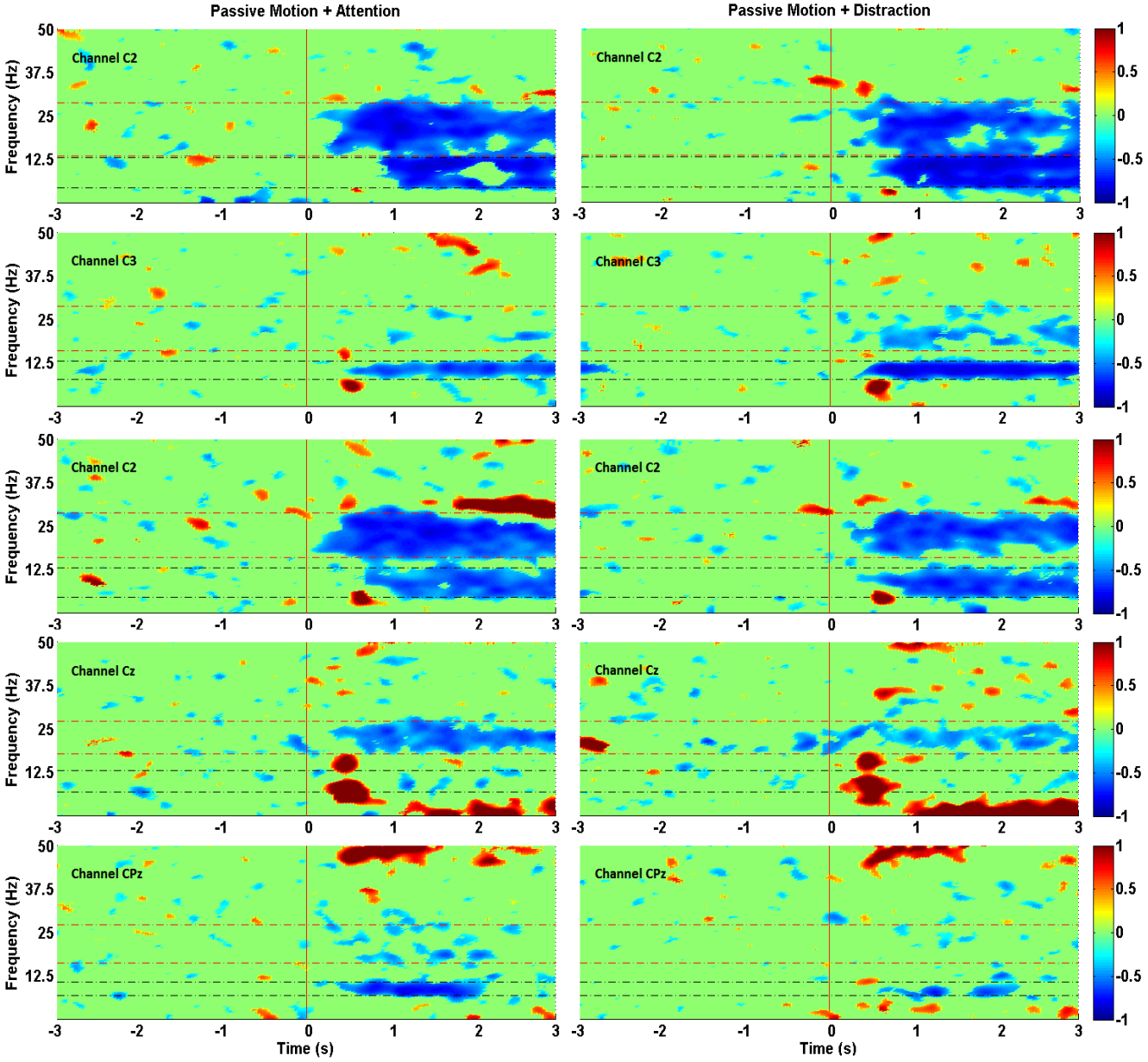

A Linear Discriminant Analysis (LDA) classifier was used to differentiate between both conditions. Three

different sets of features were used to train our classifier. In the first one only power in alpha band was used, in the second one only beta band power, and in the third one both previous features were used together. Bands and channels were visually and manually selected for each subject to calculate the features. The final results are shown in Table 6.

Subject	Accuracy alpha	Accuracy beta	Accuracy alpha+beta
1	75.00	63.33	**81.67**
2	62.86	**82.86**	80.00
3	57.14	**70.00**	64.29
4	61.67	**70.00**	66.67
5	76.67	75.00	**81.67**

Table 6 Results for each band of each subject

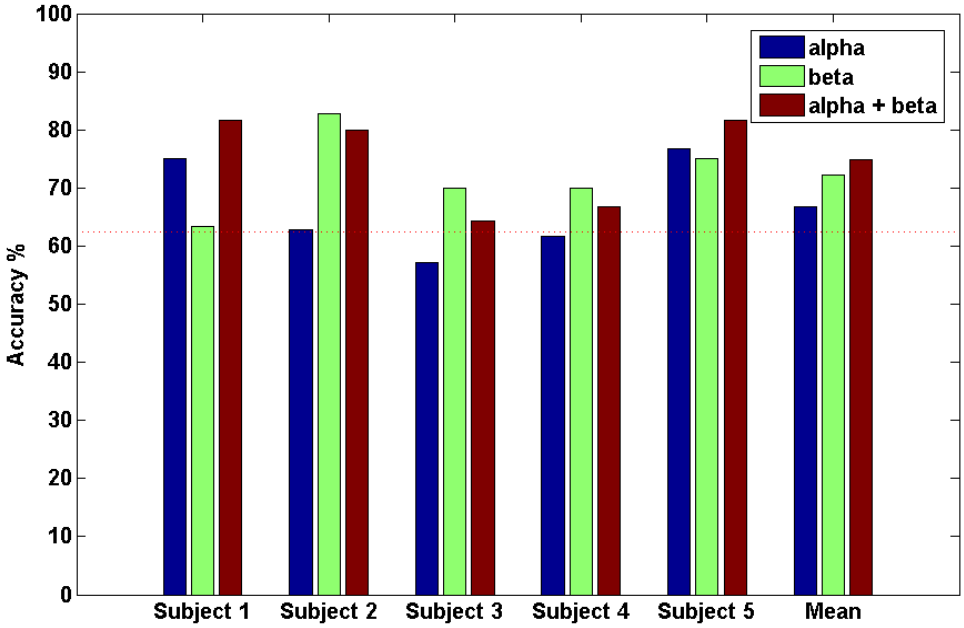

Figure 57 Results for each band of each subject (dotted line = chance level according to [Müller-Putz et al. 2008] (p<0.05))

As shown in Table 6, the classifier performance for all subjects is over the chance level which is situated in 62.5 % according to [Müller-Putz et al. 2008]. Beta band features achieved higher accuracy for subjects 2, 3 and 4 while for subjects 1 and 5 the combination of both bands features was the better election. The mean accuracy is 77.24% (selecting the best result of each subject), showing that it is possible to build a classifier over the chance level and thus showing the feasibility of building an off-line system to differentiate the two conditions.

3.3.4 Discussion

Cognitive processes such as attention affect rehabilitation exercises and they play a key role in the result of the therapy. Presented work shows that the attention modulates brain activity during passive leg movements as observed in the EEG signal. An off-line classifier was developed to differentiate between two states (attention or distraction to the motor task). The results show the feasibility to distinguish between both conditions above the chance level for all the subjects. This is the first step in the development of the attention decoding unit of CORBYS. This research could be improved in several directions. For instance, source localization techniques will be needed to confirm that the EEG changes observed between conditions have the neural origin in the motor cortex (as demonstrated by fMRI studies [Johansen-Berg et P. Matthews 2002]). In addition to this, the subjects had to focus in the screen but their legs were not concealed from his or her gaze, which could have an influence on the motor activity. Although this aspect influences both conditions, further investigation is required. Future work will consider the movement artifacts (analysed in the section 3.2, Analysis and removal of movements' artifacts during locomotion, of this deliverable) and the automation of feature selection process. Eventually, notice that the final next step is to build an online classifier to assess the feasibility of decoding attention during motion in real time which is the user scenario in the CORBYS project.

4 Safety

Work with safety aspects of the CORBYS demonstrator I and of all its components is started and will be documented in documents that will accompany the deliverable on the final demonstrator D7.4 (M36), covering safety standards and procedures. In the following safety aspects of HSS and BCI module are given together with FMEA risk analysis

4.1 Chest unit

The chest unit is a battery powered device using wireless communication. This ensures patient safety with respect to electrical shock.

The CORBYS Chest Unit uses conductive rubber electrodes for ECG measurement. These gives signal quality comparable to the medical electrodes, also when the patient is very active. A disadvantage is possible skin irritation when sweat collects under the rubber and this may cause some skin irritation during prolonged use. However CORBYS training sessions will be of limited duration. The sensors are integrated in the chest unit, and automatically placed correctly when the patient puts on the device.

The sensor belt will attract sweat and dirt after use and should be rinsed in lukewarm water (no soap) once a week, and then left to air-dry. However one must remember to detach both the chest unit and the IMU-unit from the belt before washing as the units are not water-resistant. The units can be wiped with a soft damp cloth and towel-dried.

4.2 IMU unit

The IMU unit is a battery powered device using wireless communication. This ensures patient safety with respect to electrical shock. The unit has no electrical contact with the patient.

4.3 EMG units

The EMG sensors will be covered in D3.4

4.4 HSS controller computer

The HSS Controller will be located on the mobile platform for CORBYS demonstrator I. The controller is powered from the mobile platform batteries (24VDC). It will not be physically connected to the patient. Electrical safety insulation towards the grid power supply (220VAC) is handled by the Central Power System on the mobile platform.

4.5 Offline charger

The sensor unit shall not be charged while attached to the patient. This means that the offline charger will not be physically connected to the patient. The charger will be powered from the HSS controller or by use of a separate power supply.

4.6 Safety analysis:

As part of the safety work for demonstrator I, FMEA safety analysis has been performed for all components of the system as reported in Deliverable 7.1. The analysis for the HSS is shown in the figure below. It shows that there are no high risks connected to the HSS. The medium risks will be addressed at the system level risk analysis and handled by other modules. Incomplete datasets due to failing or missing sensors must be handled by receivers of data from HSS, all sensor data shall be defined with a valid range of values. To avoid incorrect data due to incorrect sensor location there will be a therapist procedure to validate sensor data before each training session.

Pos.	FUNCTION	POTENTIAL failure MODE	POTENTIAL CAUSES	POTENTIAL EFFECTS	DETECTION METHOD	SEV	OCC	DET	RPN	Recommended Action(s)	SEV	OCC	DET	RPN
1	**Human Sensory System Controller**	connection loss to GPN	Network error	no sensor data to cognitive modules	ROS heartbeat	7	5	1	**35**	FS must check HSS heart beat and handle any detected errors according to FS specification.				0
		failure / time lag	runtime error for HSS controller hardware	delay on sensor data to cognitive modules, may lead to incorrect cognitive recognition	Timestamped sensor data. Timestamps are synchronized by ROS framework.	7	5	3	**105**	Cognitive modules must check timestamps.	7	5	2	**70**
		failure / time lag	Configuration error	missing or delay on sensor data to cognitive modules, may lead to incorrect cognitive recognition	Timestamp on sensor data/ cognitive modules detects missing data. Timestamps are synchronized by ROS framework.	7	5	3	**105**	Cognitive modules must check timestamps. Cognitive modules should handle incomplete datasets. Data from HSS to be verified in pre-session procedures.	7	5	2	**70**
2	**Human Sensory System Wireless Body Sensors**	measurement failure	Sensors pick up external noise	incorrect sensor data to cognitive modules	HSS controller detects out of range sensor data	7	4	6	**168**	Cognitive modules should validate sensor data - to be discussed with cognitive partners				0
		measurement failure	Defect sensor, incorrect sensor connection	no sensor data to cognitive modules	HSS controller detects inoperable missing sensor data	7	3	1	**21**	HSS controller reports errors to FS, which handle detected errors according to FS specification. Cognitive modules should handle incomplete datasets.				0
		measurement failure	Defect sensor or incorrect sensor location during setup	incorrect sensor data to cognitive modules	Therapist detect in pre-training session procedure	7	3	2	**42**	Therapist procedure to be developed, also included in safety document				0

		measurement failure	Defect sensor or incorrect sensor location training session	incorrect sensor data to cognitive modules	HSS controller detects out of range sensor data	7	3	6	**126**	Cognitive modules should validate sensor data - to be discussed with cognitive partners				0
		measurement failure	Sensor module run out of power	no sensor data to cognitive modules	HSS controller monitor remaining battery capacity	7	6	1	**42**	Status on sensor modules is sent via ROS heartbeat to FS. FS must handle any detected errors according to FS specification. Cognitive modules should handle incomplete datasets.				0
		biocompatibility	irritations/ inflamatic responses or pain	patient uncomfortable or unable to wear sensor	Patient response and inspection	6	5	2	**60**	Patient inspection should be added to post training session procedure.				0

Table 7 Safety analysis for HSS

The safety design of the Brain Computer Interface (BCI) submodule has two different levels of analysis: hardware and software:

4.7 EEG unit

The amplifier Porti System – TMSi of the BCI complies with the following safety requirements:

- CE0044: meets all the requirements of the MDD (93/42/EEC) MDD Classification IIa (rule 10).
- Applied standards :
    - IEC 60601-1:1988 + A1:1991 + A2:1995 : Medical electrical equipment - Part 1: General requirements for safety
    - IEC 60601-1-2:2001 : Medical electrical equipment - Part 1-2: Electromagnetic compatibility
- Safety class (IEC 60601-1): Internally or externally powered, type CF

4.8 BCI Software

The Software of the BCI submodule provides the following output regarding the state of the BCI sensors.

1. *EEG sensor failure :* information about the actual state of the EEG sensor indicating if it is working properly or not (e.g. it can happen that an electrode gets disconnected or broken during the rehabilitation session causing wrong recordings).

The EEG sensor failure will allow then to have a complete overview on the BCI submodule status.

4.9 BCI Safety analysis:

The table below presents the risk analysis for the BCI submodule. Medium and high risks are related to EEG signal contamination (i.e. patient movement noise and physiological noise); section 3.1, Analysis, evaluation and removal of movement artifacts from EEG measurement during locomotion, of this deliverable addresses the mechanical artefacts and their removal process. Removal algorithms mitigate the effect of the artifacts on the EEG signal, where the detection value in the table indicates how much the filter can reduce this contamination. This value will change since it is strictly dependent on the decoding algorithm implementation (actually under study).

Pos.	FUNCTION	POTENTIAL failure MODE	POTENTIAL CAUSES	POTENTIAL EFFECTS	DETECTION METHOD	SEV	OCC	DET	RPN	Recommended Action(s)	SEV	OCC	DET	RPN
1	**BCI software**	GPN connection loss	network error	no sensor data to other module/s	ROS heartbeat	8	4	1	**32**					
		data package loss	GPN network error	delay on sensor data	Data timestamp	7	4	1	**28**	Check Timestamp	7	4	1	**28**
2	**BCI sensors**	measurement failure	incorrect sensor setup	no sensor data to other module/s	BCI software detects incorrect sensor setup	7	5	2	**70**					
		measurement failure	incorrect sensor connection	no sensor data to other module/s	BCI software detects incorrect sensor connection	7	2	1	**14**					
		measurement failure	faulty sensor	no sensor data to other module/s	BCI software detects faulty sensor	7	3	3	**63**					
		measurement failure	sensor module out of power	no sensor data	BCI software detects when the sensor module is out of power	8	3	1	**24**					

		measurement failure	instrumental/environmental noise	incorrect sensor data to other module/s	Signal processing algorithm of the BCI software mitigate the potential effects	7	3	3	**63**					
		measurement failure	patient movement noise	incorrect sensor data to other module/s	Signal processing algorithm of the BCI software mitigate the potential effects	7	8	5	**280**					
		measurement failure	physiological noise	incorrect sensor data to other module/s	Signal processing algorithm of the BCI software mitigate the potential effects	7	9	3	**189**					

Table 8 Safety analysis for BCI

5 Requirements from D2.1

This section lists the relevant requirements for Human Sensory System and Brain Computer Interface from D2.1 and how these have been fulfilled or implemented.

Req. #	***Name***	***Description***	***Realization***
HSS1	Sensors implemented in the CORBYS system	The actual sensors selected will be defined in the detailed specification	Implemented: Heart rate and ECG Skin temperature at chest and back Humidity sensors at patient back Inertial measurement units (3 axis accelerometer, gyroscope and magnetometer) at patient chest and back To be implemented in D3.4 EMG (muscular activity) Mechanical sensing (force, torque, angular joint movements, force/pressure distribution) will be implemented by sensors in Demonstrator I in WP7.
HSS2	Sensor locations	The actual sensors selected will be defined in the detailed specification.	Implemented sensor and functionality: Homing positions of inertial sensors is handled at session start-up by therapist. A sensor for measuring environment temperature and humidity is developed and will be attached on mobile platform. Requirements that will be handled by mechanical sensors in Demonstrator I in WP7: Positions of robot mechanical support to the patient (such as limb fixation) and patient movement actuators.
HSS3	Patient user size	Adult users. Height, weight circumferences will be discussed with clinical partners	HSS will fit all patients relevant for CORBYS usage.
HSS4	Sensor output of primary parameter values	Definition on how human sensor parameters are shared with the rest of the CORBYS system, as well as in export to	Implemented: Sharing is done through ROS topics, details are described in HSS Controller section.

		log files: Details are to be defined.	Logging to file is used in early integration phases, will also be available as ROS bags. See HSS controller sections.
HSS5	Safety-related sensor output – information derived from sensor fusion of multiple sensors	Status information or flags should be raised if sensor readings indicate a potentially hazardous situation. To be discussed with partners with stakes in the design of CORBYS control system	Project has not identified need for sensor fusion from HSS for Safety. Handling of potentially hazardous situations will be discussed in D7.4.
HSS6	Sensor output related to physical effort assessments	HSS will provide human sensor data related to physical effort, which is heart rate, ECG, humidity, temperature, EMG and movement data.	Data will be processed by SAWBB (to be described in D4.3) Initial discussions have taken place between SINTEF and UR on input requirements for the Situation Assessment architecture, with respect to physiological sensor output. Based on these requirements, sampling rate, timestamp resolution etc. have been revised for heart rate, ECG. The revised ESUMS HSS dataset from SINTEF was received by UR, and is currently being utilised as part of effort undertaken in WP4. Similarly, activity sensing output (IMU data) provided as input to the Situation Assessment architecture; UR is making use of revised HSS ESUMS dataset, in which gyroscope was included. Also SOIAA will make use of this data in the adaptive walking mode that will be presented in D5.2 and D5.3
HSS7	Sensor output related to gait parameter assessments	Same data provided as listed in HSS6	Same as HSS6
HSS8	Sensor output related to identification of psyco-physiological states	Same data provided as listed in HSS6	Same as HSS6
HSS9	Sensor output related to identification of intentional states	Same data provided as listed in HSS6	This will be handled in D5.3 for adaptive walking mode. This is where SOIAA provides gait trajectories from BCI intention data, HSS sensor data, which facilitate the patient and orthosis being able to walk freely in a structured environment.

HSS10	Data processing and signal analysis requirements	The project needs to sum up all the data processing requirements, both capacity and platform wise.	HSS controller will be running on separate computer with sufficient processing power for HSS tasks.
HSS11	Integrating physiological sensor measurements (SINTEF) with BCI (BBT)	Discussions between BBT and SINTEF regarding finding a shared platform for integrating sensor signals.	All sensor measurements are presented to cognitive modules as individual ROS topics. BCI and HSS sensor data will be provided for cognitive modules with consistent timings allowing for various latencies, to provide a full picture of the patient over time.
HSS12	Interfacing physiological sensor measurement system with the main CORBYS cognitive robot control system		Wireless sensors are connected to General Purpose Network (GPN) for interfacing cognitive modules and control.
HSS13	Mains requirements	It must be anticipated that some of the measurement equipment will require 220V/50Hz	HSS Controller will be running at 24VDC
HSS14	Sensor network architecture requirements	The project needs to compile a summary of all sensors and actuators (with detailed operation characteristics and worst-case values) in order to specify the total sensor network architecture.	Worst case values will be specified as part of the GPN specifications in D3.4.
HSS15	Online access to past rehabilitation sessions	Online access to past (and possibly ongoing) therapy sessions implies a software architecture solution, as well as probably a WiFi node on the CORBYS system	Human sensory system values can be recorded at the GPN and will be described in D3.4
HSS16	CORBYS system intermittence, delay and synchronisation requirements for sensors and actuators	A shared understanding of signal propagation will have to be reached between the partners.	All sensor data will be time stamped. D3.4 will discuss synchronization of computers on GPN. HSS sensor data delays are discussed in section 2.1.2
HSS17	Number of physiological sensor probes on the patients	The detailed number is TBD. No limitations are stated at this stage.	Implemented: There will be one Chest unit at front and one IMU sensor unit at the back of the patient. One IMU sensor unit will be located at the mobile platform to measure environment humidity

			and temperature Postponed: Four EMG sensors located at each patient leg.
HSS18	Number of physiological sensor probes on the patients	For ease-of-use purposes, it will be desirable to combine several sensors into single devices, thereby reducing the experienced system complexity	See HSS17
HSS19	Signal connection of physiological sensors to the CORBYS system	Sensor data signals will be sent through electrical wires/cables	Implemented Physiological sensors are transmitted using Bluetooth to HSS controller. HSS controller use wired Ethernet for communication over GPN,
HSS20	Signal connection of physiological sensors to the CORBYS system	For ease of use purposes, possibilities to make some sensor units transmit data using wireless communication protocols will be considered	See HSS19
HSS21	Intended duration of continuous usage of physiological sensors	Anticipation: A therapy session will last up to 2 hours	The chest unit and IMU sensor unit will have battery capacity for more than 2 hours. Final battery capacity measurements will be provided in D3.4. Two sets of units will follow the demonstrator. One set for use and another charging. Charging time is less than 2 hours. There will be one charging station following the demonstrator.
HSS22	Intended duration of continuous usage of physiological sensors	Anticipation: 8 hour sessions	See HSS21
HSS23	Intended duration of continuous usage of physiological sensors	If CORBYS becomes a “community walker” gait assistance system, usage sessions could last from morning to evening.	See HSS21
HSS24	Electrical measurement system safety	Within Consortium electronic systems are acceptable as long as they are tested and deemed safe for the CORBYS users (e.g. complete user shielding from 220V/50Hz).	This requirement will be handled in the safety discussion in D7.4
HSS25	Electrical measurement system safety	CE Medical device standard electrical safety	See HSS24

HSS26	Electrical measurement system safety	Medical device CE approvals on all sensor components (For a commercial product after CORBYS)	See HSS24
HSS27	Sensor systems should not be invasive or excessively obtrusive	In vivo (implanted) sensor systems are not a part of the CORBYS physiological measurement system Sensor concepts probing human fluidic samples (blood, urine, saliva etc.) are excluded Sensor concepts probing human body openings (such as rectal core temperature measurements and breath air gas analysis) are excluded	Fulfilled in HSS designed.
HSS28	Limitations in the range of acceptable users	Based on user safety concerns, the physiological measurements system might not be used on patient groups such as: • Patients with electronic implants • Patients with certain dermatologic conditions • Patients with limitations in cognitive capabilities • Others - to be decided	HSS should not be used by patient with electronic implants.
HSS29	Mounting and removal sensors on the patient	The physiological sensors will be mounted and removed by trained clinical rehabilitation professionals	Usage scenario and sensor mounting will be described as part D7.4
HSS30	Mounting of individual sensor components directly on the user's skin	Certain physiological sensors (for example electrode based) can be placed at optimum measurement locations, directly on the skin of the patient.	See HSS29
HSS31	Mounting of individual sensor components directly on the user's skin	Less optimal, but more user friendly locations can be used.	See HSS29
HSS32	Placement of sensor components on the patient	All sensor components should be clearly marked in order to reduce the risk of placing sensors in incorrect measurement positions (e.g.	See HSS29

		mix left and right)	
HSS33	Placement of sensor components on the patient	Preferably automated detection mechanisms to avoid the risk of incorrect placement	Therapist GUI shall be used for sanity check of sensor data at session startup and during training sessions. This will be described as part of D7.4.
HSS34	Physiological sensor biocompatibility issues	Sensors should not cause irritations/inflamatic responses or pain during the designated duration of CORBYS rehabilitation sessions. Sensors can be temporarily attached to the patient using e.g. medical grade adhesive tape	The Chest belt has been tested with patients and no biocompatibility issues has been observed. EMG sensors will be covered in D3.4
HSS35	Physiological sensor biocompatibility issues	EC Medical device standard biocompatibility testing of all materials interfacing the patient	This is an optional requirement and no testing towards EC Medical device standard biocompatibility has been done. However informal testing has been dine, see HSS34.
HSS36	Physiological sensor hygienic issues	Physiological sensor interfacing the patient's skin directly should be possible to clean or replace from patient to patient: Single use probes Multiple use probes that have smooth surfaces and that can be cleaned in appropriate detergents	Cleaning and replacement of Chest Belt will be described in D7.4.
HSS37	Time required to mount or dismount all physiological sensors	For a trained user, it should be possible to mount all sensors within the maximum time required for the entire start-up and shut-down times targeted for the entire CORBYS system. Time allocated for the physiological sensor system alone is TBD.	Chest unit and IMU sensor unit should be possible to mount within one minute. EMG mounting time will be given in D3.4
CCM10	Connection to sensing network sub-system.	Sensing network sub-system should provide pre-processed sensor data for cognitive modules in appropriate time rate.	ROS is used for interfacing HSS and cognitive modules. ROS topics are described in the HSS Controller sections.
SIREF2	Sub-systems to be integrated must be accompanied by sufficient	The documentation required in order to integrate sub-system components into a	This document together with D3.4, CORBYS Users manual and source code will be sufficient

	documentation	complete system, such as: Functional specification Mechanical design drawings User manual Source code Interface definitions Installation guidelines	documentation for sub-system integration.
CTREF 7	Conformance testing test protocol design	Test plans shall have unique definition of test objects (physical components shall be uniquely marked and software shall have correct version numbering). It shall further contain information about test site, test date and test personnel The test protocol when feasible will be designed with the following information for each test item: Unique test item number Description of test activity Description of expected test result (which should be in accordance with target specifications) Check box field for entering test result with the following alternatives: Passed/Failed Field for entering test observation (in particular observations when the "Failed" box was checked.	HW replaceable components will be marked with serial number. SW replaceable components will be marked with ID and revision.

Req. #	***Name***	***Description***	***Realization***
BCISW1	BCI communication interface	External interface that communicates with other subsystems using a TCP/IP messages protocol.	To be addressed in WP6 (i.e. ROS)
BCISW2	Therapist GUI	The graphical user interface (GUI) allows the therapist to interact with the BCI software.	To be addressed in WP6 and WP7 (i.e. User interface design and implementation, Demonstrator development)
BCISW3	Subject GUI / User GUI	In the training and decoding process subjects are asked to perform some tasks.	It has been already addressed in D2.2. Further analysis will be

			addressed in WP6 and WP7 (i.e. User interface design and implementation, Demonstrator development)
BCISW4	BCI software portability	The BCI software can run over different operating systems (Windows, Linux, etc.)	To be addressed in Task 3.4/Deliverable D3.4
BCISW5	EEG sensor cap size	The cap is available in 3 sizes (small, medium and large); the most appropriate one needs to be chosen depending on the subject head circumference. Anyway the medium-sized cap is suitable for over 95% of all adult subjects.	Requirement that needs always to be accomplished since the quality of the signal depend on it. In the present deliverable it was accomplished.
BCISW6	EEG Electrodes location and number	The EEG electrodes are inserted via small holes in the cap. Their position on the scalp, indicated on the cap according to the extended international 10/20 system, and number depends on what brain areas are activated during a specific cognitive task. Ongoing CORBYS research will identify those (Tasks 3.3 and 3.5).	In this deliverable different EEG setup has been used depending on the task to focus on. This issue will be addressed in detail during the development of Task 3.3 and 3.5/ Deliverable D3.4
BCISW7	Subject screen / User screen	The graphical user interface (GUI) displays commands to the subject (e.g. a visual cue indicating that the subject has to start walking).	To be addressed in WP7 (i.e. Demonstrator development)
BCISW8	Therapist screen	The graphical user interface (GUI) allows the therapist to interact with the BCI software.	To be addressed in WP6 and WP7 (i.e. User interface design and implementation, Demonstrator development)
BCISW9	BCI processing unit	The minimum computing power needed depend on the results of the ongoing CORBYS research (e.g. laptop, netbook, personal digital assistant, etc.).	To be addressed in Task 3.4/Deliverable D3.4
BCISW10	EEG system montage	A fast and easy EEG system montage, cap and electrodes placement is required. Associated with these requirements the most appropriate system will be used.	The choice of the CORBYS EEG hardware has been addressed in the current deliverable (section 3.1). The EEG system chose is water-based; log time and uncomfortable preparation issues have been solved.
BCISW11	EEG system portability	A reduced size and weight EEG system is required. Associated with these requirements the most appropriate system will be used.	The choice of the CORBYS EEG hardware has been addressed in the current deliverable (section 3.1). Even if the priority in the EEG hardware selection has been given to the performance of the EEG

			system in a noisy scenario, this requirement has been accomplished.
BCI1	Execution Mode	Indicates which operation between training and decoding is going to be used. BCI requires a machine free training stage before users can work the technology. The training process modifies some internal parameters that successively the decoding process uses. This procedure must be observed for each cognitive-related task is planned to be used. A training phase is also needed for the artefacts removal processing (Training artefacts). The possible values of the execution mode input are - Training motion * - Training feedback - Training attention - Training artefacts - Decoding motion - Decoding feedback - Decoding attention - Decoding motion & feedback - Decoding motion & attention - Decoding feedback & attention - Decoding motion & feedback & attention - Stop The independence of the cognitive-related tasks allows their simultaneous execution in the decoding process (i.e. Decoding motion & feedback, Decoding attention & feedback, etc.). A stop input value has been also added to	Signal processing/Decoding part of the requirement will be addressed in Task 3.3 and 3.5/Deliverable D3.3; Integration in the BCI architecture will be addressed in Task 3.4/Deliverable D3.4

		allow the interruption of the running processes. *Motion, feedback and attention are the abbreviations for intention of legs motion, feedback error-related potential and attention states respectively.	
BCI2	Configuration File	Values of the optional parameters, a default setting is provided A list of possible optional parameters is available below: - Number of electrodes to be used. - Sampling rate of the EEG signal. - Decoders parameters. A complete list will be provided depending on the results of the ongoing CORBYS research.	To be addressed in Task 3.4/Deliverable D3.4
BCI3	Raw EEG	Electroencephalographic signal acquired by the BCI hardware	Integration in the BCI architecture will be addressed in Task 3.4/Deliverable D3.4 Integration in the CORBYS system will be addressed in WP6.
BCI4	Filtered EEG	Electroencephalographic signal filtered from occurring artefacts	Signal processing/Decoding part of the requirement has been partially addressed in the current deliverable (i.e. section 3.1 and 3.2) where an analysis of EEG hardware and EEG artefacts has been performed. Further analysis will be addressed in Task 3.3 and 3.5 / Deliverable D3.3 Integration in the BCI architecture will be addressed in Task 3.4 / Deliverable D3.4 Integration in the CORBYS system will be addressed in WP6.
BCI5	Intention of legs motion decoding flag	Information about which leg the subject is going to move. It also provides a “no	Signal processing/Decoding part of the requirement will

		movement" output value. The intention of legs motion decoding flag output can take the following values: *right leg*, *left leg* and *no movement*.	be addressed in Task 3.3/Deliverable D3.3; Integration in the BCI architecture will be addressed in Task 3.4/Deliverable D3.4
BCI6	Decoding accuracy	It provides a numerical value (e.g. a percentage) related to the ability of the BCI subsystem in detecting the intention of legs motion	Refer to BCI5
BCI7	Error marker	Feedback stimulus that informs the subject about the correctness of their response to a specific task. The feedback stimulus presented after the accomplishment of a task, informs the subject about the correctness of his response and therefore provide the critical information that would enable the error detection. Feedback stimulus, provided by other subsystems, can be auditory, visual, somatosensory, etc. The error marker input is a time marker that informs the BCI subsystem when the feedback is presented to the subject.	Signal processing/Decoding Refer to BCI8
BCI8	Feedback error-related potential decoding flag	Information about the presence of the feedback error-related potential in the brain signal The feedback error-related potential decoding flag output can take the following values: *present* and *absent* depending on the presence of the feedback error-related potential in the brain signal.	Signal processing/Decoding part of the requirement will be addressed in Task 3.5/Deliverable D3.3; Integration in the BCI architecture will be addressed in Task 3.4/Deliverable D3.4
BCI9	Decoding accuracy	It provides a numerical value (e.g. a percentage) related to the ability of the BCI subsystem in detecting the feedback error-related potential.	Refer to BCI8
BCI10	Attention states decoding flag	Information about the subject's attention level during a specific task The attention states decoding flag output provides a numerical value indicating the user's level of attention.	Progress report on the Signal processing/Decoding related part of the requirement has been addressed in the current deliverable. Final analysis will be addressed in D3.3.

			Integration in the BCI architecture will be addressed in Task 3.4/Deliverable D3.4
BCI11	Decoding accuracy	It provides a numerical value (e.g. a percentage) related to the ability of the BCI subsystem in detecting the attention states.	Refer to BCI10

6 Conclusions and future work

This report describes the work related to development of Human Sensory System (HSS) and Brain Computer Interface (BCI) performed in Work Package 3 "Sensing systems for assessing dynamic system environments including humans".

The human sensory system has been realized through development of a lightweight chest belt with sensors at chest and back of patient measuring physiological parameters during gait rehabilitation training sessions. Infrastructure for transmitting sensor data wirelessly with a predictable low latency to a computer, synchronizing and time-stamping data and interfacing the user interface and cognitive modules has been provided. The sensor modules are based on state of the art low power components that are highly integrated and optimized for long term wireless physiological monitoring. The Chest Belt can easily be fit to and removed from the patient at start and end of a training session and will not cause any discomfort, but still provide relevant physiological sensor data to the cognitive modules of the CORBYS Demonstrator I. Patient safety is handled by using a wireless battery powered sensor modules.

The remaining work for the Human Sensory System will be presented in D3.4 in month 26. This will include:

- EMG system
  - Description of the sensor modules
  - Time to mount sensors on patient
  - Driver component for the EMG sensors.

- Complete testing description
  - Chest unit
  - IMU unit
  - HSS controller SW

- Complete specification of charging of wireless devices
  - Operational and charging time for all units
  - Localization of charging station

- ROS network integration
  - Complete set of test data exploitable for simulating the execution of the HSS Controller without actual sensors.
  - Front-end implementation fully compliant with the final CORBY ROS Guideline.
  - Implementation of the training initialization process and supporting GUI.
  - Integration with Task Manager and Executive Supervisor

- Synchronization issues
  - Implementation of an appropriate mechanism for time synchronization with the wireless sensor (either "over the air" or through serial communication on the charging station).
  - Evaluation of latency and time-stamping offsets at the different layers of the HSS Controller.

- Evaluate effect of noise for human sensory system
  Electromagnetic noise from actuators, motors, radios etc. at the mobile platform and in the environment may interfere with senor measurements. The possible effect of this will be investigated and reported in D3.4.

- Physical integration
  The Human Sensory System will be integrated with Demonstrator I from WP7 as a part of WP8, System Integration. When Demonstrator I is ready for integration this work will start by integrating the HSS computer in the carrier frame together with external antennas and cabling to the general purpose network. HSS will then be tested in Demonstrator I environment and results will be compared to results from similar tests prior to integration. This activity is dependent on WP7 and WP8 work and may not be completed for D3.4

In this present deliverable three topics related to the design of a BCI submodule within the CORBYS gait rehabilitation system have been addressed:

In section 3.1, Evaluation of EEG acquisition systems that could reduce the noise level, two EEG systems, i.e. TMSi and g.Tec, have been analysed in order to choose the most appropriate for the CORYS gait rehabilitation system. Due to the results obtained where the g.Tec system showed to be more affected by electrical noise contamination, TMSi has be chosen as EEG system for the CORBYS 1st demonstrator.

In section 3.2, Analysis and removal of movement artifacts from during locomotion, the description of temporal and spectral characteristics of the main contamination introduced in the EEG by locomotion and head movements have been described. ICA technique was applied to remove the artifacts contamination generated showing its feasibility within a simulation of the CORBYS rehabilitation user scenario. Due to the importance of the decoder-specific analysis in the removing process of gait-related artifacts, further evaluations are needed once the CORBYS decoders have been implemented.

Section 3.3, Detection of attention during assisted passive leg motion, shows how the attention modulates brain activity during passive leg movements. An off-line classifier has been developed to differentiate between attention and non-attention to the motor task. Results showed the feasibility to distinguish between both conditions above the chance level for all the subjects. This is the first step in the design a BCI system to decode passive lower limb movements with attention and non-attention to the motor task. Future work will consider the automation of the features selection process and build an online classifier to assess the feasibility of decoding attention during real time motion.

The remaining work for the Brain Computer Interface will be presented mainly in D3.3 (month 38) and D3.4 (month 26). This will include:

- Design of a Brain Computer Interface software architecture:
  -Analysis
  -Design

-Implementation
-Documentation

- Development of the CORBYS-related decoding algorithms:
  - Attention states
  - Feedback error-related potential

  - Integration of the decoding algorithms in the BCI software architecture

- BCI module testing:
  - Bluetooth acquisition
  - Decoders activation/deactivation
  - Measurement failure
  - Training procedures
  - Decoding Procedure

- ROS network integration
  - Generation and integration of simulated EEG data (node version for simulation)
  -Design of BCI output messages (including EEG data and decoding outputs)
  - Design of BCI configuration parameters (from Parameter Server)
  - Integration of BCI architecture in ROS node template
  - Development of GUI ROS node

- Synchronization
  - Evaluation of BCI processing delays
  - Evaluation of submodule sampling frequency and cycle time
  - Evaluation of synchronization between HSS and BCI data

- Integration and Testing

The Brain Computer Interface submodule will be integrated and tested within the CORBYS mobile platform in WP7 and WP8. Testing of functional and other requirements will be analysed in WP8.

7 References

Anderer P, Roberts S, Schlogl A, Gruber G, Klosch G, Herrmann W, Rappelsberger P, Filz O, Barbanoj MJ, Dorffner G, Saletu B .Artifact processing in computerized analysis of sleep EEG – a review .Neuropsychobiology 1999;40:150-157.

Antelis J.M., Montesano L., Giralt X., Casals A. and Minguez J., "Detection of movements with attention or distraction to the motor task during robot-assisted passive movements of the upper limb", *International Conference of the IEEE Engineering in Medicine and Biology Society*, San Diego (USA) , 2012.

Costa D, Vitti M, De Oliveira Tosello D., *Electromyographic study of the sternocleidomastoid muscle in head movements*, Electromyogr Clin Neurophysiol,1990.

Croft RJ, Barry RJ. Removal of ocular artifact from the EEG: a review. Neurophysiol Clin 2000;30(1):5–19.

Dyson M, F. Sepulveda, J.Q. Gan, Localisation of cognitive tasks used in EEG-based BCIs, Clinical Neurophysiology, Volume 121, Issue 9, September 2010

Gargiulo G, Calvo RA, Bifulco P, Cesarelli M, Jin C, Mohamed A, van Schaik A. (2010)A new EEG recording system for passive dry electrodes. Clin Neurophysiol, 121(5):686-93.

Gomez J., Aguilar M., Horna E., and Minguez J.**, "**Quantification of Event-Related Desynchronization / Synchronization at Low Frequencies in a Semantic Memory Task", *International Conference of the IEEE Engineering in Medicine and Biology Society, San Diego (USA)*, 2012 .

Goncharova II, McFarland DJ, Vaughan TM, Wolpaw JR., *EMG contamination of EEG: spectral and topographical characteristics*.,Clin Neurophysiol. 2003

Graimann B, Huggins J.E, Levine S.P and Pfurtscheller G, "Visualization of significant ERD/ERS patterns in multichannel EEG and ECoG data", *Clinical neurophysiology : official journal of the International Federation of Clinical Neurophysiology,* 1 January 2002, volume 113, issue 1, Pages 43-47.

Graimann B. and Pfurtscheller G., "Quantification and visualization of event-related changes in oscillatory brain activity in the time frequency domain", *Progress in Brain Research*, no. 159, pp. 79–97, 2006.

Groppe DM, Makeig S, Kutas M., *Identifying reliable independent components via split-half comparison,*. Neuroimage, 2000

g.Tec Technologies, n.d. g.Tec EEG system [online] Available at < http://www.gtec.at/> [Accessed 20 September 2012].

Gwin, J.T., Gramann, K., Makeig, S. and Fer, D. P. (2010). Removal of movement artifact from highdensity eeg recorded during walking and running. J Neurophysiol., 103:3526–3534.

Hanakawa T, Immisch I, Toma K, Dimyan MA, Van Gelderen P, Hallett M., Functional properties of brain areas associated with motor execution and imagery, J Neurophysiol. 2003 Feb;89(2):989-1002.

Hirasaki E., Moore S., Raphan T. Cohen B., Theodore, *Effects of walking velocity on vertical head and body movements during locomotion,* Exp Brain Res,1999

Hyvärinen, A; Oja, E . *Independent Component Analysis: Algorithms and Applications*, Neural Networks 2000.

Johansen-Berg H. and Matthews P., "Attention to movement modulates activity in sensori-motor areas, including primary motor cortex", *Experimental Brain Research*, vol. 142, pp. 13–24, 2002.

Liverud A.E, Vedum J., Fleurey F. and Seeberg T.M. (2012). "Wearable Wireless Multi-parameter Sensor Module for Physiological Monitoring." pHealth 2012 Proceedings of the 9th International Conference on Wearable Micro and Nano technologies for Personalized Health, pages 210-215, 2012

Matteucci, M., Carabalona, R., Casella, M., Di Fabrizio, E., Gramatica, F., Di Rienzo, M., Snidero, E., Gavioli, L. and Sancrotti, M. (2007). Micropatterned dry electrodes for braincomputer interface. Journal Microelectronic Engineering, 84(2).

Müller-Putz G. R., Scherer R., Brunner C., Leeb R., and Pfurtscheller G., "Better than random? A closer look on BCI results", *International Journal of Bioelectromagnetism*, vol. 10, pp. 52–55, 2008.

Pascual-Marqui R. Standardized low resolution brain electromagnetic tomography (sLORETA): technical details. Methods Find Exp Clin Pharmacol 2002;24D: 5–12.

Pfurtscheller G., Lopes da Silva F.H., "Event-related EEG/MEG synchronization and desynchronization: basic principles", *Clinical neurophysiology : official journal of the International Federation of Clinical Neurophysiology*, 1 November 1999 (volume 110 issue 11 Pages 1842-1857)

Pfurtscheller G., Müller-Putz G. R., Pfurtscheller J. and Rupp R., "EEG-Based Asynchronous BCI Controls Functional Electrical Stimulation in a Tetraplegic Patient", EURASIP J. Adv. Sig. Proc., 2005(19):3152-3155, 2005.

Pons J.L., "Wearable Robots: Biomechatronic Exoskeletons", *Wiley Books*, 2008.
Searle, A. and Kirkup, L. (2010). A direct comparison of wet, dry and insulating bioelectric recording electrodes. Physiological Measurement, 21(2):271–283.

Popescu, F., Fazli, S., Badower, Y., Blankertz and Mller, KR. (2007). Single trial classification of motor imagination using 6 dry eeg electrodes. PLoS ONE, 2(2).

Schlögl A, Keinrath C, Zimmermann D, Scherer R, Leeb R, Pfurtscheller G. , A fully automated correction method of EOG artifacts in EEG recordings. Clin Neurophysiol. 2007

Tee K. P., Guan C., Ang K. K., Phua K. S., Wang C., and Zhang H., "Augmenting Cognitive Processes in Robot-Assisted Motor Rehabilitation," *Proceedings of the 2nd Biennial IEEE/RAS-EMBS International Conference on Biomedical Robotics and Biomechatronics*, pp. 698–703, 2008

Teplan, M., *Fundamentals of EEG measurement*., Measurement Science Review, 2002

TMSi: Twente Medical Systems International, n.d. EEG TMSi system [online] Available at < http:// http://www.tmsi.com/> [Accessed 20 September 2012].

Tzyy-Ping Jung, Colin Humphries, Te-Won Lee, Scott Makeig, Martin J. Mckeown, Vicente Iragui, and Terrence J. Sejnowski. *Extended ICA removes artifacts from electroencephalographic recordings*, In NIPS '97, 1998. MIT Press.

Van de Velde M, van Erp G, Cluitmans PJ., Detection of muscle artefact in the normal human awake EEG, Electroencephalogr Clin Neurophysiol. 1998 Aug;107(2):149-58.